EUMETSAT Satellite Application Facility on
Support to Operational Hydrology and Water Management

Product Validation Report (PVR-15A) for product H15A (PR-OBS-6A)

Blended SEVIRI Convection area/ LEO MW Convective Precipitation

Reference Number:	SAF/HSAF/PVR-15A
Issue/Revision Index:	1.1
Last Change:	10 April 2015
About this document	This Document has been prepared by the Product Validation Cluster Leader, with the support of the Project Management Team and of the Validation and Development Teams of the Precipitation Cluster

DOCUMENT CHANGE RECORD

Issue / Revision	Date	Description
1.0	16/02/2015	Baseline version prepared for CDOP2 ORR1 Part5.
1.1	10/04/2015	Revised version which acknowledges the outcomes of ORR1 Part5

Index

List of tables

List of figures

1. Introduction to product H15A (PR-OBS-6A)

2.1 Sensing principle

Product PR-OBS-6A (Blended SEVIRI Convection area/ LEO MW Convective Precipitation) is based on the SEVIRI instrument onboard Meteosat Second Generation satellites. The whole H-SAF area is covered (see Figure 1, same as for PR-OBS-3, PR-OBS-4 and PR-OBS-5). An objective analysis of the equivalent blackbody temperatures (TBB) is implemented to detect the convective structures of cloudy areas, by means of NEFODINA, an automatic tool running at CNMCA dedicated to now-casting applications. A map of convective clouds is performed to combine precipitation fields from MW channels. The product is generated accordingly SEVIRI acquisition time plus a delay of few minutes. The delay is in the range of 3 to 5 minutes with a potential maximum of 10, after end of reception of whole disk SEVIRI data at CNMCA. Processing duration is principally dominated by convection identification algorithm. The more is HSAF area affected by convection areas the more is processing time to analyze the whole scene. The SEVIRI channels utilised for convective area identification are 6.2, 7.3 and 10.8 μm. The calibration of TBB in terms of precipitation rate by means of MW measurements, as reconstructed in PR-OBS-1 and PR-OBS-2, implies the existence of good correlation between behaviour of TBB and precipitation rate in case of convection phenomena. PR-OBS-6A assigns precipitation to SEVIRI pixels after the convection filtering via an algorithm that remap PR-OBS-1 and PR-OBS-2 estimation, in reason of the dynamical behaviour of clouds, to a new rain field. Being connected only with convective systems this rain fields is no more only a lookup of latest SEVIRI acquisition but has inside the capacity to diagnose clouds, individuating ones vertically changing, and to prolong rain precipitation in the dissipating phase of convection systems, contributing adequately to accumulated precipitation (product PR-OBS-5). For more information, please refer to the Products User Manual (specifically, PUM-15A).

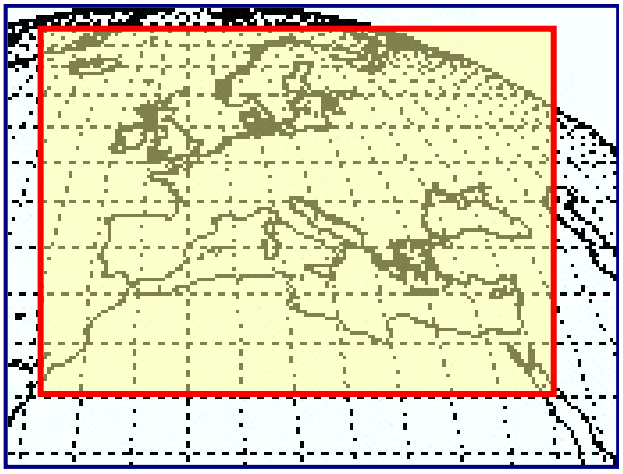

Figure 1 The H-SAF required coverage in the Meteosat projection

2.2 Algorithm principle

The baseline algorithm for H15A processing is described in ATBD-15A. Only essential elements are highlighted here.

The PR-OBS-6A product is based on MW-derived precipitation measurements PR-OBS-1 and PR-OBS-2 and NEFODINA products on HSAF area (1900x900).

The fields of precipitation are retrieved directly from HSAF components, instead the convective areas are identified with an automatic tool running at CNMCA dedicated to now-casting applications. It allows the automatic detection and classification of convective cloud systems and the monitoring of their lifecycles.

The algorithm classifies and groups neighbouring SEVIRI fields of view that show convective characteristics. Based on the hypothesis that deep convective clusters are associated with local rapid horizontal variation of cloud volume and WV content, it is possible to classify a collection of pixels as convective by looking for temporal variations in cloud top temperatures seen in IR at 10.8 m, and for changes in WV content seen in the 6.2 m and at 7.3 m channels. The IR channel provides cloud top temperature and morphology, while WV channels provide information on the spatial distribution of the WV content in the neighbouring cloud-free area and above the cloud.

NEFODINA produces images that identify detected cells, their development, and their movement (Fig. 5). These output images are associated to ASCII files which contain quantitative information of the IR1, WV1 and WV2 channels BTs along with CO shape, slope index (spatial BT gradient), CO area and CO mean and minimum BTs.

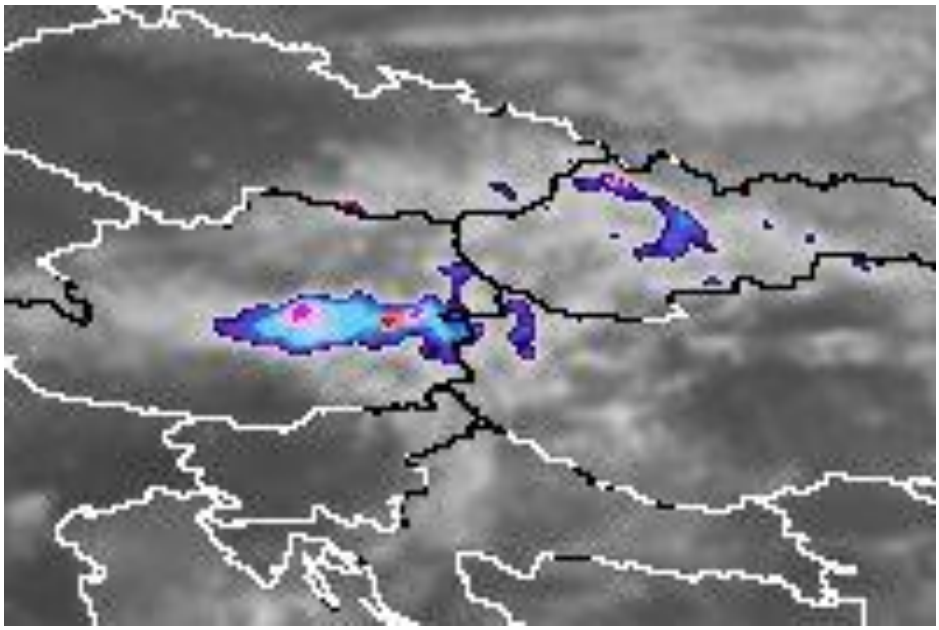

Figure 2 Example of NEFODINA image detected objects - red and pink colours show convective regions: red for growing objects and pink for those disappearing

PR-OBS-6A SW package includes auxiliary files as seasonal and latitude configuration file, orography map, land/sea mask.

The SW inputs, are:

- PR-OBS-1.
- PR-OBS-2.
- NEFODINA CO data.
- Auxiliary files.

The SW outputs are:

- Maps of precipitation rain rate.
- Precipitation rain rate maps encoded in GRIB2 format.

The main functions (described in Fig. 8) are:

- PR-OBS-1 and PR-OBS-2 data (in BUFR format) decoding and extraction.
- NEFODINA run over H-SAF area and data extraction.
- Association between NEFODINA CO and MW retrieved precipitation rain rate.
- Precipitation rain rate maps, both in graphical and numerical (GRIB2) format.

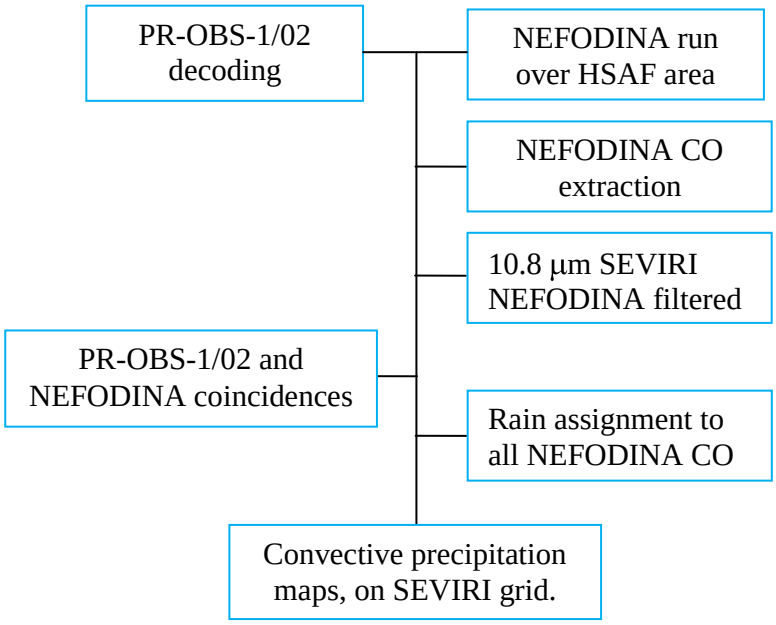

Figure 3 SW package main functions

2.3 Main operational characteristics

Main operational characteristics are connected with the identification of convection and the association of MW retrieved rain rate present in the same area with only active SEVIRI pixels, this by recomposing rain intensity that the system as in input from PR-OBS-1 and PR-OBS-2A towards the only part of clouds that NEFODINA individuate in the growing, mature and dissipating convective cell. While PR-OBS-3A performs a rain lookup of SEVIRI image, without any connection to preceding SEVIRI image that permit to classify cloud status and behaviour, with PR-OBS-6A there the possibility to observe principally heavy shower of rain connected with vertical development of thunderstorm clouds.

The operational characteristics of PR-OBS-6A are discussed in PUM-15A. Here are the main highlights.

The horizontal resolution (□x). The IFOV of SEVIRI images is 4.8 km at nadir, and degrades moving away from nadir, becoming about 8 km in the H-SAF area. A figure representative of the PR-OBS-6A resolution is: ~ 8 km. Sampling is made at ~ 5 km intervals, consistent with the SEVIRI pixel over Europe. Conclusion:

- resolution □x ~ 8 km - sampling distance: ~ 5 km.

The observing cycle (□t) is defined as the average time interval between two measurements over the same area. In the case of PR-OBS-6A the product is generated soon after each SEVIRI new acquisition, Thus:

- observing cycle □t = 15 min - sampling time: 15 min.

The timeliness (□). For PR-OBS-6A, the time of observations is 1-5 min before each quarter of an hour, ending at the full hour. To this, ~ 5 min have to be added for acquisition through EUMETCast and ~ 5 min for processing at CNMCA, thus:

- timeliness □ ~ 15 min.

The accuracy is defined into phases: in the first phase, for this document, the accuracy values which have been agreed into the PRD and PRT for the product H03 are adopted:

<VERIFICARE REQUIREMENTS>

The architecture of the PR-OBS-6A products generation chain is shown in the Fig. 4.

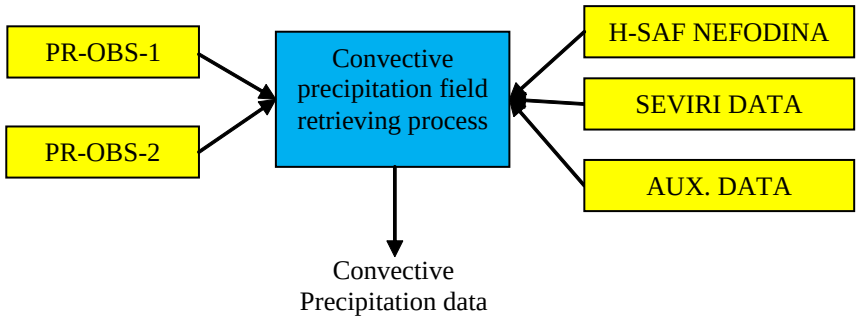

Figure 4 PR-OBS-6A production chain architecture

The logical model above represents a schematic description of the PR-OBS-6A products chain architecture. This also represents the product context diagram by identification of inputs, outputs and application processes. It includes:

- PR-OBS-1, PR-OBS-2, H-SAF dedicated NEFODINA data, SEVIRI raw image at 10.8 □m and auxiliary data as inputs;
- "Convective precipitation field retrieving process" able to decode PR-OBS-1 and PR-OBS-2, retrieve suitable NEFODINA information, calculate the convective precipitation associated to NEFODINA Convective Objects,
- "Convective Precipitation data" as processing output in terms of maps and encode data (GRIB2).

In the architecture of PR-OBS-6A production chain are also included (not shown in the Fig. 3) data archiving and dissemination functions and log of events module in order to verify the SW performance.

2. Validation strategy, methods and tools

3.1 Validation team and work plan

Whereas the previous operational characteristics have been evaluated on the base of system considerations (number of satellites, their orbits, access to the satellite) and instrument features (IFOV, swath, MTF and others), the evaluation of accuracy requires validation, i.e. comparison with the ground truth or with something assumed as "true". PR-OBS-4, as any other H-SAF product, has been submitted to validation entrusted to a number of institutes (see next figure).

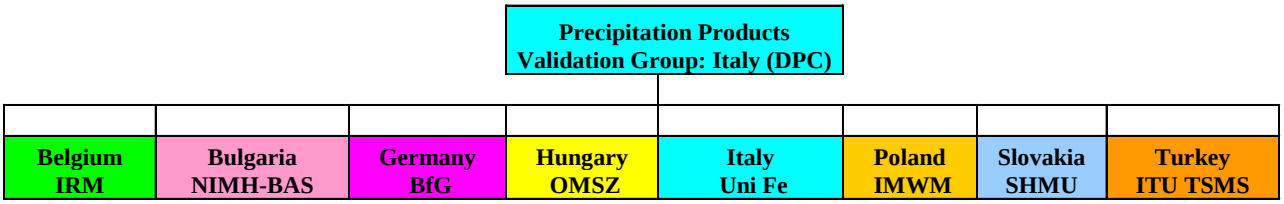

Figure 5 Structure of the Precipitation products validation team

Next table lists people involved in the validation of H-SAF precipitation products:

Validation team for precipitation products			
Silvia Puca (Leader)	Dipartimento Protezione Civile (DPC)	Italy	silvia.puca@protezionecivile.it
Emanuela Campione	Dipartimento Protezione Civile (DPC)	Italy	emanuela.campione@protezionecivile.it
Gianfranco Vulpiani	Dipartimento Protezione Civile (DPC)	Italy	gianfranco.vulpiani@protezionecivile.it
Alexander Toniazzo	Dipartimento Protezione Civile (DPC)	Italy	alexander.toniazzo@protezionecivile.it
Angelo Rinollo	EUMETSAT and Dipartimento Protezione Civile (DPC)	Italy	angelo.rinollo@protezionecivile.it
Emmanuel Roulin	Institut Royal Météorologique (IRM)	Belgium	Emmanuel.Roulin@oma.be
Pierre Baguis	Institut Royal Météorologique (IRM)	Belgium	Pierre.Baguis@oma.be
Gergana Kozinarova	National Institute of Meteorology and Hydrology Bulgarian Academy of Sciences (NIMH-BAS)	Bulgaria	gkozinarova@gmail.com
Georgy Koshinchanov	National Institute of Meteorology and Hydrology Bulgarian Academy of Sciences (NIMH-BAS)	Bulgaria	georgy.koshinchanov@meteo.bg
Claudia Rachimow	Bundesanstalt für Gewässerkunde (BfG)	Germany	rachimow@bafg.de
Peter Krahe	Bundesanstalt für Gewässerkunde (BfG)	Germany	krahe@bafg.de
Eszter Lábó	Hungarian Meteorological Service (OMSZ)	Hungary	labo.e@met.hu
Judit Kerenyi	Hungarian Meteorological Service (OMSZ)	Hungary	kerenyi@met.hu
Federico Porcu'	Ferrara University, Department of Physics (UniFe)	Italy	porcu@fe.infn.it
Lisa Milani	Ferrara University, Department of Physics (UniFe)	Italy	milani@fe.infn.it
Bozena Lapeta	Institute of Meteorology and Water Management (IMWM)	Poland	Bozena.Lapeta@imgw.pl
Rafal Iwanski	Institute of Meteorology and Water Management (IMWM)	Poland	Rafal.Iwanski@imgw.pl
Ján Kaňák	Slovenský Hydrometeorologický Ústav (SHMÚ)	Slovakia	jan.kanak@shmu.sk

Ľuboslav Okon	Slovenský Hydrometeorologický Ústav (SHMÚ)	Slovakia	luboslav.okon@shmu.sk
Ladislav Méri	Slovenský Hydrometeorologický Ústav (SHMÚ)	Slovakia	ladislav.meri@shmu.sk
Mariàn Jurasek	Slovenský Hydrometeorologický Ústav (SHMÚ)	Slovakia	marian.jurasek@shmu.sk
Ahmet Öztopal	Istanbul Technical University (ITU)	Turkey	oztopal@itu.edu.tr
Ibrahim Sonmez	Turkish State Meteorological Service (TSMS)	Turkey	isonmez@dmi.gov.tr
Aydin Gurol Erturk	Turkish State Meteorological Service (TSMS)	Turkey	agerturk@dmi.gov.tr

Table 1 List of the people involved in the validation of H-SAF precipitation products

The Precipitation products validation programme started with a first workshop in Rome, 20-21 June 2006, soon after the H-SAF Requirements Review (26-27 April 2006). After the first Validation Workshop in 30 September 2006, other ones followed, at least one per year to exchange experiences, problem solutions and to discuss possible improvement of the validation methodologies. Often the Precipitation Product Validation workshop are joined with the Hydrological validation group. The precipitation products validation programme was finalised during the H-SAF Products and Hydro Validation Workshops hosted in 2011 by the Italian Civil Protection and, in 2013, by the Hungarian Meteorological Service (OMSZ).

The results of the Product Validation activities are reported in this Product Validation Report (PVR) and are published in the validation section of the H-SAF web page. A new structure and visualization of the validation section of H-SAF web page is in progress to take into account the user needs. This validation web section will be continuously updated with the last validation results and studies coming from the Precipitation Product Validation Group (PPVG).

3.2 Validation objectives and issues

The products validation activity has to serve multiple purposes:

- to provide input to the product developers for improving calibration for better quality of baseline products, and for guidance in the development of more advanced products;
- to characterise the product error structure in order to enable the Hydrological validation programme to appropriately use the data;
- to provide information on product error to accompany the product distribution in an open environment, after the initial phase of distribution limited to the so-called “beta users”.

Validation is obviously a hard work in case of precipitation, either because the sensing principle from space is very indirect, or because of the natural space-time variability of the precipitation field (sharing certain aspects with fractal fields), that determines severe sampling problems.
It is known that an absolute ‘ground truth’ does not exist. In the H-SAF project the validation is based on comparisons of satellite products with ground reference data: radar, rain gauge and radar integrated with rain gauge. During the Development phase some main problems have been pointed out. First of all the importance to characterize the error associated to the ground data used by PPVG. Secondly to develop software for all steps of the Validation Procedure, a software available to all the members of the PPVG. Two Working Groups (WG) (radar, rain gauge) have been composed in PPVG in order to solve these problems. The first results obtained by the working groups are reported in annex 1-5, a complete documentation shall be available in the H-SAF web page Precipitation Validation Section. In addition to the radar and rain gauge WG other WGs have been composed to integrate various sets of precipitation data sources – raingauge network, radar network, NWP models outputs and climatological standards - into additional precipitation products, which can describe the areal instantaneous and cumulated precipitation fields (*INCA -WG*) and to

investigate the opportunity to create geographical maps of error distribution for providing information on test catchments to the Hydrological Validation Group *(GEO MAP –WG)*.

3.3 Validation methodology

From the beginning of the project it was clear the importance of defining a common validation procedure to make the results obtained by several institutes comparable and to better understand their meanings. The main steps of this methodology have been identified in collaboration with the product developers, and with the support of ground data experts. The common validation methodology is based on the comparison with ground data (radar and rain gauge observations) to produce **large statistic** (multi-categorical and continuous), and **case study analysis.** The two approaches (large statistic and case study analysis) are considered complementary in assessing the accuracy of the implemented algorithms. Large statistics helps in identifying existence of pathological behaviour; selected case studies are useful in identifying the roots of such behaviour, when present.
The main steps of the validation procedure are the following:

- ground data error analysis: radar and rain gauge;
- point measurements (rain gauge) spatial interpolation;
- up-scaling of radar data versus SSMI grid;
- temporal comparison of precipitation products (satellite and ground refeference);
- statistical scores (continuous and multi-categorical) evaluation;
- case study analysis.

3.4 Ground data and tools used for validation

Rain gauge and radar data have been both used until for the validation. The knowledge of the ground data characteristics used by the PPVG, i.e., the instrumental error and retrieval algorithms, is necessary to understand the validation results and define the procedure to select the most reliable data to be considered as “ground reference”. A complete report on the results obtained by the Working Group on rain gauge, radar and ground data integration are reported in the Chapter 4 with a complete inventory of the ground data used by the PPVG.

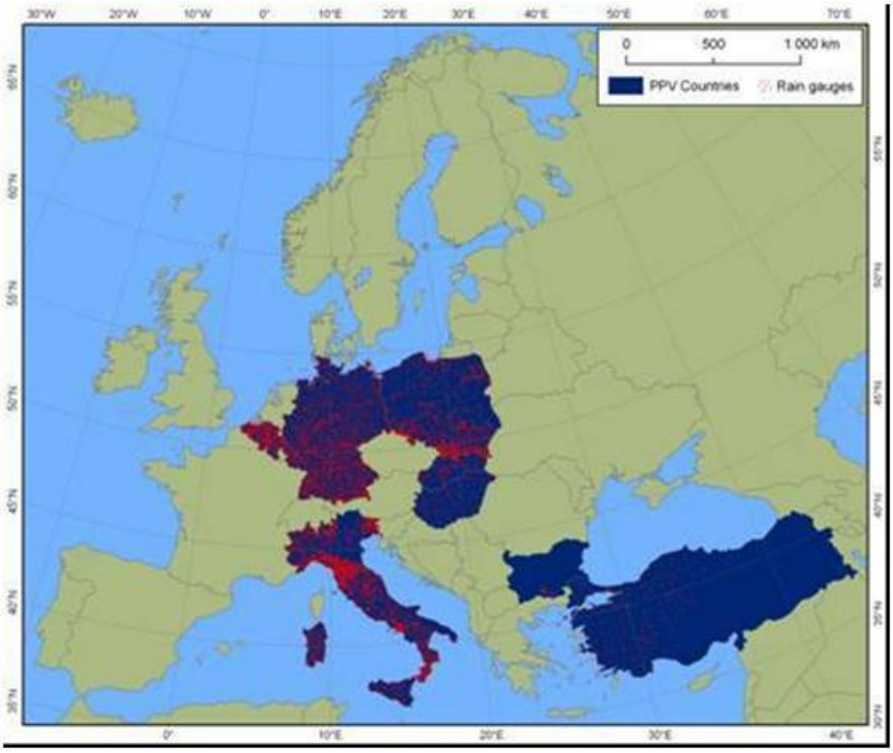

Figure 6 The network composed by more than 4000 rain gauges used for H-SAF precipitation products validation

The rain gauge networks managed by the PPVG are composed by more than 4000 stations across 6 Countries (Figure 6). The average distance between nearby raingauges, a measure of the raingauge density, is a key characteristic of these networks. The number of raingauge and density per country are summarized in Table 2.

Country	Total number of gauges *	Average minimum distance (km)
Belgium	91**	11.2
Germany	1300	17
Hungary	267	N.A.
Italy	2600	9.5
Poland	330-475	13.3
Turkey	356	27

Table 2 Number and density of raingauges within H-SAF validation area

* the number of raingauges could vary from day to day due to operational efficiency within a maximum range of 10-15%.
** only in the Wallonia Region

Most of the gauges used in the National networks by the PPVG Partners are of the tipping bucket type, providing hourly cumulated rainfall observations (see Table 3).

The rain gauge inventory (see annex 1) on the instruments, the operational network and the approach to match gauge data with the satellite estimates in the PPVG, has pointed out that the rain gauge networks available in the PPVG are surely appropriated for the validation of cumulated products (1 hour and higher), but probably not for instantaneous estimates. The comparison of satellite rain rate with hourly cumulated

ground measurements surely introduces intrinsic errors in the matching scores, that can be estimated as very large. The validation of instantaneous estimates should be carried on only when gauges cumulation interval is 10 to 15 minutes (as in Poland). Values cumulated over shorter intervals (5 or even one minute, as it is done in Turkey) are affected by large relative errors in cases of low/moderate rain rates. Studies are undertaken in order to quantitatively estimate the errors introduced in the validation procedure comparing the instantaneous satellite precipitation estimation with the rain gauge precipitation cumulated on different intervals.
Moreover the revisiting time (3,4 hours) of the product makes impossible or not reasonable to validate the product for 1-24 hours cumulated interval.
The WG has also pointed out that different approaches for the estimates matching are considered in the PPVG. One of the next step of the WG will be to define in collaboration with the *GeoMap-WG* (Annex 7) the spatial interpolation technique and to develop the related software to be used in side the PPVG.

Country	Minimum detectable rainrate (mm h^{-1})	Maximum detectable rainrate (mm h^{-1})	Heating system (Y/N)	cumulation interval (min)
Belgium	0.1	N/A	N	60
Germany	0.05	3000	Y	60
Hungary	0.1	360	Y	15
Italy	0.2	300	Y	5
Poland	0.1	300	Y	10
Turkey	0.2	288	Y	1

Table 3 Summary of the raingauge characteristics

An inventory on radar data (see annex2), networks and products used in PPVG (Chapter 4), has pointed out that all the institutes involved in the PPVG declared the system are kept in a relatively good status and all of them apply some correction factors in their processing chain of radar data. In Figure 7 there is the map showing part of the 56 C-band radars available for validation by the PPVG. Only the radar data passing the quality control conceived by the owner Institute are used by the PPVG for validation activities. However, the applied data correction methodology is not unique, depending on the system characteristics, the environmental scenario, the operational strategy. This implies that the uncertainty retrieval cannot be homogenized within the H-SAF domain. However, each country can provide useful information of the error structure of its rainfall products based on its own resources. The *Radar-WG* (Annex 3) is now working to define an approach which ingest the data quality information to constraint the validation onto the "reliable" pixels. Quality information should take into account the radar site/geographical areas/event type/radar products. The study performed by the Slovakian team (Annex 4) and the scheme published by J. Szturc *et al* 2008, on the quality index evaluation was considered by the *Radar-WG*. Additionally, a sensitivity study on the impact of the radar data quality on the validation activity was carried out by Rinollo et al. (2013). Future developments will be aimed at considering the radar data quality as up-scaling criterion (pixels weight) and to make a conditional validation, i.e. for different data quality thresholds.
The studies that have been carried out in the PPVG on comparison of radar data with rain gauge data have shown that RMSE error associated with radar fields depends considerably on radar minimum visible height above the rain gauge in mountainous terrains like Slovakia, but less importantly in flat terrains like Hungary. In Slovakia, the RMSE% error (see Section 3.7) of radar accumulated fields is between 70-90%, whereas in Hungary, it is slightly lower, between 60-80%. Dataset for May-September 2010 have been used to derive these parameters.

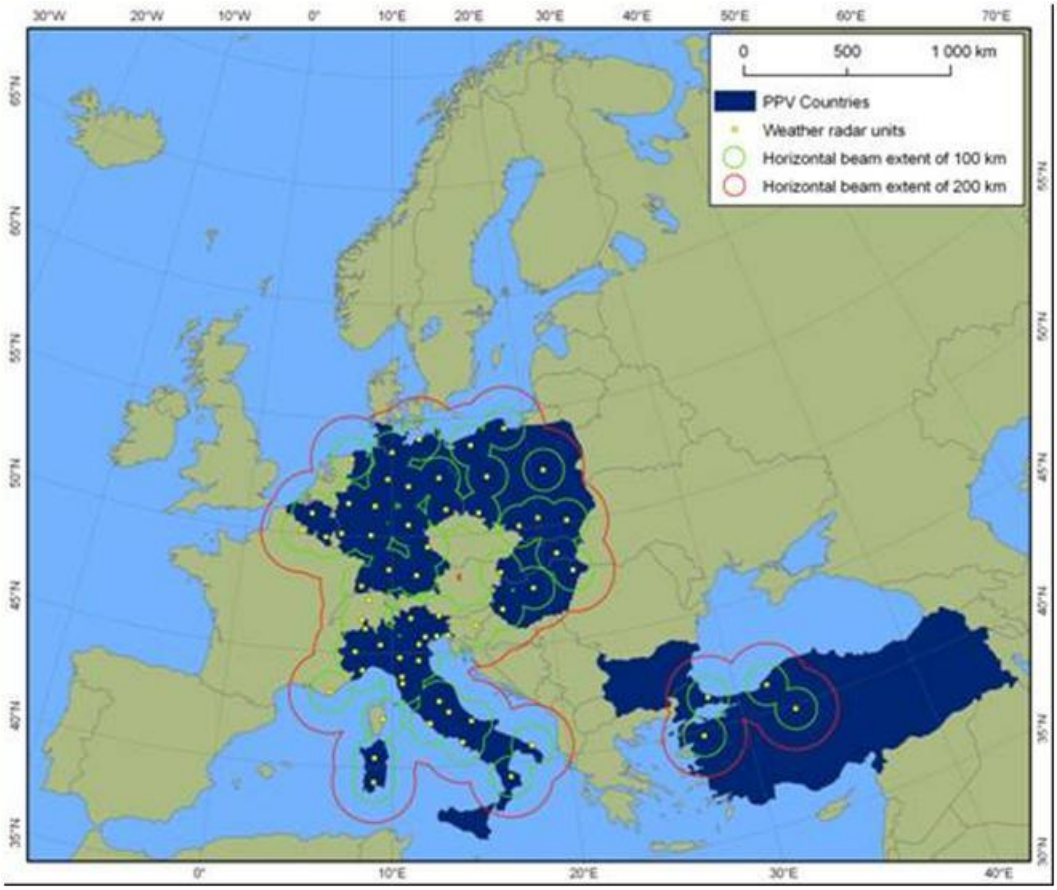

Figure 7 The network of C-band radars available in the H-SAF PPVG (situation updated on 2010).

In PPVG it is under investigation the possibility to use ground data integrated software to produce precipitation field. The results obtained by *INCA-WG* are reported in the chapter 4.

References

Rinollo, A., Vulpiani, G., Puca, S., Pagliara, P., Kănák, J., Lábó, E., Okon, L'., Roulin, E., Baguis, P., Cattani, E., Laviola, S., and Levizzani, V.: Definition and impact of a quality index for radar-based reference measurements in the H-SAF precipitation product validation, Nat. Hazards Earth Syst. Sci., 13, 2695–2705, doi:10.5194/nhess-13-2695-2013, 2013.

Szturc, J., Ośródka, K., and Jurczyk, A., 2008. Parameterization of QI scheme for radar-based precipitation data. Proceedings of ERAD 2008.

3.5 Common procedure for the validation of H15A

Following the common validation methodology validation codes have been developed for validation using radar and rain gauge data as ground reference.

Common procedure for the validation of H15A with RADAR data

Selection of satellite pixels falling into the region of interest:

In order to avoid time-consuming useless calculation, every country restricts the validation to a specific Area of Interest (normally the area covered by the RADAR data of the country), which is detected implicitly by the common validation algorithm.

Taking into account quality index information
The code is predisposed to read a quality index for each radar pixel. In the present phase of the project, this quality information is not used for validation purposes, but it will be in CDOP2.

Selection of the RADAR data synchronous with the satellite ones:
The RADAR instantaneous image which is the closest in time, either preceding or ensuing the satellite time, is chosen. The image is chosen among the ones referring to the same month of the satellite (so no satellite file can be validated with RADAR file of the following or preceding month, even if closer in time), because validation is provided on monthly basis. If there is no RADAR file within 20 minutes from a satellite file, this is not validated.

Up-scaling of RADAR data at the resolution of the native satellite grid
A grid in which every cell is centred around an IFOV is constructed, so that all the radar pixels are assigned to a certain cell, and the satellite measurement is validated with the average of the radar pixels falling into the corresponding cell.
The edge of radar horizon, where only part of satellite IFOV is covered by radar pixels from validation, is excluded.

Calculation of corresponding satellite and RADAR rain rate values
For each single satellite file, a separate up-scaling procedure reads the look up table and assigns to each satellite pixel the RADAR rain rate average calculated from the values of the radar pixels belonging to the satellite pixel in the look-up table.
Averaging is simply arithmetical; as investigations so far have shown that the averaging method does not have an impact on the statistical scores.
The flag indicating if the satellite pixel is coast, land or sea is matched to each satellite-radar data pair calculated in this step.

Common procedure for the validation of H15A with RAIN GAUGE data

Selection of satellite pixels falling into the region of interest:
In order to avoid time-consuming useless calculation, every country restricts the validation to a specific Area of Interest (normally the area covered by the rain gauge data of the country), which is detected implicitly by the common validation algorithm.

Taking into account quality index information
The validation code is predisposed to read a quality index for each rain gauge. In the present phase of the project, this quality information is not used for validation purposes, but it will be in the near future.

Selection of rain gauge data synchronous with the satellite ones
Gauges with different cumulation intervals are considered, and if the interval is longer than the time resolution of the product (15 minutes), more satellite images are averaged.

interpolation of the rain gauge data:
The partners of the Validation Group have been using a variety of different strategies to treat gauge data. Some are using interpolation algorithms to get spatially continuous rainfall maps, while others process directly the measurements of individual gauges.

Country	Type of interpolation
Belgium	Barnes over 5x5 km grid
Germany	Inverse square distance
Italy	Barnes over 5x5 km grid
Poland	No
Turkey	No

Table 4 Data pre-processing strategies

The kriging technique is the interpolation method chosen for the common validation.

matching between satellite and rain gauge data:
The satellite data is matched with the rain gauge interpolated grid using the nearest-neighbour method.

Techniques to make observation comparable

Due to the time and space structure of precipitation and to the sampling characteristics of both the precipitation products and ground data used for validation, care has to be taken to bring data comparable. At a given place, precipitation occurs intermittently and at highly fluctuating rates. Over space, precipitation is distributed with a high variability, in cells of high intensity nested in larger area with lower rain rate. Aimed at observing this complex phenomenon, the satellite-based products are defined with a spatial resolution of several kilometres and with different sampling rate. On the other hand, reference ground data used to validate precipitation data from satellite are also characterized by their own spatial resolution ranging from point information measured on rain-gauge networks to grids with cells of several hundreds of meters to several kilometres for weather radar. Furthermore, none of these reference observations are without error. For this reason it was decided to compare the satellite data with ground data on the satellite product native grid (see Chapter 2). All the institutes applied the same up-scaling method to compare the satellite precipitation estimations with ground data as described in the previous section 3.5.

Large statistic: Continuous and multi-categorical

The large statistics analysis allows to point out the existence of pathological behaviour in the satellite product performance. It requires the application of the same validation technique step by step in all the institutes take part of the PPVG.

The large statistics analysis in PPVG is based on the evaluation of monthly and seasonal *Continuous verification* and *Multi-Categorical* statistical scores on one year of data for three precipitation classes.

It was decided to evaluate both continuous and multi-categorical statistic to give a complete view of the error structure associated to H15A. Since the accuracy of precipitation measurements depends on the type of precipitation or, to simplify matters, the intensity, the verification is carried out on two classes indicated by hydrologists during the development phase (see **Errore. L'origine riferimento non è stata trovata.**).

	1	2
Precipitation Classes	1 - 10 mm/h (medium precipitation)	> 10 mm/h (intense precipitation)

Table 5 Classes for evaluating Precipitation Rate products

The rain rate lower than 1 mm/h is considered no precipitation.

The main steps to evaluate the statistical scores are:

- all the institutes up-scale the national radar and rain gauge data on the satellite native grid using the up-scaling techniques before described;
- all the institutes compare H15A with the radar precipitation intensity and the rain gauge cumulated precipitation;
- all the institutes evaluate the monthly and seasonal continuous scores (below reported) and contingency tables for the precipitation classes producing numerical files called 'CS' and 'MC' files;
- all the institutes evaluate PDF producing numerical files called 'DIST' files and plots;
- the precipitation product validation leader collects all the validation files (MC, CS and DIST files), verifies the consistency of the results and evaluates the monthly and seasonal common statistical results;

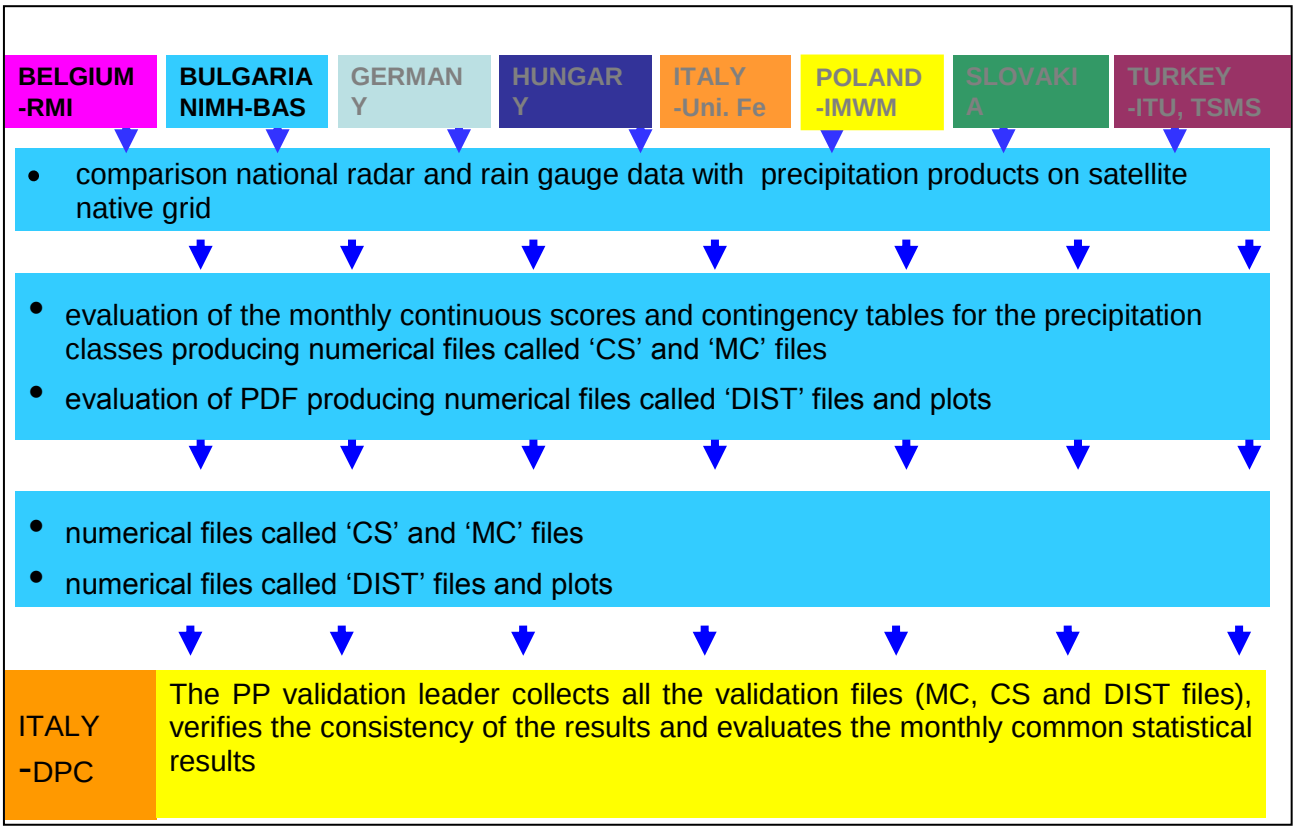

Figure 8 Main steps of the validation procedure in the PPVG.

Statistical scores

The statistical scores evaluated in PPVG *for continuous statistics* are*:*

- Mean Error (ME)

$$ME = \frac{1}{N}\sum_{k=1}^{N}(sat_k - true_k)$$ Range: - ∞ to ∞. Perfect score: 0

- Mean Absolute Error (MAE)

$$MAE = \frac{1}{N}\sum_{k=1}^{N} |sat_k - true_k|$$ Range: 0 to ∞. Perfect score: 0

- Standard Deviation (SD)

$$SD = \sqrt{\frac{1}{N}\sum_{k=1}^{N} (sat_k - true_k - ME)^2}$$ Range: 0 to ∞. Perfect score: 0

- Multiplicative Bias (MBias)

$$MB = \frac{\frac{1}{N}\sum_{1}^{N} sat_K}{\frac{1}{N}\sum_{1}^{N} true_K}$$ Range: - ∞ to ∞. Perfect score: 1

- Correlation Coefficient (CC)

$$CC = \frac{\sum_{k=1}^{N} (sat_k - \overline{sat})(true_k - \overline{true})}{\sqrt{\sum_{k=1}^{N} (sat_k - \overline{sat})^2 \sum_{1}^{N} (true_k - \overline{true})^2}}$$ with $\overline{sat} = \frac{1}{N}\sum_{k=1}^{N} sat_k$ and $\overline{true} = \frac{1}{N}\sum_{k=1}^{N} true_k$;

Range: -1 to 1. Perfect score: 1

- Root Mean Square Error (RMSE)

$$RMSE = \sqrt{\frac{1}{N}\sum_{k=1}^{N} (sat_k - true_k)^2}$$ Range: 0 to ∞. Perfect score: 0

- Root Mean Square Error percent (RMSE %), used for precipitation since error grows with rate.

$$PR\text{-}RMSE\ \% = \sqrt{\frac{1}{N}\sum_{k=1}^{N} \frac{(sat_k - true_k)^2}{true^2{}_k}} * 100$$ Range: 0 to ∞. Perfect score: 0

The statistical scores evaluated in PPVG for *multi categorical statistic* are derived by the following contingency table:

		ground		
		yes	no	total
satellite	yes	hits	false alarms	forecast yes
	no	misses	correct negatives	forecast no
	total	observed yes	observed no	total

Table 6 Contingency Table for statistical scores in PPVG

where:
- hit: event observed from the satellite, and also observed from the ground
- miss: event not observed from the satellite, but observed from the ground

- false alarm: event observed from the satellite, but not observed from the ground
- correct negative: event not observed from the satellite, and also not observed from the ground.

The scores evaluated from the contingency table are:

- Probability Of Detection (POD)

$$POD = \frac{hits}{hits + misses} = \frac{hits}{observed\ yes}$$

Range: 0 to 1. Perfect score: 1

- False Alarm Rate (FAR)

$$FAR = \frac{false alarms}{hits + false alarms} = \frac{false alarms}{forecast\ yes}$$

Range: 0 to 1. Perfect score: 0

- Critical Success Index (CSI)

$$CSI = \frac{hits}{hits + misses + false alarm}$$

Range: 0 to 1. Perfect score: 1

- Equitable Threat Score (ETS)

$$ETS = \frac{hits - hits_{random}}{hits + misses + false alarm - hits_{random}} \quad \text{with} \quad hits_{random} = \frac{observed\ yes * forecast\ yes}{total}$$

ETS ranges from -1/3 to 1. 0 indicates no skill. Perfect score: 1.

- Frequency BIas (FBI)

$$FBI = \frac{hits + false alarms}{hits + misses} = \frac{forecast\ yes}{observed\ yes}$$

Range: 0 to ∞. Perfect score: 1

- Probability Of False Detection (POFD)

$$POFD = \frac{false alarms}{correct negatives + false alarms} = \frac{false alarms}{observed\ no}$$

Range: 0 to 1. Perfect score: 0

- Fraction correct Accuracy (ACC)

$$ACC = \frac{hits + correct negatives}{total}$$

Range: 0 to 1. Perfect score: 1

- Heidke skill score (HSS)

$$HSS = \frac{(hits + correct negatives) - (expected\ correct)_{random}}{N - (expected\ correct)_{random}} \quad \text{with}$$

$$(expected\ correct)_{random} = \frac{1}{N}\left[(observed\ yes)(forecast\ yes) + (forecast\ no)(observed\ no)\right]$$

Range: -∞ to 1. 0 indicates no skill. Perfect score: 1.

- Dry-to-Wet Ratio (DWR).

$$DWR = \frac{false\ alarm + correct\ negative}{hits + misses} = \frac{observed\ \ no}{observed\ yes}$$

Range: 0 to ∞. Perfect score: n/a.

Case study analysis

Each Institute, in addition to the large statistic verification produces a case study analysis based on *the knowledge and experience of the Institute itself*. Each institute, following a standard format here reported decides whether to use ancillary data such as lightning data, SEVIRI images, the output of numerical weather prediction and nowcasting products.

The main sections of the standard format are:

- description of the meteorological event;
- comparison of ground data and satellite products;
- visualization of ancillary data;
- discussion of the satellite product performances;
- indications to Developers;
- indication on the ground data (if requested) availability into the H-SAF project.

More details on case study analysis will be reported in the Chapter 5.

3. Ground data used for validation activities

4.1 Introduction

In the following sections the precipitation ground data networks used in the PPVG are described: radar and rain gauge data the following countries: Belgium, Germany, Hungary, Italy, Poland, Slovakia, and Turkey. H04. It is well know that radar and rain gauge rainfall estimation is influenced by several error sources that should be carefully handled and characterized before using these data as reference for ground validation of any satellite-based precipitation products.

In this chapter a description of the ground data available in the PPVG is reported country by country. chapter has the object to provide ground data information and to highlight their error sources

4.2 Ground data in Belgium (IRM)

Radar Data

The network

Belgium is well covered with three radars (see Figure 9). Further radar is currently under construction in the coastal region.

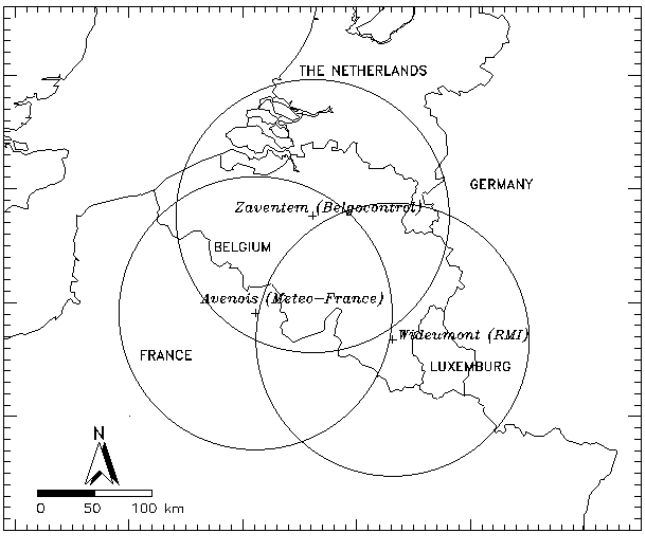

Figure 9 Meteorological radar in Belgium

The instruments

These are Doppler, C-band, single polarization radars with beam width of 1° and a radial resolution of 250 m. Data are available at 0.6, 0.66 and 1 km horizontal resolution for the Wideumont, Zaventem and Avesnois radars respectively.

In this report, only the Wideumont radar has been used. The data of this radar are controlled in three steps.

Data processing

First, a long-term verification is performed as the mean ratio between 1-month radar and gauge accumulation for all gauge stations at less than 120 km from the radar. The second method consists in fitting a second order polynomial to the mean 24 h (8 to 8 h local time) radar / gauge ratio in dB and the

range; only the stations within 120 km and where both radar and gauge values exceed 1 mm are taken into account. The third method is the same as the second but is performed on-line using the 90 telemetric stations of the SETHY (Ministry of the Walloon Region). Corrected 24 h images are then calculated. New methods for the merging of radar and raingauge data have been recently evaluated (Goudenhoofdt and Delobbe 2009)[1].In this report, only instantaneous radar images are used.

4.3 Ground data in Germany (BfG)

The H-SAF products are validated for the territory of Germany by use of two observational ground data sets: SYNOP - precipitation data based on the network of synoptical stations, provided by the German Weather Service (DWD) and RADOLAN-RW - calibrated precipitation data based on the radar network of DWD and calibrated by DWD by use of measurements at precipitation stations.

Data	Number/Resolution	Time interval	Delay	Annotation
Synoptical stations	~ 200	6h / 12h	Near-real-time	
Precipitation stations	~ 1100	hourly	Near-real-time	Automatic precipitation stations
RADOLAN RW	16 German radar sites, ~1 km x ~1 km	1 hour,	Near-real-time	Quantitative radar composite product RADOLAN RW (Radar data after adjustment with the weighted mean of two standard procedures)

Table 7 Precipitation data used at BfG for validation of H-SAF products

Rain gauge

The network

The data used are compiled from ~1300 rain gauges. About 1000 are operated by DWD while about 300 are operated by other German authorities. The average minimum distance between stations is 17 km.

The instruments

The measurement instruments are precipitation sensors OTT PLUVIO of Company Ott[2] [3]. They continually and precisely measure quantity and intensity of precipitation in any weather, based on balance principle with temperature compensation (heated funnel) and by an electronic weighing cell. The absolute measuring error is less than 0.04 mm for a 10 mm precipitation amount and the long-term (12months) stability is better than 0.06 mm. The operating temperature ranges from –30°C to +45°C. The minimum detected quantity (sensitivity) is 0,05 mmh^{-1}. The maximum possible measured rain rate is 3000 mmh^{-1}. The operational accumulation interval theoretically is one minute.

The data processing

[1] Goudenhoofdt E. and L. Delobbe, 2009: "Evaluation of radar-gauge merging methods for quantitative precipitation estimates". *Hydrol. Earth Syst. Sci.,* 13, 195-203.

[2] http://www.ott.com/web/ott_de.nsf/id/pa_ottpluvio2_vorteile.html?OpenDocument&Click=

[3] **Precipitation amount and intensity measurements with the Ott Pluvio, Wiel Wauben, Instrumental Department, INSA-IO, KNMI, August 26, 2004**

Continuous, automatic measurement of liquid and solid precipitation data are collected, accumulated (intervals: from 1hour until 1day) and provided as SYNOP tables by DWD. These data are error corrected and quality controlled in four steps with checks of completeness, climatologic temporal/spatial consistency and marginal checks.

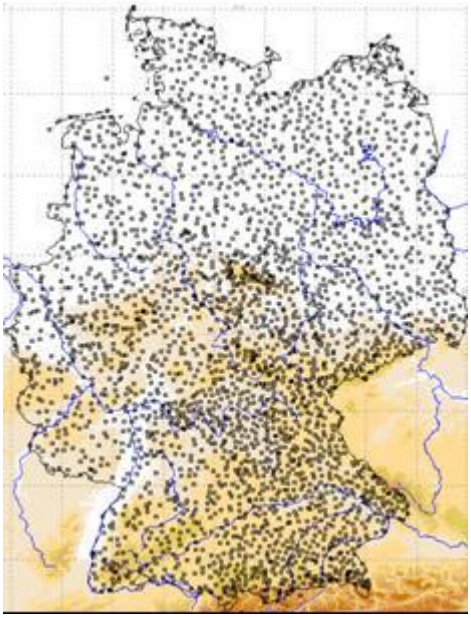

Figure 10 (left): Network of rain gauges in Germany - Figure 11 (right): Pluvio with Remote Monitoring Module

Radar data

Radar-based real-time analyses of hourly precipitation amounts for Germany (RADOLAN) is a quantitative radar composite product provided in near-real time by DWD. Spatial and temporal high-resolution, quantitative precipitation data are derived from online adjusted radar measurements in real-time production for Germany. Radar data are calibrated with hourly precipitation data from automatic surface precipitation stations. [4]

The combination of hourly point measurements at the precipitation stations with the five-minute-interval radar signals of the 16 weather radars (C-Band Doppler) provides gauge-adjusted hourly precipitation sums for a ~1km x ~1km raster for Germany in a polar stereographic projection.

Radar site	Latitude (N)	Longitude (E)	WMO No.	Radar site	Latitude (N)	Longitude (E)	WMO No.
München	48° 20’ 14’’	11° 36’ 46’’	10871	Rostock	54° 10’ 35’’	12° 03’ 33’’	10169
Frankfurt	50° 01’ 25’’	08° 33’ 34’’	10630	Ummendorf	52° 09’ 39’’	11° 10’ 38’’	10356
Hamburg	53° 37’ 19’’	09° 59’ 52’’	10147	Feldberg	47° 52’ 28’’	08° 00’ 18’’	10908
Berlin-Tempelhof	52° 28’ 43’’	13° 23 17’’	10384	Eisberg	49° 32’ 29’’	12° 24’ 15’’	10780
Essen	51° 24’ 22’’	06° 58’ 05’’	10410	Flechtdorf	51° 18’ 43’’	08° 48’ 12’’	10440
Hannover	52° 27’ 47’’	09° 41’ 54’’	10338	Neuheilenbach	50° 06’ 38’’	06° 32’ 59’’	10605
Emden	53° 20’ 22’’	07° 01’ 30’’	10204	Türkheim	48° 35’ 10’’	09° 47’ 02’’	10832
Neuhaus	50° 30’ 03’’	11° 08’ 10’’	10557	Dresden	51° 07’ 31’’	13° 46’ 11’’	10488

Table 8 Location of the 16 meteorological radar sites of the DWD

4 http://www.dwd.de/bvbw/appmanager/bvbw/dwdwwwDesktop?_nfpb=true&_windowLabel=dwdwww_main_book&T14609949251144921180881gsbDocumentPath=Navigation%2FWasserwirtschaft%2FUnsere__Leistungen%2FRadarniederschlagsprodukte%2FRADOLAN%2Fradolan__node.html%3F__nnn%3Dtrue&switchLang=en&_pageLabel=_dwdwww_spezielle_nutzer_forschung_fkradar

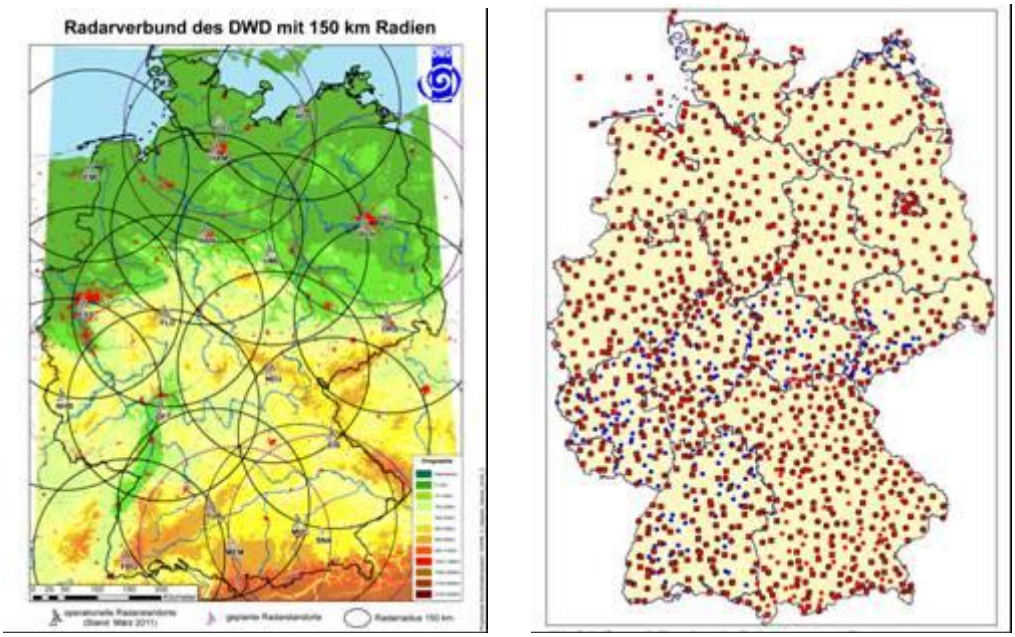

Figure 12 (left): radar compound in Germany (March 2011) ; Figure 13 (right): location of ombrometers for online calibration in RADOLAN; squares: hourly data provision (about 500), circles: event-based hourly data provision (about 800 stations)5.

The flowchart of online calibration method applied in RADOLAN is depicted in Figure 14

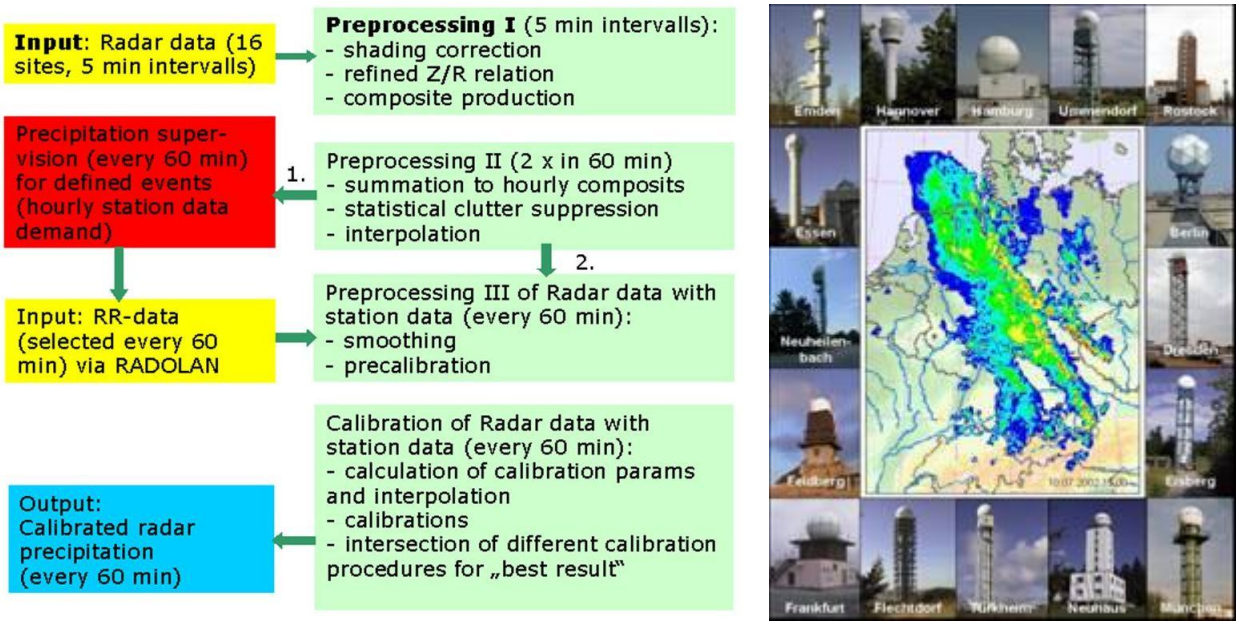

Figure 14 Flowchart of online calibration RADOLAN (DWD, 2004)

4.4 Ground data in Hungary (OMSZ)

Radar data

The network

[5] Bartels, H.: Projekt RADOLAN. Routineverfahren zur Online-Aneichung der Radarniederschlagsdaten mit Hilfe von automatischen Bodenniederschlagsstationen (Ombrometer), Abschlussbericht 2004

The main data used for validation in Hungary would be the data of meteorological radars. There are three C-band dual polarized Doppler weather radars operated routinely by the OMSZ-Hungarian Meteorological Service. The location and coverage of the three Hungarian radars are shown in Figure 15; the measurement characteristics are listed in Table 9.

All three radars are calibrated periodically, with an external (calibrated) TSG, the periodicity is kept every 3 months.

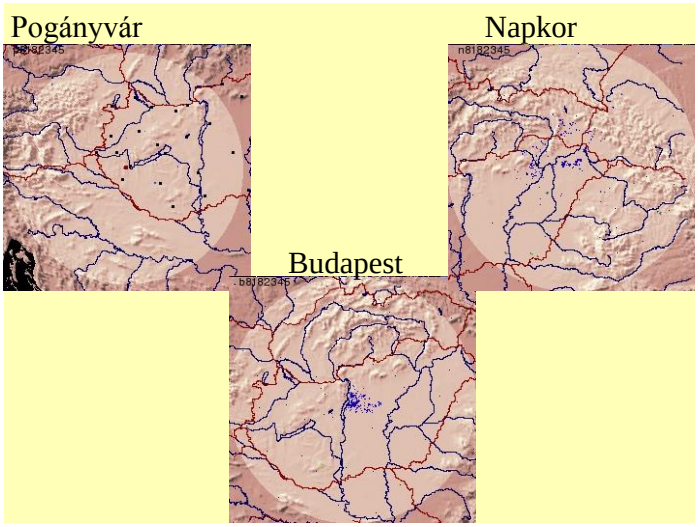

Figure 15 The location and coverage of the three meteorological Doppler radars in Hungary

Year of installation	Location	Radar type	Parameters measured
1999	Budapest	Dual-polarimetric Doppler radar	Z, Z_{DR}
2003	Napkor	Dual-polarimetric Doppler radar	Z,Z_{DR},K_{DP},Φ_{DP}
2004	Poganyvar	Dual-polarimetric Doppler radar	Z,Z_{DR},K_{DP},Φ_{DP}

Table 9 Main characteristics of the Hungarian radar network

The instruments

The Hungarian radar network is composed by three Doppler radars, which are measuring in the C-band, mainly at same frequencies. The scan strategy is the same for all the radars, the Budapest radar has a resolution lower than the two other radars which are newer types. The parameters of the instruments and the measurement campaigns are listed in Table 10

	Budapest	Napkor	Poganyvar
Frequency band	C-Band, 5625MHz	C-Band, 5610MHz	C-Band, 5610MHz
Polarization (Single/Double)	single	single	single
Doppler capability (Yes/No)	Yes	Yes	Yes

Scan strategy: elevations, maximum nominal range distance, range resolution	scan freq: 15 min Elevaions(deg): 0 0.5 1.1 1.8 2.7 3.8 5.1 6.6 8.5 Range 240 Km Resolution:500m	scan freq: 15 min Elevaions(deg): 0 0.5 1.1 1.8 2.7 3.8 5.1 6.6 8.5 Range 240 Km Resolution:250m	scan freq: 15 min Elevaions(deg): 0 0.5 1.1 1.8 2.7 3.8 5.1 6.6 8.5 Range 240 Km Resolution:250m

Table 10 Characteristics of the three radar instruments in Hungary

The data processing

Radar measurements are influenced by many error sources that should be minimized as much as possible. As such, in case of the Hungarian radar data many correction methods are applied, or planned to be applied int he near future to filter out false radar reflectivity measurements. Clutter removal, and WLAN filter is already implemented int he processing chain of all three radar data; and a filter to disregard signals below 7dBz is also applied because in general, these data is not coming from real rain drops, but false targets.

According to experiences, beam blockage can result in serious underestimation of precipitation amounts (e.g. behind the Börzsöny mountains at the north of Budapest). So the bleam blockage correction is planned to be implemented during year 2012. Also, the attenuation correction (the attenuation of electromagnetic waves in water environment, water drops) is planned for 2012. Hungary does not apply VPR (Vertical Profile Reflectivity) correction.

Precipitation intensity is derived from radar reflectivity with the help of an empirical formula, the Marshall-Palmer equation (R=a*Z^b, where a=200, b=1.6). From the three radar images a composite image over the territory of Hungary is derived every 15 minutes applying the maximum reflectivity in one column method, in order to make adjustments in overlapping regions.

Description of instantaneous and accumulated radar product used in HSAF Validation Activities

Rain gauge correction

The non-corrected precipitation field can be corrected by rain gauge measurements. In Hungary, we do not make corrections to instantaneous 15 minutes radar data. In our institute, we only use a correction for the total precipitation for 12 and 24 hour periods.

For the 3h and 6h accumulated products, we use a special method to accumulate rainfalls: we interpolate the 15-minutes measurements for 1-minute grid by the help of displacement vectors also measured by the radar, and then sum up the images which we got after the interpolation. It is more precise especially when we have storm cells on the radar picture, because a storm cell moves a lot during 15 minutes and thus we do not get continuous precipitation fields when we sum up only with 15.minutes periods. This provides satisfying results. However, there is still a need for rain-gauge adjustment because there are obviously places (behind mountains) that the radar does not see.

The radars are corrected with rain gauge data every 12 hours. The correction method using rain gauge data for 12 hour total precipitation consists of two kinds of corrections: the spatial correction which becomes dominant in the case of precipitation extended over a large area, whereas the other factor, the distance correction factor prevails in the case of sparse precipitation. These two factors are weighted according to the actual situation. The weighting factor depends on the actual effective local station density, and also on the variance of the

differences of the bias between radar and rain gauge measurements. On the whole, we can say that our correction method is efficient within a radius of 100 km from the radar. In this region, it gives a final underestimation of about 10%, while at bigger distance; the underestimation of precipitation fields slightly increases. Besides, we also produce 12 hour total composite images: first the three radar data are corrected separately, and then the composite is made from them. The compositing technique consists of weighting the intensity of each radar at a given point according to the distance of the given point from the radars. This is also true for the 24-hourly accumulations.

Resolution, projection, threshold of detection

The resolution of the radar data used for validation is 2km by 2km. This is true for the accumulated and the instantaneous products as well. As We have already mentioned, the threshold of detection in Hungary is 7dB. Hungarian radar data is available operationally in stereographic (S60) projection.

References

Péter Németh: Complex method for quantitative precipitation estimation using polarimetric relationships for C-band radars. Proceed. of 5th European Radar Conference (ERAD), Helsinki (Finland) (http://erad2008.fmi.fi/proceedings/extended/erad2008-0270-extended.pdf)

4.5 Ground data in Italy (DPC, Uni Fe)

Rain gauge

The network

The maximum number of available raingauges is about 1800, irregularly distributed over the surface. On the average, however, a number of stations have low quality data, failure or data transmission problems and their data are missing (-9999 recorded). This number of no data stations is highly varying on hourly/daily basis and ranges from few units to a hundred. In case of data acquired but not transmitted/recorded, the first transmitted measure is the cumulated value over the time when the data were not transmitted.

The average minimum distance between closest stations is about 9.5 km, with a very high variance: in some regions (such as Tuscany in central Italy) it is below 5 km, while in Emilia Romagna (Po Valley) it is more than 20 km. A study of the decorrelation distance between stations as function of the mutual distance has been carried out for the 2009 dataset. The decorrelation distance is defined as the minimum distance between two observations that makes the Pearson correlation coefficient between the two measures decrease below e^{-1}. Results are shown in next figure, where the decorrelation distance is plotted as function of the distance between stations. It appears that there is a large variability of this parameter from higher values (around 60 km for cold months when large precipitating systems dominate and reduces to roughly 10 km when small scale convection is more likely to occur (warm months).
This points out that the distribution of gauges could be able to describe the spatial structures of precipitation fields in case of wintertime rainfall, while may be inadequate for spring/summer convective events.

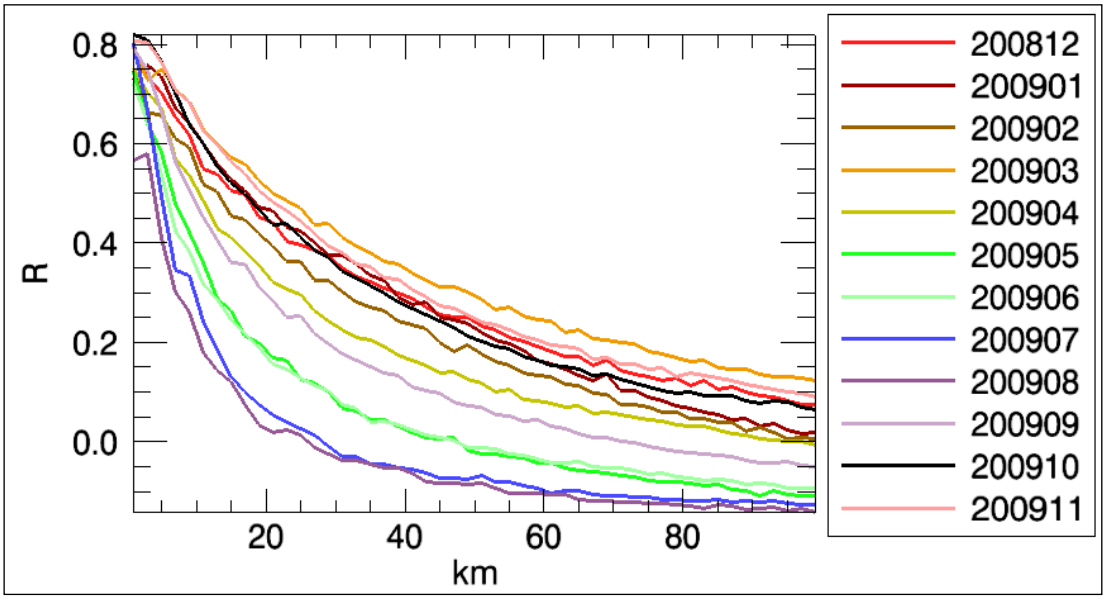

Figure 16 Correlation between rainrates detected by two close by stations as function of the distance between the two stations. Colors refer to the month along 2009

In following figure the distribution of working stations over Italy is shown for a given day.

Figure 17 Distribution of the raingauge stations of the Italian network collected by DPC.

The instruments

The following information should be provided in this section:

- All the available raingauge are of tipping bucket type;
- Most of the raingauge have a minimum detected quantity of 0.2 mm, others have 0.1 mm.
- The maximum rainrate that can be measured by the gauges ranges between 300 and 500 mm^{-1} over one minute, depending on the manufacturer.

The rainrate is measured over different cumulation intervals by the different local administrations managing the network, but the data disseminated are all integrated over 60 minutes.

At the moment, the National network made available by DPC provides only hourly data, Shorter cumulation times could be available for case studies after specific agreements with local management authorities.

Only a small subset (about 300 stations) of gauges have heated funnel, especially in alpine regions (such as Valle d'Aosta and Piedmont), and this is a clear source of errors in both summer (due to hailfall) and in autumn/winter (due to snowfall).

The data processing

No quality control is performed on the data right now.

In this Project the point-like gauges data are interpolated by using the Barnes method (Barnes, 1964; Koch et al, 1983) widely used to interpolate station data. It works by defining a regular output grid (5x5 km in our case) and a "radius of influence" of each station (in our case it was 10 km). The point information from a raingauge is "spread" in the neighbour by an exponential function, limited by the influence radius, and the rainfall value for each grid-point is computed as the contribution of all the closest measurements.
The resulting grid is a 5x5 km regular grid with 240 columns and 288 lines. Moreover, a Digital elevation model is used to provide a mask of Italy in order to: 1) screen out sea-pixels too far from the coastlines and 2) process the pixels with the elevation above sea level.

Radar data

The network

The Italian Department of Civil Protection (DPC) is the authority leading the national radar coverage project in order to integrate the pre-existent regional systems. Currently, the radar network is composed by 20 systems, most of them with dual-polarization. The network is composed by 8 C-band fixed regional installations (five of them are polarimetric), two systems owned by the Italian company for air navigation services (ENAV), 8 dual-polarization systems managed by DPC (6 using C-band and 2 X-band).
The image 21 shows the spatial radar coverage of the Italian territory.

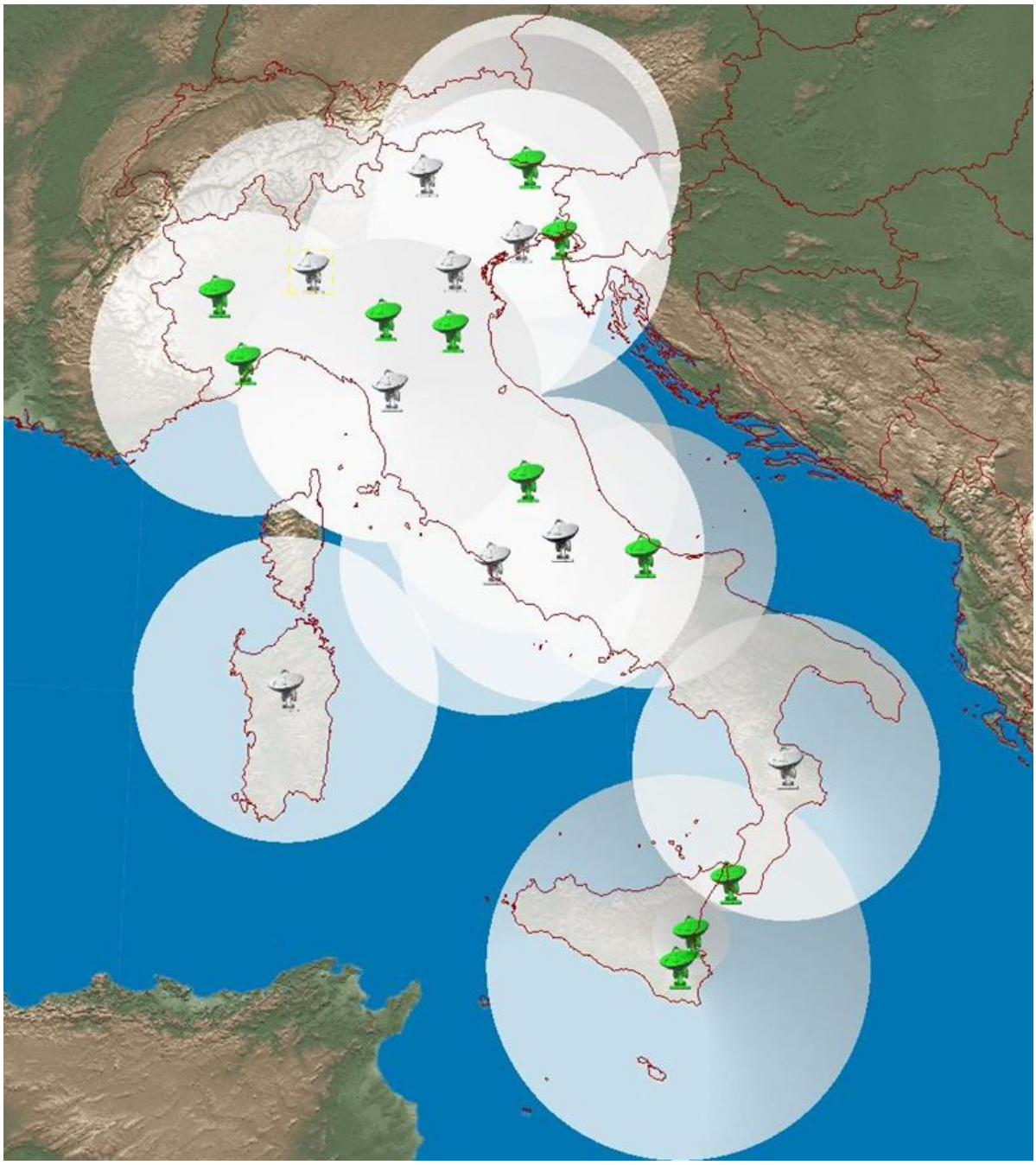

Figure 18 Italian radar network coverage. The green and grey radar symbol stands for dual- and single-polarization system, respectively.

Radar Data processing

The operational radar processing chain, currently under testing within the H-SAF project, is briefly described in this section.
It aims at compensating or at least identifying most of the uncertainty sources conditioning the radar rainfall estimation process (Friedrich et al., 2006). Among them, the following error sources are primarily considered: contamination by non-weather returns (clutter), Partial Beam Blocking (PBB), beam broadening at increasing distances, vertical variability of precipitation (Germann and Joss, 2002; Joss and Lee, 1995; Marzano et al., 2004) and rain path attenuation (Bringi and Chandrasekar, 2001; Carey et al., 2000; Testud et al., 2000; Vulpiani et al., 2008). Every error source is quantified through specific tests ending with the estimation of specific (partial) quality matrices and, when possibile, is compensated for. The overall data quality (Q) is then obtained as a combination of the partial quality matrices. The quality model described in Rinollo et al. (2013) is embedded within the overall processing chain schematically depicted in Figure 24.
In this schematic representation, the sequential flow among consecutive computational steps is specified by black arrows, while the blue ones identify the data input (or output) to (or from) a specific processing module.
The processing chain can be summarized through the following few steps as follows:

i. As typical, the raw volumetric data must be first filtered from non-weather returns. This step is here achieved using the fuzzy-logic approach proposed in Vulpiani et al. (2012) for polarimetric radar systems.
ii. The next step is the correction for Partial Beam Blocking (PBB) based on the retrieved 3-D cocclusion map (Bech et al., 2003) that, assuming the e.m. waves propagate in a standard atmosphere, is evaluated only once for a given radar scanning strategy.
iii. The rain path attenuation is just qualitatively evaluated in case the considered radar system has single-polarization capability (Rinollo et al., 2013), otherwise it is compensated for by means of the differential phase shift that needs to be preliminarly processed. In this framework, the iterative moving-window range derivative approach proposed in Vulpiani et al. (2012) is applied here.
iv. The range-related deterioration of radar data quality is modeled through a non-linear function as in Rinollo et al. (2013).
v. Once the attenuation is evaluated and, eventually, compensated for through the so-called ZPHI method (Testud et al., 2000), the overall data quality is computed as geometric mean of the partial quality matrices.

$$Q = q_{clutter} \cdot q_{vertical} \cdot q_{PBB} \cdot q_{distance} \cdot q_{attenuation}$$

vi. The retrieved mean Vertical Profile of Reflectivity (VPR) is applied to the entire volumetric scan with the aim to use all the observations along the vertical to retrieve the surface rainfall rate. All the clutter-filtered and attenuation-corrected (if applicable) PPIs are projected at ground by means of the average Vertical Profile of Reflectivity (VPR).

vii. The Surface Rainfall Intensity (SRI) map is computed as a quality-weighted average of each rain rate map, obtained by each ground-projected reflectivity sweep (Vulpiani et al., 2014).

viii. The SRI composite is built by combining the single-radar rainfall maps through a squared-quality-weighted approach. In case of dual-polarization systems, the composite rainfall retrieval algorithm proposed in Vulpiani and Baldini (2013)

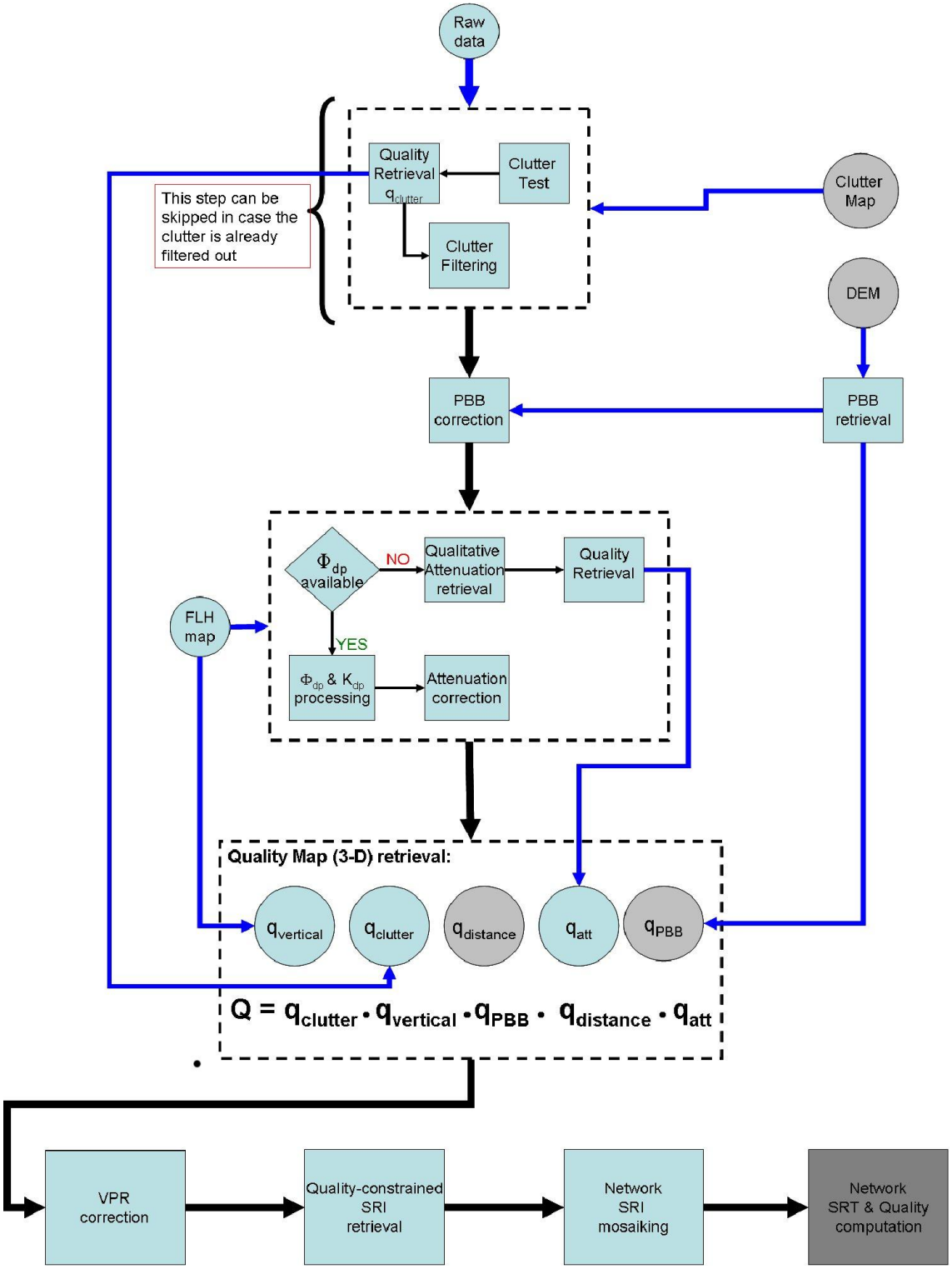

Figure 19 Schematic representation of the Italian radar data processing chain.

References

Bech, J., B. Codina, J. Lorente, and D. Bebbington, 2003: The sensitivity of single polarization weather radar beam blockage
correction to variability in the vertical refractivity gradient. J. Atmos. Oceanic Technol., 20, 845–855.
Bringi, V. N. and V. Chandrasekar, 2001: Polarimetric doppler weather radar. Cambridge University Press, 636 pp.
Carey, L. D., S. A. Rutledge, and D. A. Ahijevych, 2000: Correcting propagation effects in c-band polarimetric radar observations of tropical convection using differential propagation phase. J. Appl. Meteor., 39, 1405–1433.
Friedrich, K., M. Hagen, and T. Einfalt, 2006: A quality control concept for radar reflectivity, polarimetric parameters, and doppler velocity. J. Atmos. Ocean. Tech., 23, 865–887.
Germann, U. and J. Joss, 2002: Mesobeta profiles to extrapolate radar precipitation measurements above the alps to the ground level. J. Appl. Meteorol., 41, 542–557.
Joss, J. and R. Lee, 1995: The application of radar-gauge comparisons to operational precipitation profile corrections. J. Appl. Meteorol., 34, 2612–2630.
Rinollo, A., et al., 2013: Definition and impact of a quality index for radar-based reference measurements in the h-saf precipitation product validation. Nat. Hazards Earth Syst. Sci., 13, 1–11.
Testud, J., E. L. Bouar, E. Obligis, , and M. Ali-Mehenni, 2000: The rain profiling algorithm applied to polarimetric weather radar. J. Atmos. Oceanic Technol., 17, 332–356.
Vulpiani, G. and L. Baldini, 2013: Observations of a severe hail-bearing storm by an operational X-band polarimetric radar in the mediterranean area. Proceed. of the 36th AMS Conference on Radar Meteorology, Breckenridge, CO, USA.
Vulpiani, G., M. Montopoli, L. D. Passeri, A. Gioia, P. Giordano, and F. S. Marzano, 2012: On the use of dual-polarized C-band radar for operational rainfall retrieval in mountainous areas. J. Appl. Meteor and Clim., 51, 405–425.
Vulpiani, G., P. Tabary, J. P. D. Chatelet, and F. S. Marzano, 2008: Comparison of advanced radar polarimetric techniques for operational attenuation correction at c band. J. Atmos. Oceanic Technol., 25, 1118–1135.
Vulpiani, G., A. Rinollo, S. Puca, m. Montopoli, 2014: A quality-based approach for radar rain field reconstruction and the H-SAF precipitation products validation. The eighth European Radar conference on radar in meteorology and hydrology. Garmish-Partenkirken (Germany) 1-5 Sept., 2014 ,

4.6 Ground data in Poland (IMWM)

Rain gauge

The network

The maximum number of rain gauges in the Polish ATS (Automatic Telemetric Station) national network is 950. Each ATS post is equipped with two independent rain gauges of the same sort. One of them is heated during the winter period and the other one is not. Therefore precipitation information is derived from 475 points at the time. Fact that rainfall is measured by two equally sensitive instruments two meters away from each other at the same post, enables to apply simple in situ data quality control during summertime. During winter non-heated rain gauge is covered with a cup to prevent it from being clogged by the ice and damaged. Because of that the precipitation information derived from ATS network in winter cannot be verified using this method. It can be stated that during the wintertime precipitation information might be bPR-RMSEened by a slightly bigger measuring error.

The number of rain gauges available for H-SAF validation activities varies from day to day due to operational efficiency of ATS network in Poland and depends on large number of independent factors. It can be stated that the number varies between 330 and 475 rain gauges for each day of operational work.

Mean minimum distance between precipitation measuring ATS posts (between each pair of rain gauges) in Polish national network is 13,3 km.

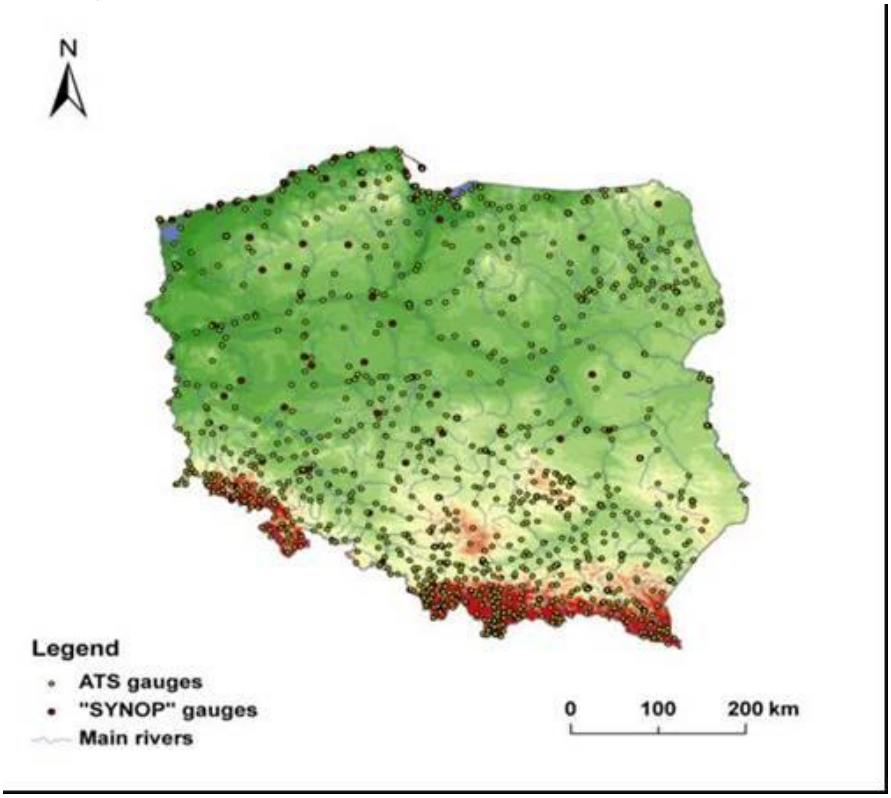

Figure 20 ATS national network in Poland

The instruments

All rain gauges working within Polish ATS national network are MetOne tipping bucket type instruments. Minimum detected quantity that can be measured by those rain gauges is 0,1 mm/h which means that each tilt of rain gauge bucket adds 0,1mm to the total sum of the measured precipitation. During very heavy precipitation events MetOne rain gauges tend to underestimate real precipitation by factor of 10%. Maximum measured rainrate *(mmh^{-1})* by MetOne instruments in Poland was recorded in 5.06.2007 at ATSO Koscielisko Kiry at the foot of Tatra Mountains. The recorded values reached 65 mm/h. Operational cumulation interval *(min)* of ATS network rain gauges is set for

10 minutes and can be adjusted according to given needs. There is possibility to have very short cumulation intervals for case studies - theoretically 1 minute - but not on every given precipitation post. It depends on local DCS settings.

The data processing

As stated above the data quality control can be achieved by comparison on two rainfall datasets collected by two independent rain gauges at the same ATS post. It is done operationally during summertime. There is no such possibility during the winter because of lack of non-heated rain gauge dataset. In case that one pair of rain gauges at the same ATS post provide two different rainfall readings the higher one is taken into account.

No specialization technique is used for standard validation process. However, for some case studies, the Natural Neighbor technique is applied for satellite and ground precipitation data. To match the precipitation information with satellite data spatial and temporal matching are applied.

- Spatial matching: for each given satellite pixel, the posts situated within that pixel were found. The pixel size was taken into account, however, its shape was assumed to be rectangular. If more than one rain gauge were found within one satellite pixel, the ground rain rate value was calculated as a mean of all rain gauges measurements recorded within that pixel;
- Temporal matching: satellite derived product is combined with the next corresponding ground measurement. As the ground measurements are made with 10 minute time resolution, the maximum interval between satellite and ground precipitation is 5 minutes.

4.7 Ground data in Slovakia (SHMÚ)

Rain gauge

The network

In Slovakia there are overall 98 automatic rain gauge stations potentially available for the H-SAF project. The real number of usable gauges varies with time because on average about 20 of them are out of operation.

Mean minimum distance between rain-gauges in the complete network is 7,74 km. Map of the rain gauge network in Slovakia containing also climatological and selected hydrological stations is shown in next figure.

Figure 21 Map of SHMÚ rain gauge stations: green – automatic (98), blue – climatological (586), red - hydrological stations in H-SAF selected test basins (37)

The instruments

Type of all the automatic rain gauges is tipping bucket (without heating of the funnel). The gauges are able to measure precipitation rates ranging from 0,1 to 200 mm/h at 10 min operational accumulation interval. Shorter accumulation interval of 1 min is also possible which makes the instruments suitable for case studies in the H-SAF project.

The data processing

The rain gauge data are not used at SHMÚ directly for the H-SAF precipitation validation but they are utilized as the input to the INCA precipitation analysis system which is supposed to become a new validation tool. Prior the INCA analysis the rain gauge data are interpolated onto the regular 1x1 km grid using the inverse-distance-squared (IDS) interpolation method. Only the 8 nearest rain gauge stations are taken into account in the interpolation in order to reduce occurrence of precipitation bull-eyes artifact.

SHMÚ performs the offline automatic and manual quality check of the rain gauge data. In frame of the INCA system a quality control technique called blacklisting has been developed which avoids the data from systematically erroneous rain gauges to enter the analysis. Currently the blacklisting is used in manual mode only.

Radar data

The network

The Slovak meteorological radar network consists of 2 radars (see next figure). One is situated at the top of Maly Javornik hill near city Bratislava and second one is on the top of Kojsovska hola hill close to the city Kosice. Both are Doppler, C-band radars; the newer one at Kojsovska hola is able to measure also the dual polarization variables (non-operational).

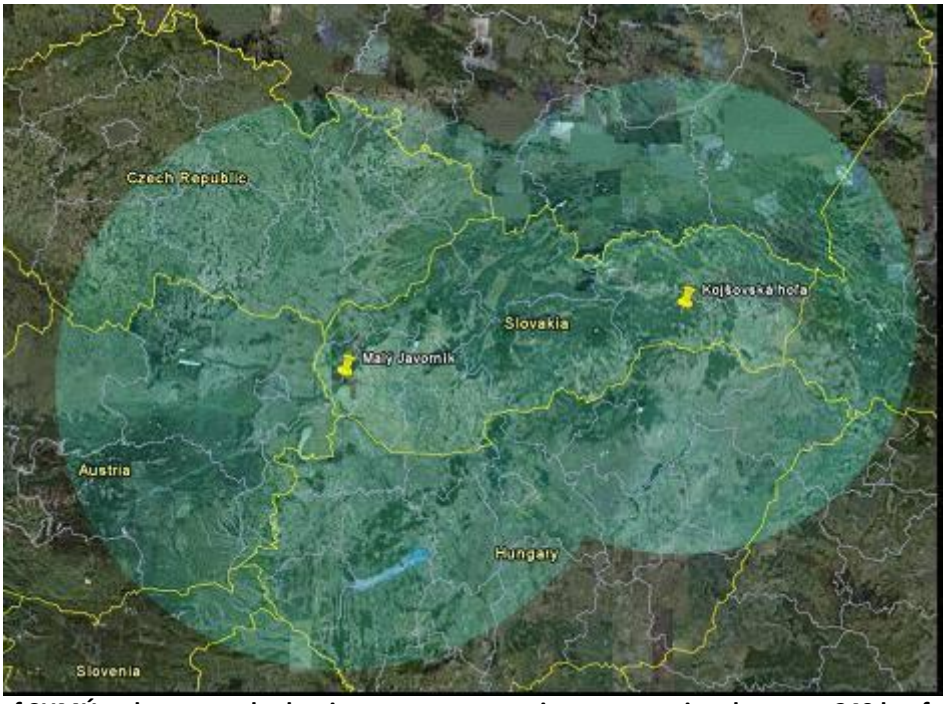

Figure 22 Map of SHMÚ radar network; the rings represent maximum operational range – 240 km for radar at Maly Javornik (left), 200 km for radar at Kojsovska hola (right)

The instruments

The radars are operated and technically maintained by SHMÚ. Receivers of radars are calibrated regularly by means of internal test signal generator (TSG). In case of radar at Maly Javornik calibration is performed every 3 months and in case of radar at Kojsovska hola every 1 month.

The basic parameters of both SHMÚ radars are summarized in following table.

	Maly Javornik	Kojsovska hola
Frequency band	C-Band, 5600 MHz	C-Band, 5617 MHz
Polarization (Single/Double)	Single	Double (but so far only single pol. products generated)
Doppler capability (Yes/No)	Yes	Yes
Scan strategy: scan frequency, elevations, maximum nominal range distance, range resolution	Scan frequency: 5 min Elevations (deg): 0.2 0.7 1.4 2.5 3.8 5.4 7.3 9.5 13.0 17.0 25.0 Range: 240 Km Resolution: 1000m	Scan frequency: 5 min Elevations (deg): -0.5 0.0 0.5 1.0 1.5 2.5 4.0 6.0 10.0 20.0 Range: 200 Km Resolution: 125m

Table 11 Characteristics of the SHMÚ radars

The data processing

For ground clutter removal the Doppler filtering is used. In case of radar at Maly Javornik the frequency-domain IIR filter is used, at Kojsovska hola the Doppler filtering is supplemented with moving target

identification (MTI) technique. Isolated radar reflectivity and Doppler velocity bins are removed by the Speckle removal filter. The data with signal to noise ratio below the specified threshold are also eliminated. The measured radar reflectivity is corrected for atmospheric (clear-air) attenuation of the radar beam.
Neither beam blocking correction nor vertical profile of reflectivity (VPR) is applied at SHMÚ. However implementation of the beam blocking correction is being considered for the H-SAF validation due to complicated orographical conditions in Slovakia.

Precipitation intensity is derived from radar reflectivity according to the Marshall-Palmer equation (Z=a*R^b) with constant coefficients valid for stratiform rain (a=200, b=1.6). Polarimetric techniques for quantitative precipitation estimation in case of dual polarization radar at Kojsovska hola are not used because the measured polarimetric data are not operational (calibration would be required).
Software filter for the RLAN interference detected by radars is currently in development at SHMÚ.

Radar composite based on CAPPI 2 km products from both radars is used for the H-SAF validation. The composition algorithm used selects the higher value measured by the two radars in the overlapping area.
No raingauge correction of the derived instantaneous precipitation is applied. Effect of elevating radar beam with increasing range and beam attenuation is reduced by limiting the validation area to rain effective range of 120 km for both radars in the composite.
The instantaneous precipitation products are provided in Mercator projection with approximately 1 km resolution. Threshold for precipitation detection is 0,02 mm/h. Time resolution of the current instantaneous products is 5 minutes, for the products prior to April 2010 it was 10 minutes and prior to August 2009 15 minutes.
Precipitation accumulation in case of 3-hourly interval is based on integration of 5 (10 or 15) minutes instantaneous measurements in time period of 3 hours. Accumulated precipitation for intervals of 6, 12 and 24 hours is calculated as a sum of the 3-hourly accumulated precipitation. At least 92% of instantaneous measurements must exist in relevant time period for the 3-hourly accumulated product to be produced.
No rain gauge correction of the accumulated precipitation is applied but the same limitation of validation area is used as for the instantaneous product. Threshold for precipitation detection of the 3-hourly accumulated product is 0,5 mm. Geographical projection and space resolution of the accumulated products are the same as those of instantaneous product (see above).

For validation of H-SAF precipitation products it is necessary to know errors distribution of used ground truth data – in case of SHMÚ it is precipitation intensity and accumulated precipitation measured by Slovak radar network. For this purpose a study called “SHMU study on evaluation of radar measurements quality indicator with regards to terrain visibility” has been elaborated. To find distribution of errors in radar range next steps had to be done:

- simulations of terrain visibility by radar network using 90m digital terrain model
- statistical comparison of radar data against independent rain gauge data measurements
- derivation of dependence (regression equation) describing the errors distribution in radar range with regard to terrain visibility, based on rain gauge and radar data statistical evaluation computation of error distribution maps using regression equation and terrain visibility

Main results of this study are shown in next figure. It is evident that the best visibility of SHMU radars corresponds to the lowest PR-RMSE-RMSE of 60% displayed by light violet colors. PR-RMSE-RMSE is of quite homogeneous distribution with average of 69% in prevalent lowlands of Slovakia displayed by bluish colors. But in central and north-west mountainous areas this error exceeds 100%.

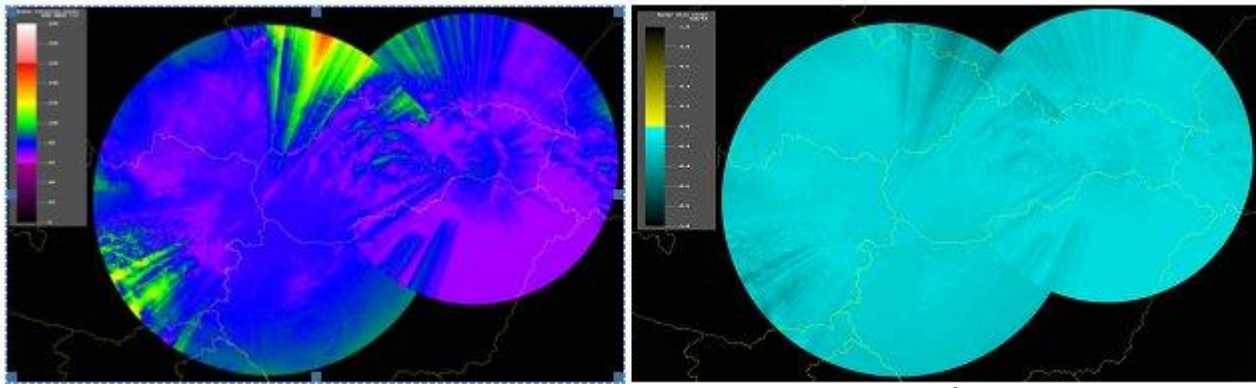

Figure 23 Map of relative RMSE (left) and Mean Error (right) over the SHMÚ radar composite

Similar studies that have been carried out in the PPVG on comparison of radar data with rain gauge data have shown in general that RMSE error associated with radar fields depends considerably on radar minimum visible height above the rain gauge especially in mountainous countries. In lowlands this dependence is not so significant, but no negligible. The reason can be the location of radar sites at the top of hills and impossibility of the lowest elevation to reach the lowland's surface. In case of Slovakia The PR-RMSE-RMSE error of radar accumulated fields is between 60-90%, with an average PR-RMSE-RMSE value of 69,3%. Mean Error specified for 24-hours cumulated precipitation is -4,42mm or converted into instantaneous precipitation -0,184 mm/h. RMSE specified for 24-hours cumulated precipitation is 9,48mm or converted into instantaneous precipitation 0,395 mm/h.

Complete SHMU study is available on the H-SAF ftp server:
/hsaf/WP6000/WP6100/precipitation/WG_groups/WG2-radar/WG-2-3_radar quality indication_v1.doc

4.8 Ground Data in Turkey

Rain gauge

The network

356 Automated Weather Observation Station (AWOS) distributed over the country are used for the validation of the satellite precipitation products in the HSAF project. The average distance between the AWOS sites is 40.5 km.

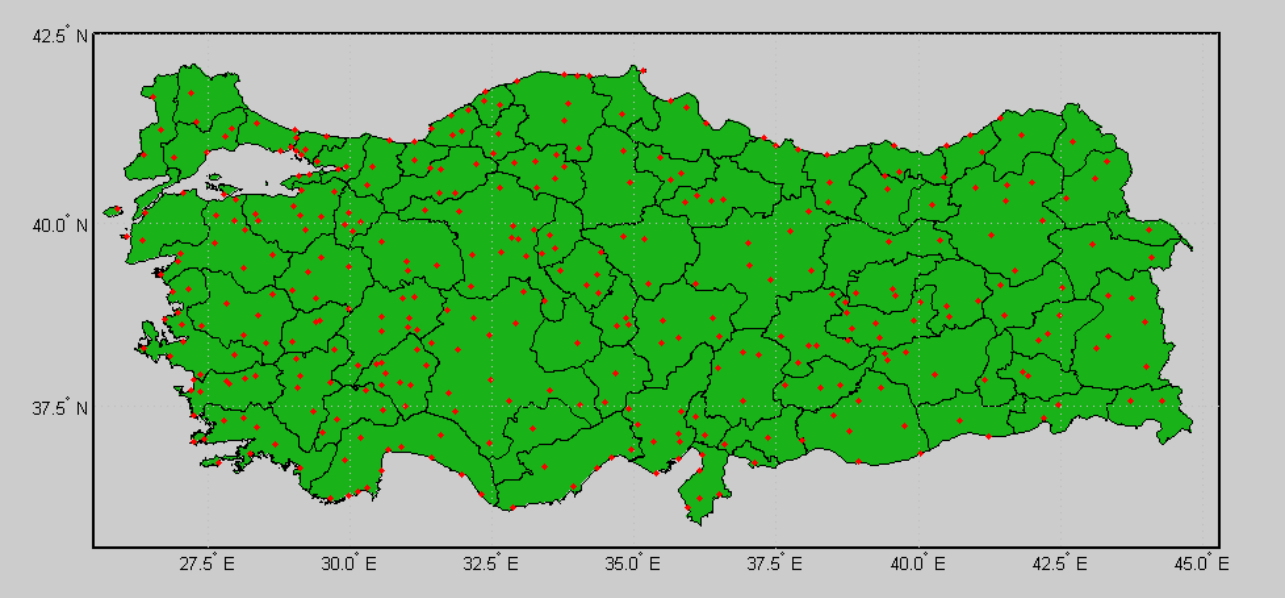

Figure 33 Map Turkish rain gauge stations

The instruments

The gauge type of the network is tipping bucket where each has a heated funnel. The minimum detection capability of the gauge is 0.2 mm per tip. In the maximum capacity of the instrument is 720 mm/h at most. The operational accumulation interval is 1 minute, so that alternative cumulation intervals such as 5, 10, 20, 30 minutes are possible.

Data processing

Quality control

High quality of the ground data is critical for performing the validation of the precipitation products. The validation results or statistics can provide meaningful feedbacks for the product developers and additionally the products can be used reliably only if there is a confidence present about the ground data at a certain level. For this reason, some predefined quality assurance (QA) tests are considered for the precipitation data in order to define the confidence level. First of all, a flagging procedure is defined as described in next table

QA Flag Value	QA Status	Brief Description
0	Good	Datum has passed all QA Test
1	Suspect	There is concern about accuracy of datum
2	Failure	Datum is unstable

Table 12 The precipitation data QA tests are summarized as follows.

Range Test

This test is used to see if any individual precipitation observation falls within the climatological lower and upper limits. The test procedures applied in the study are as follows.

IF $Lim_{Lower} \leq Obser_{j,t} \leq Lim_{Upper}$ **THEN** $Obser_{j,t}$ flag is **'Good'**
IF $Obser_i > Lim_{Upper}$ **OR** $Obser_{j,t} < Lim_{Lower}$ **THEN** $Obser_{j,t}$ flag is **'Failure'**

Lim_{Lower} and Lim_{Upper} thresholds are separately determined for each station on a monthly basis. At any specific site, all the observed monthly data is considered for determination of the upper and lower limits.

By applying this test, each observation is flagged either by 'Good' or 'Failure' label depending on the comparison tests mentioned above.

Step Test

It is used to see if increment/decrement between sequential observations in time domain is in acceptable range or not. The applied test procedure is,

IF $|Obser_{j,t}-Obser_{j,t-1}| < Step_j$ **THEN** $Obser_{i,t}$ flag is **'Good'**
IF $|Obser_{j,t}-Obser_{j,t-1}| > Step_j$ **THEN** $Obser_{i,t}$ flag is **'Suspect'**

$Step_j$ threshold is determined again for each site on a monthly basis. For each site, the dataset containing the absolute difference of the sequential observations is determined by considering the observations for the matching month. The 99.9 % cumulative histogram value of the dataset is set as the $Step_j$ threshold for the related site and month.

Persistence Test

Persistence test is used to determine if any group of observations are due to instrument failures. The test procedure applied is defined as,

IF T < Δ THEN Flag for all Obser in T **: 'Good'**
IF T > Δ THEN Flag for **all** Obser in T **: 'Suspect'**

where T is the total number of the sequentially repeating observations forward in time and Δ is the possible maximum number of sequentially repeating observations. As in the other two tests, Δ threshold is determined for each site on a monthly basis. For any site, the data belonging to the same month is taken into account to determine the repeating number of the sequential observations. Then, 99.9 % cumulative histogram value of the repeating number dataset is assigned as the Δ amount for the corresponding site and month. Since there is a high possibility of no-precipitation data (zero), the sequential zero observations are excluded in this test during the determination of the Δ threshold amount and application of the test.

QA Test procedure

By applying the control procedures of the QA test mentioned above, each individual precipitation observation receives three flags referring to the corresponding test. For the corresponding observation if all the test flag is not 'Good' then the observation is excluded from the validation process.

Use of spatialization technique

Due to the time and space structure of precipitation and to the sampling characteristics of both the precipitation products and observations used for validation, care has to be taken to bring data into comparable and acceptable range. At a given place, precipitation occurs intermittently and at highly fluctuating rates. Various maps, time series analysis, statistical and probabilistic methodologies are employed in the validation procedure classically, but some additional new aspects such as the spatial coverage verification model of point cumulative semivariogram (PCSV) approach (Şen and Habib, 1998) are proposed for usage in this work.

Each precipitation product within the H-SAF project represents a foot print geometry. Among these, H01 and H02 products represent an elliptical geometry while H03 and H05 have a rectangular geometry. On the other hand, the ground observation (rain gauge) network consists of point observations. The main problem in the precipitation product cal/val activities occurs in the dimension disagreement between the product space (area) and the ground observation space (point). To be able to compare both cases, either area to point (product to site) or point to area (site to product) procedure has to be defined. However, the first alternative seems easier. The basic assumption in such an approach is that the product value is

homogenous within the product footprint. Next figure presents satellite foot print (FOV) centers of the H01 and H02 products, an elliptical footprint for the corresponding center (area within the yellow dots) and Awos ground observation sites. The comparison statistic can be performed by considering just the sites in the footprint area. Although this approach is reasonable on the average but it is less useful in spatial precipitation variability representation. The comparison is not possible when no site is available within the footprint area.

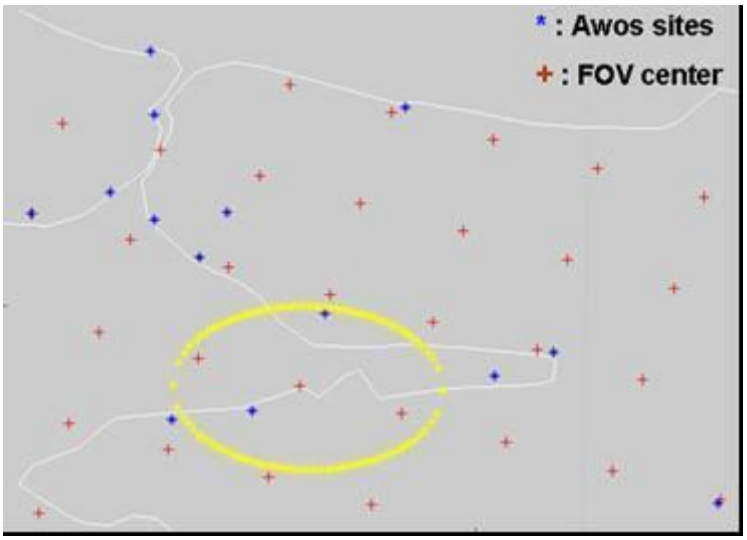

Figure 24: H01 and H02 products footprint centers with a sample footprint area as well as the Awos ground observation sites.

Alternatively, the point to area approach is more appealing for the realistic comparison of the precipitation product and the ground observation. This approach is simply based on the determination of the true precipitation field underneath the product footprint area. To do so, the footprint area is meshed and precipitation amounts are estimated at each grid point by using the precipitation observations at the neighboring Awos sites as shown in Figure 25. A 3x3 km grid spacing is considered for the products with elliptical geometry while 2x2 km spacing is considered for the products with rectangular geometry. For any grid point, Awos sites within the 45 km for the time period of April-September (convective type) and 125km for the rest(stratiform type) are taken into consideration. At each grid point, the precipitation amount is estimated by,

$$Z_m = \frac{\sum_{i=1}^{n} W(r_{i,m}) Z_i}{\sum_{i=1}^{n} W(r_{i,m})} \qquad (4.13.1)$$

where Z_m is the estimated value and $W(r_{i,m})$ is the spatially varying weighting function between the i-th site and the grid point m.

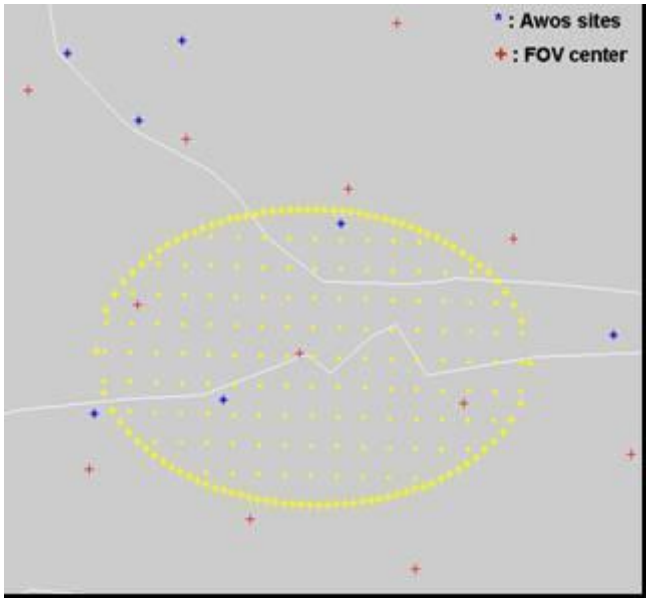

Figure 25: Meshed structure of the sample H01 and H02 products footprint.

Determination of the $W(r_{i,m})$ weighting function in Equation 1 is crucial. In open literature, various approaches are proposed for determining this function. For instance, Thiebaux and Pedder (1987) suggested weightings in general as,

$$W(r_{i,m}) = \begin{cases} \left(\dfrac{R^2 - r_{i,m}^2}{R^2 + r_{i,m}^2} \right)^{\alpha} & \text{for} \quad r_{i,m} \le R \\ 0 & \text{for} \quad r_{i,m} \ge R \end{cases} \qquad (4.13.2)$$

where R is the radius of influence, $r_{i,m}$ is the distance from point i to point m to the point and α is a power parameter that reflects the curvature of the weighting function. Another form of geometrical weighting function was proposed by Barnes (1964) as,

$$W(r_{i,m}) = \exp\left[-4 \left(\frac{r_{i,m}}{R} \right)^{\alpha} \right] \qquad (4.13.3)$$

Unfortunately, none of these functions are observation dependent but suggested on the basis of the logical and geometrical conceptualizations only. They are based only on the configuration, i.e. geometry of the measurement stations and do not take into consideration the natural variability of the meteorological phenomenon concerned. In addition, the weighting functions are always the same from site to site and time to time. However, in reality, it is expected that the weights should reflect to a certain extent the regional and temporal dependence behavior of the phenomenon concerned.

For the validation activities, the point cumulative semi-variogram technique proposed by Şen and Habib (1998) is used to determine the spatially varying weighting functions. In this approach, the weightings not only vary from site to site, but also from time to time since the observed data is used. In this way, the spatial and temporal variability of the parameter is introduced more realistically to the validation activity.

Matching approach

The temporal and spatial matching approaches are applied separately in the validation of the satellite products. As for the temporal matching, the product time is taken into account and 5 minute window(t-2 to t+3) is considered for estimation of the average rainrate for each site.

For the spatial matching, the mesh grid size of 3kmX3km is constructed for each IFOV area. For each grid point, the rainrate is estimated by taking the 5 minute averaged rainrate amounts observed at the nearby AWOS sites within the radius distance of 45 km(for convective type) or 125 km(for stratiform type) considering the weighting of each site with respect to the grid point(Equation 1). The weighting amounts are derived from the spatially varying weighting functions obtained by using the semi-variogram approach(Şen and Habib,1998). Finally, the Gaussian filter is applied to the estimations at the mesh grid of the IFOV area to get the average rainrate. Then, this amount is compared with the satellite precipitation product amount for the validation purposes.

Conclusions

After these inventories some conclusions can be drawn.

The rain gauge in PPVG is composed by more than 4000 instruments across the partner Countries. These data are, as usual, irregularly distributed over ground and are generally deduced by tipping bucket type instruments. Moreover most of the measurements are hourly cumulated. So probably the raingauge networks used in this validation activities are surely appropriated for the validation of cumulated products (1 hour and higher), while for the validation of instantaneous estimates the use of hourly cumulated ground measurements could introduce a large error. Moreover the revisiting time (3,4 hours) of the product makes impossible or not reasonable to validate the product for 1-24 hours cumulated interval. The first object of PPVG *(Rain Gauge- WG)* in the next future it will be to quantitatively estimate the errors introduced in the validation procedure comparing the instantaneous satellite precipitation estimation with the rain gauge precipitation cumulated on different intervals (the Polish and Turkish data will be used for this purpose).

The rain gauge inventory has also pointed out that different approaches for the estimates matching are considered in the PPVG. The second steps in the next future will be to define the rain gauge spatial interpolation technique and to develop the related software.

The radar data in the PPVG is composed by 56 C-band radars across the 7 countries: Belgium, Germany, Hungary, Italy, Slovakia, Poland, Turkey. The rain gauge network responsible declared that the systems are kept in a relatively good status. The rain gauge inventory pointed out that different correction factors are applied. This means that the corresponding rainfall estimates are diverse, and the estimation of their errors cannot be homogenized. The first step in PPVG *(Radar –WG)* will be to define a quality index on the base of the study performed by the Slovakian team (Annex 4) and the scheme published by J. Szturc et all 2008. The main difficulty consists on the definition of a quality index computable for every radar networks of PPVG. The evaluation of this quality index will allow to evaluate the rain gauge error in the same way and to select the more reliable radar data in the PPVG.

In this chapter the first example of precipitation fields integration has been provided (Section 4.4.3): INCA and RADOLAN products. The INCA system, a tool for the precipitation products validation, is available in Slovakia and Poland, in both countries being run in pre-operational mode. In Germany similar precipitation analysis system called RADOLAN is being run operationally. This tool is already used for validation of the H-SAF precipitation products in Germany. The study performed in the PPVG *(INCA-WG)* showed that the accuracy and reliability of the raingauge stations significantly affect final precipitation analysis of the INCA or INCA-like systems. In order to solve this problem an automated blacklisting technique is going to be developed at SHMÚ (currently blacklisting is used in manual mode). The next step will be to develop the software for up-scaling the INCA precipitation field into the satellite product grid. The grids of INCA and RADOLAN have similar horizontal resolution to the common radar grid. The up-scaling software will allow to provide case study analysis and statistical score evaluation for future considerations on the opportunity to use these precipitation integration products in the H-SAF validation programme.

4. Validation results: case study analysis

Introduction

As reported in the Chapter 3 the common validation methodology is composed of large statistic (multi-categorical and continuous), and case study analysis. Both components (large statistic and case study analysis) are considered complementary in assessing the accuracy of the implemented algorithms. Large statistics helps in identifying existence of pathological behaviour, selected case studies are useful in identifying the roots of such behaviour, when present.

This Chapter collects the case study analysis performed by PPVG on H15A for the period June 2013 –June 2014. The Chapter is structured by Country / Team, one section each. The analysis has been conducted to provide information to the User of the product on the variability of the performances with climatological and morphological conditions, as well as with seasonal effects.

Each section presents the case studies analysed giving the following information:

- description of the meteorological event;
- comparison of ground data and satellite products;
- visualization of ancillary data deduced by nowcasting products or lightning network;
- discussion of the satellite product performances;
- indications to satellite product developers;
- indication on the ground data (if requested) availability into the H-SAF project.

In the future the PPVG will test the possibility to present case study analysis in the test sites, indicated by the hydrological validation team, in order to provide a complete product accuracy and hydrological validation analysis to the users.

4.1 Case study analysis in Hungary

4.1.1 Case Study 1: 30th January, 2014

METEOROLOGICAL EVENT DESCRIPTION

A front system from Barents Sea to North Italy derived the weather of the North Europe. In Hungary afternoon lot of thunderstorms developed causing showers, hailstorms.

DATA/PRODUCTS USED
precipitation rate information from the Hungarian radar network (top middle panel),
precipitation rate information from the H15A product (old version) (top left panel),
precipitation rate information from the H03 product (top right panel),
visible image (bottom left panel), IR brightness temperature image (bottom middle panel), lightning image (bottom right panel)

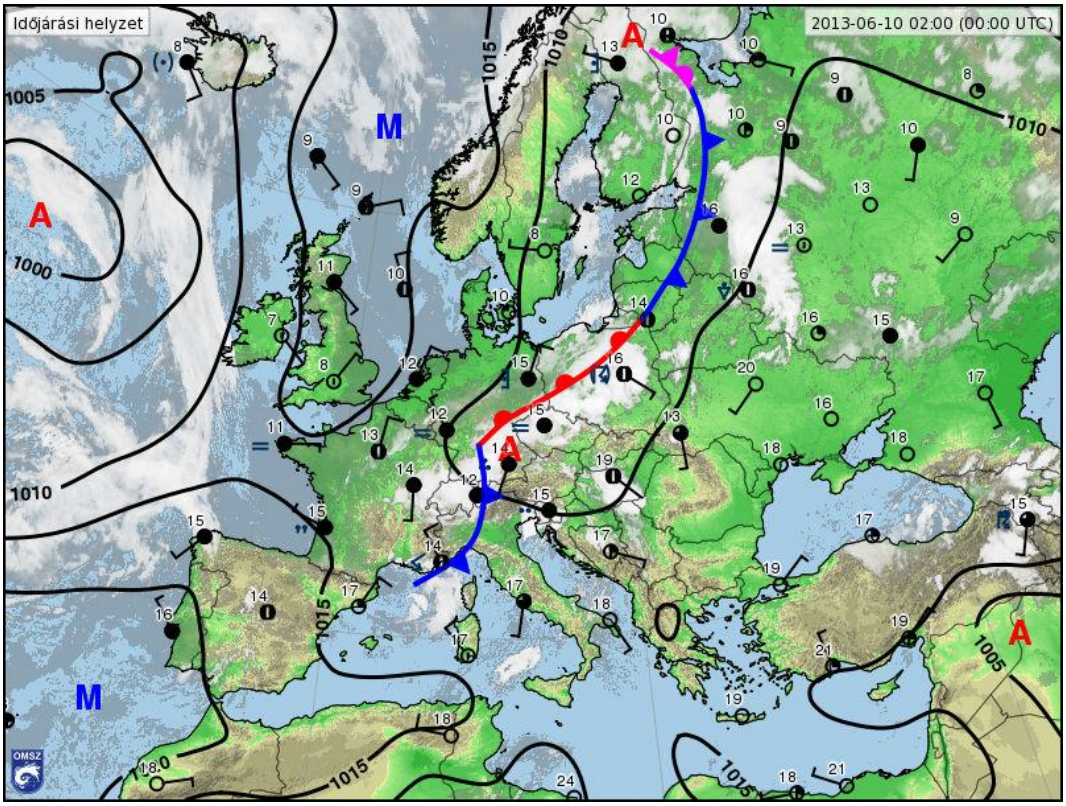

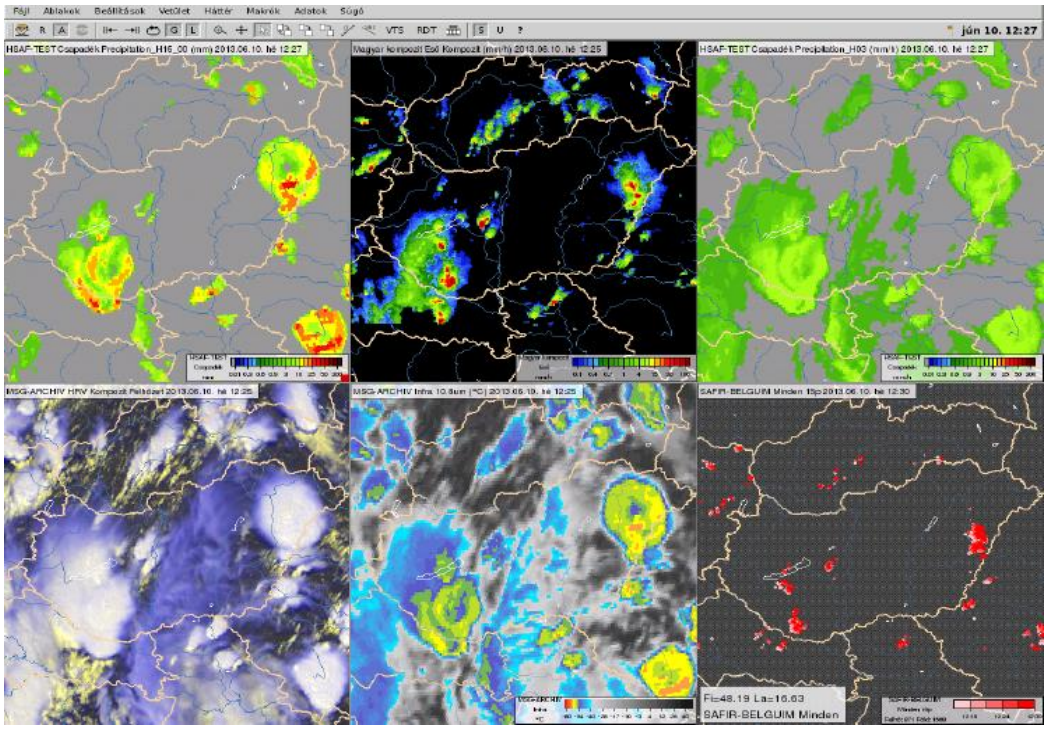

Figure 1.

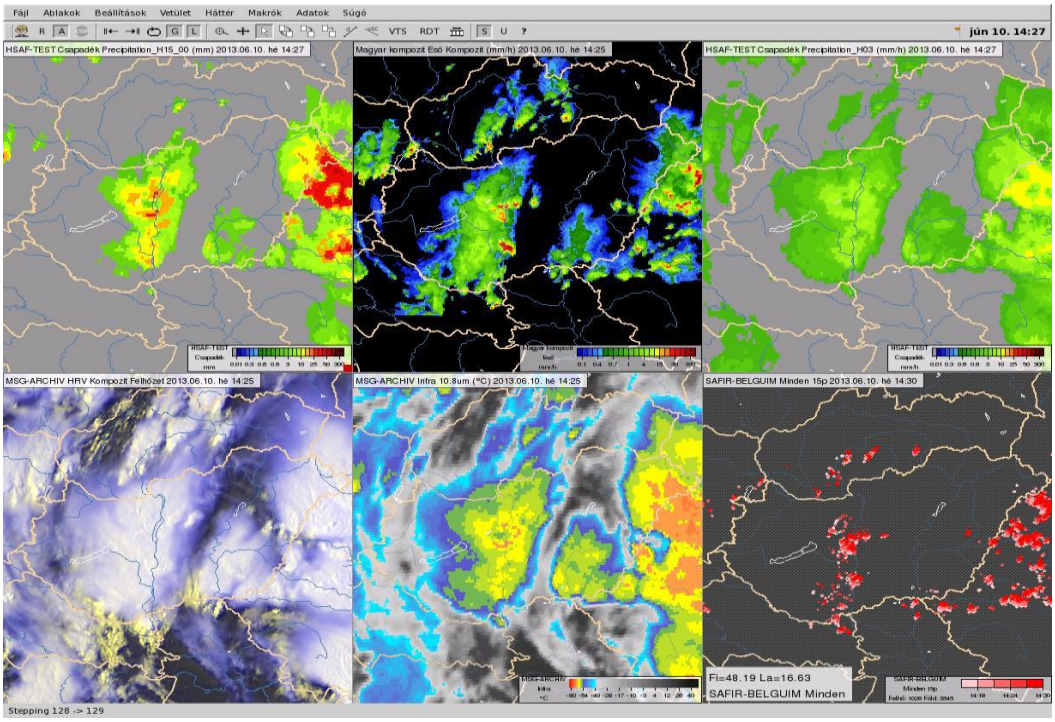

Figure 2.
precipitation rate information from the Hungarian radar network (right panel)
precipitation rate information from the H15A product (reprocessed version) (left panel)

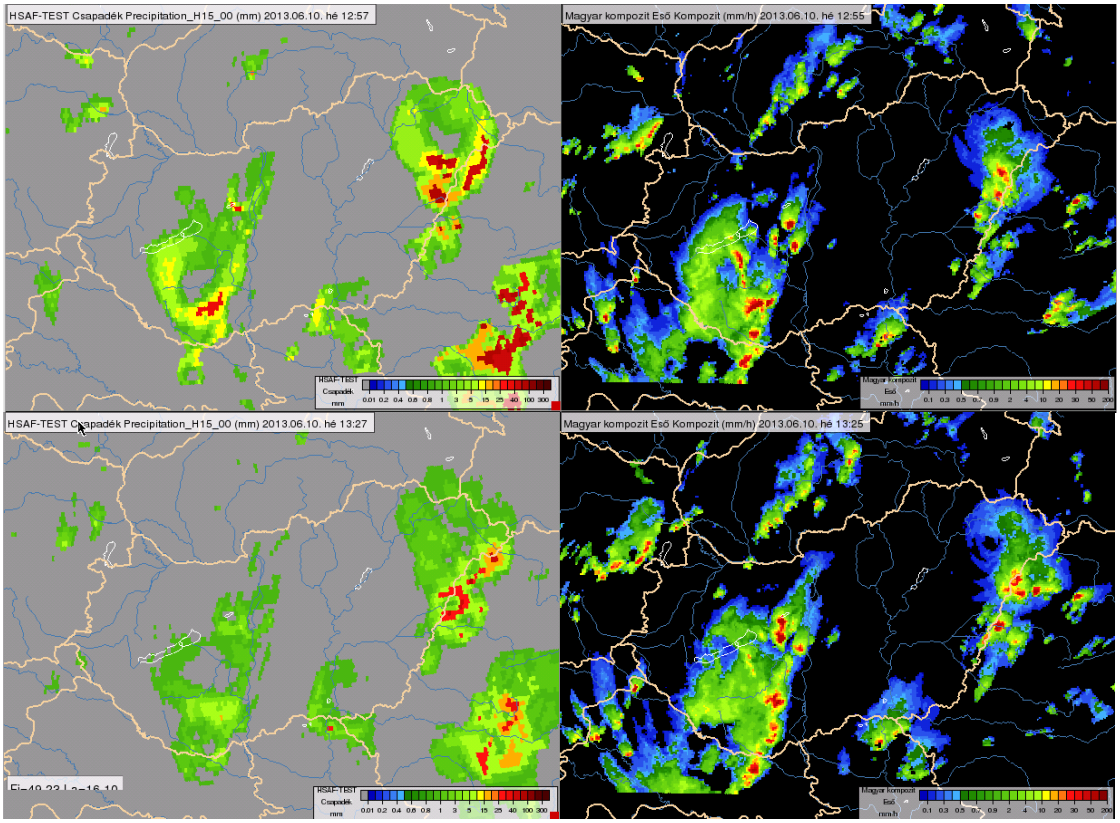

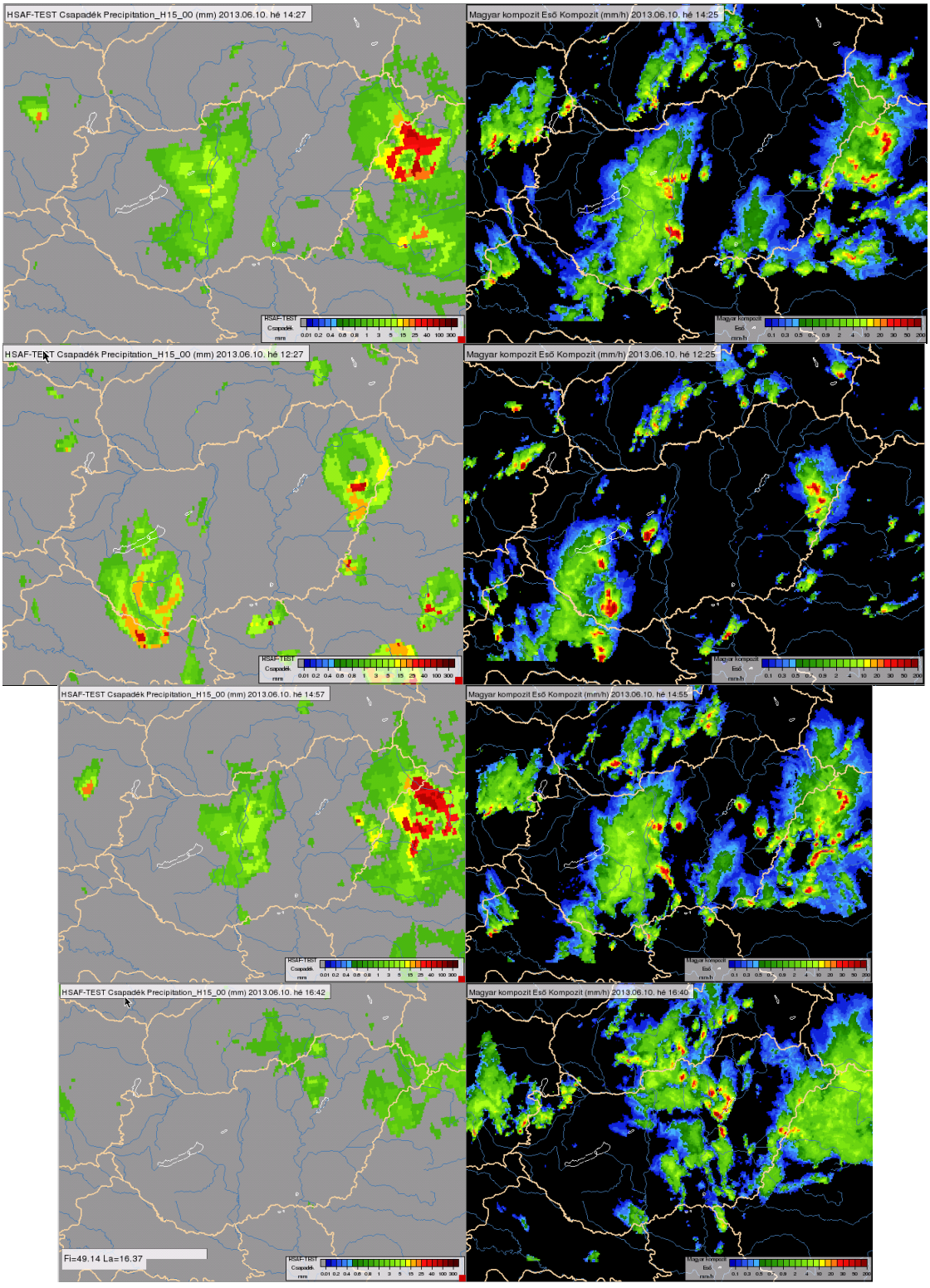

Figure 3.

RESULTS OF COMPARISON

The Figure 1 and 2 shows the old version H15A product, while Figure 3. the new version of it.
Cold-ring pattern can be seen at both H-SAF products and the IR 10.8 µm image. Comparing the two H-SAF products to the radar images we can see the H15A derives more correctly the precipitation area and

intensity than H03. The H15A precipitation intensity shows the same form as the coldest part of the cloud in the IR 10.8 µm image.
The lightning data, the highest precipitation intensity measured by radar show good agreement. While the H15A product overestimated the highest precipitation intensity area, until H03 underestimated the intensity except the light intensity, which was overestimated.
The next images show the convective clouds 2 hours later. As we can see at the previous images the H15A detects the precipitation area more correctly than h03, but 2 hour later we can see at the convective cloud developed on the east part of Hungary the H15A overestimated the high precipitation intensity area. If we look at the IR image and H-SAF products, we can see the cold-ring form disappeared, and the coldest area increased.

Comparing the old and new version of H15A product we can see that the moderate precipitation intensity was detected more correctly at the new version, but the highest precipitation intensity was overestimated significantly. The highest intensity values in all cases are very high.

As you can at the last image some convective precipitation areas were not detected.

COMMENTS
In most cases the H15A detects correctly the wide spread of convective precipitation area, but the smaller areas in more cases are not detected.
The H15A product overestimates the high precipitation intensity area. At the new version the highest precipitation intensity increased significantly.

4.2 Case study analysis in Italy

4.2.1 Case Study 1: 11-13 November, 2013

METEOROLOGICAL EVENT DESCRIPTION

In November 2013 frequent and intense perturbations affected the Mediterranean area. Between 11th and 12th of November a strong Mediterranean cyclone affected Italy and brought bad weather in the central and southern Italy, with heavy precipitation especially in the central Adriatic regions.
In the evening of 10th a vast Atlantic cyclonic wave, extending from Scandinavia to France, moved towards northern Italy and cut-off rapidly.

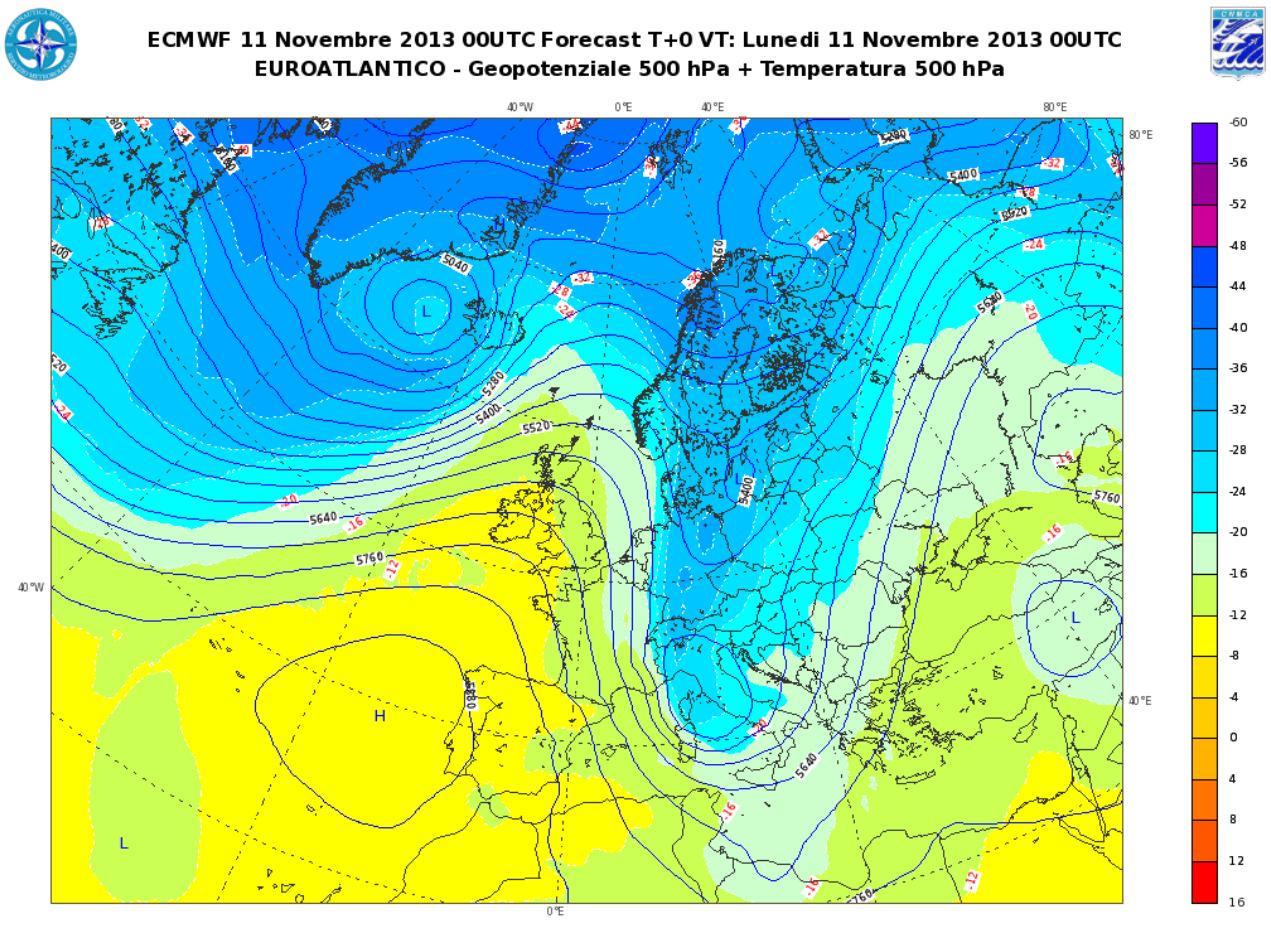

Geopotential height and temperatures 500 hPa, ECMWF analysis (11.11.2013, 00.00 UTC)

The analysis of ECWMF in the early morning of 11th (00 UTC, 01 local time) shows the cut-off of the cyclonic wave over Italy, with cold polar air masses flowing in from the North. Thus a cyclogenesis took place over the

Tyrrhenian Sea, a very common phenomena in Autumn, when strong low pressure systems bring heavy rainfall over Italy.

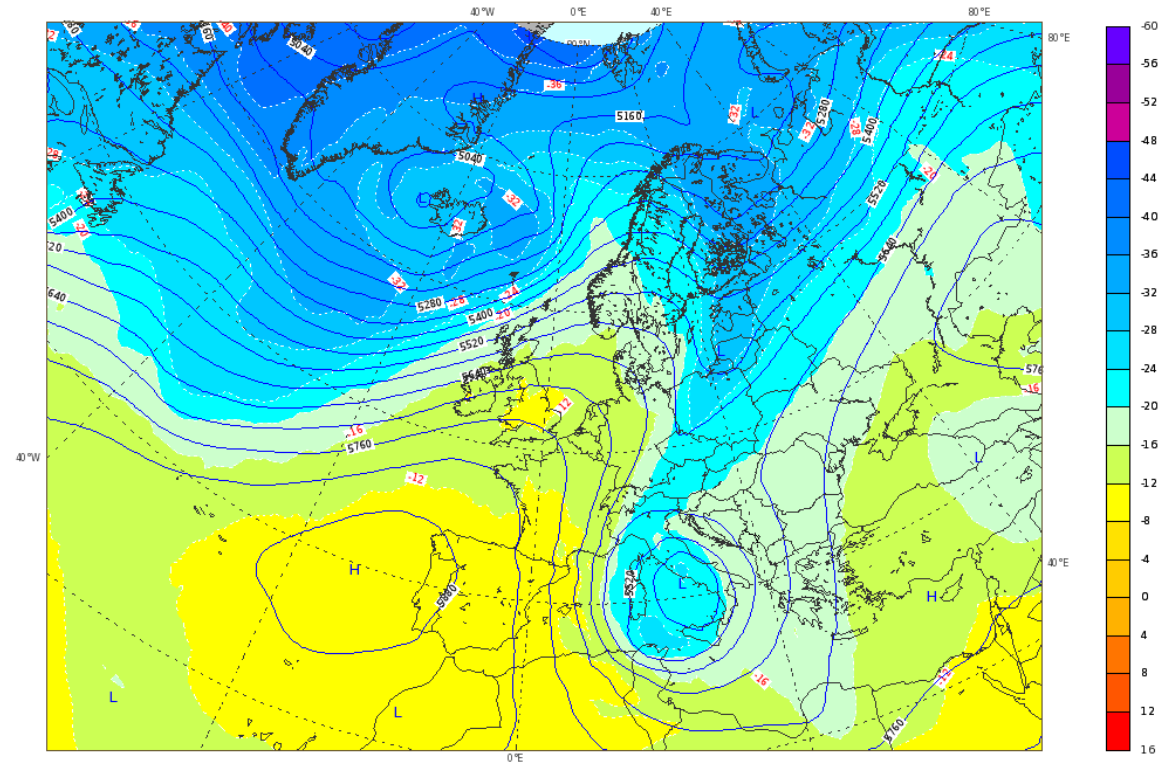

Geopotential height and temperatures 500 hPa, ECMWF analysis (11.11.2013, 12.00 UTC)

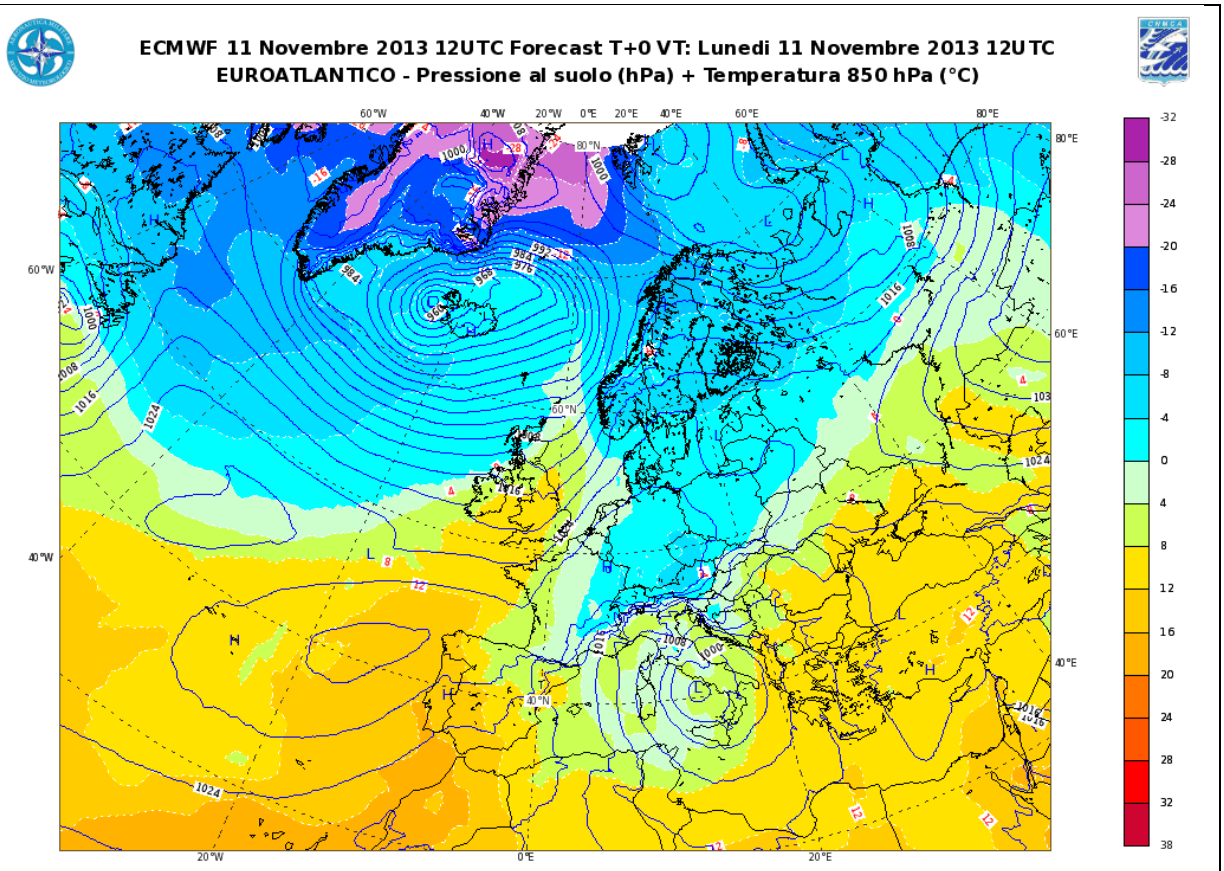

Mean sea level pressure and temperature at 850 hPa, ECMWF analysis (11.11.2013, 12.00 UTC)

The 2 analysis of ECWMF above show that in the early afternoon of 11th the low pressure system has already developed and is centered on the sea, before the coast of Latium. The low pressure in low layers (under 995 hPa) is a Mediterranean cyclone, almost in phase with the high level low, which cut-offed from the main zonal flow in northern Europe. In high layers cold air masses dominate, in low levels air mass separation is less evident, which in characteristic of Mediterranean cyclones, where occlusions and convective systems are main weather driving phenomena.

Bad weather affects the whole of center- and southern Italy, with rain, strong winds and high seas. In the north of the cyclone the isobars in low levels point to a strong pressure gradient and therefore very a strong easterly flow over central Adriatic regions, announcing the arrival of the occluded front.

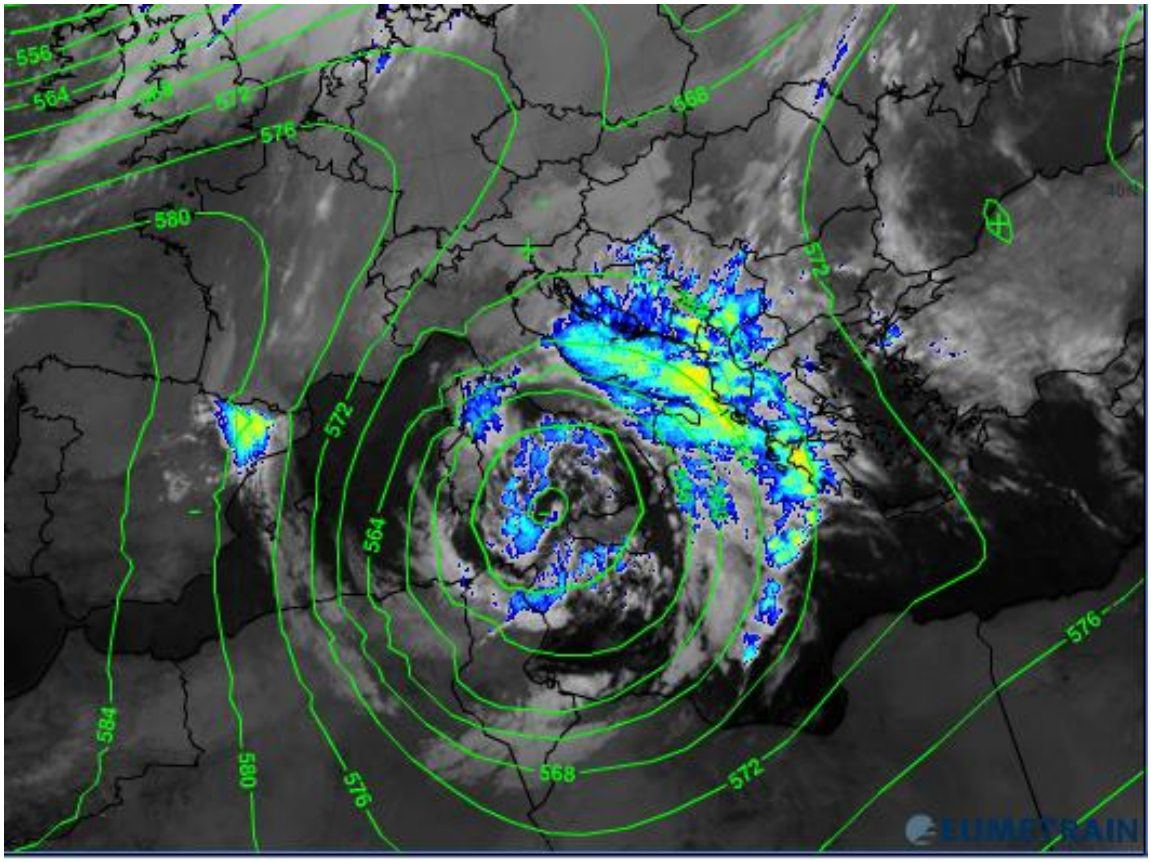

Meteosat 8 IR 10.8 + enhanced IR10.8 + ECMWF geopotential height 500 hPa; 12/11/2013 00 UTC

12 hours later, an analysis of 500 hPa geopotential, combined with Meteosat IR imaging is shown above. The low pressure system moved slowly southward to Sicily, and there it will be almost stationary till the 13th of November, bringing strong showers and thunderstorms in southern Italy, especially in Basilicata and Puglia.

Further to the east, the satellite image shows clearly the occluded front over the Adriatic sea reaching central Italy, with an intake of very moist maritime air from the southeast.

Till the morning of 13th in the center of Italy rainfall will be widespread and persistent, with embedded showers, especially in in the Adriatic regions of Abruzzi and Marche, where very high rain amounts, due to additional Stau effects, fall on the upward side of the Apennines. Lesser, but also relevant rain amounts, are recorded in the eastern zones of Umbria and Lazio.

In the afternoon of 13th the low pressure system dissipates and then moves to Greece; in Italy weather improves gradually, with ceasing rainfall.

DATA/PRODUCTS USED

The gauge-estimated rain rates are used to validate the product PR-OBS3 v1.4 (H03).

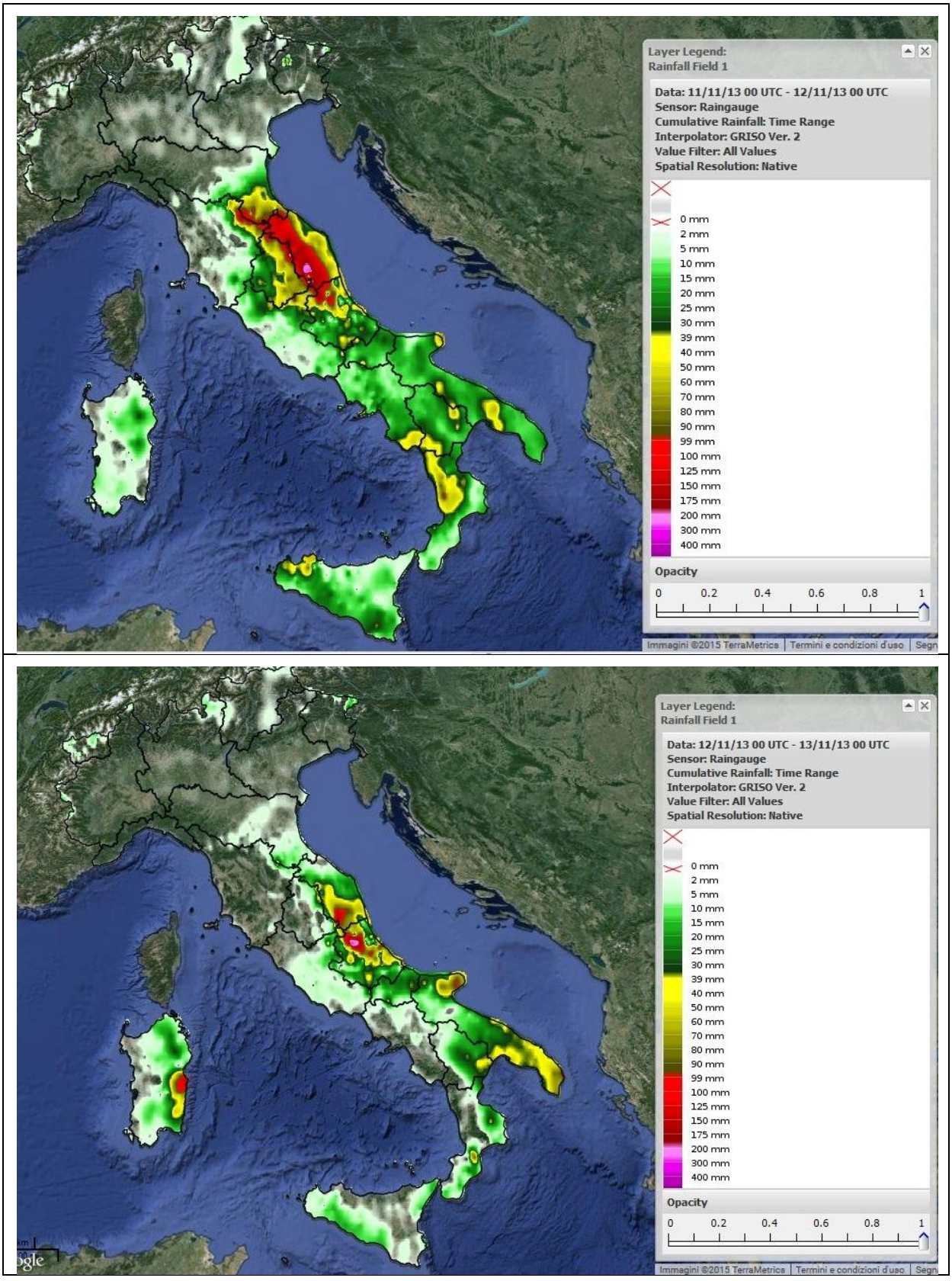

Figure 24-hour cumulated precipitation as retrieved by the Italian rain gauge network on the 11th November 2013 (upper panel) and 12th November 2013 (lower panel).

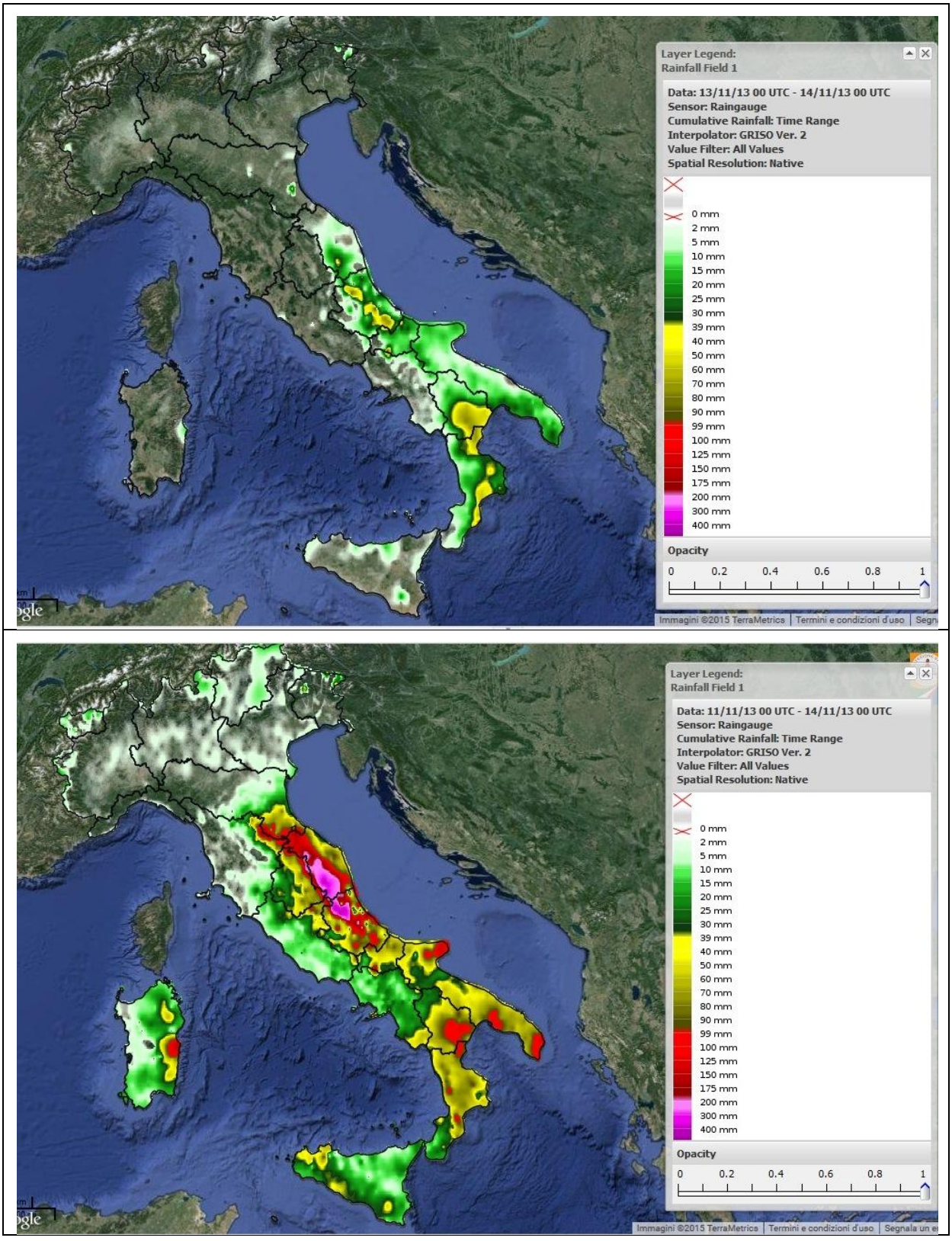

Figure Cumulated precipitation as retrieved by the Italian rain gauge network. The upper panel shows the 24-hour cumulated rainfall registered on the 11th November 2013. The lower panel shows the 72-hour cumulated precipitation observed between 11th November and 13th November 2013.

RESULTS OF COMPARISON

The validation results are shown in terms of continuous and multi-category statistics.

Prec. Class	ME (mm/h)	SD (mm/h)	MAE (mm/h)	MB (adim)	RMSE (mm/h)	PR-RMSE (%)
1≤PR<10	-2.49	2.22	2.69	0.27	3.32	84
PR≥10	-11.48	4.91	11.54	0.19	12.48	84
PR≥1.0	-3.08	3.27	3.26	0.25	4.49	83

Table 1 Continuous statistics for H15A as obtained considering the rain gauge as ground reference over land areas.

Prec. Class	ME (mm/h)	SD (mm/h)	MAE (mm/h)	MB (adim)	RMSE (mm/h)	PR-RMSE (%)
1≤PR<10	-1.73	2.34	2.34	0.40	2.91	105
PR≥10	-12.82	5.35	12.82	0.11	13.89	90
PR≥1.0	-2.41	3.71	3.01	0.33	4.42	105

Table 2 Continuous statistics for H15A as obtained considering the rain gauge as ground reference over coastal areas.

	Land Areas	Coastal Areas
POD (%)	31	27
FAR (%)	54	55
CSI (%)	23	20

Table 3 Multi-category scores for H15A as obtained considering the rain gauge as ground reference over land (left column) and coastal (right column) areas.

COMMENTS

The product performed relatively well for all precipitation regimes, the accuracy being between target and threshold.

4.3 Case study analysis in Poland

4.3.1 Case Study 1: 29th July, 2013

METEOROLOGICAL EVENT DESCRIPTION

On the 29th of July 2013 the weather phenomena over Poland were determined by the front coming to the NW parts of Poland from Germany fed by the thermal contrast between extremely hot and dry air masses of tropical origin and humid but also cooler polar air masses of Atlantic provenience. As a result only the SE part of the country was cloud free – the rest of the country was obscured by clouds connected with storm events encountered all over the country. The forecasted liquid precipitation (connected with hail) during the storms was estimated as of 15 mm up to 30 mm (at night in the Pomerania region) and 25mm to 35 mm during the day, especially in the close vicinity of Cb clouds. In the storm area wind gusts were reaching 85 km/h while predominant wind direction was SE. The min temperature at night was estimated at 15°C in SE and 23°C in SW while max temperature during the day in the W regions of Poland 29°C, in the east parts 31°C and 36°C in the S and center of the country. The above mentioned weather conditions were increasing in intensity during the day and following night.

Data and products used

Reference data: data from Polish automatic rain gauges network (IMWM-NRI)
data from Polish meteorological radar network (IMWM-NRI)
H-SAF product: PR-OBS-6A
Ancillary data (used for case analysis):
Polish Lighting Detection System, PERUN (IMWM-NRI)

Comparison

Convective storms where observed over the NW regions of the country on that day. The precipitation was accompanied by lightning activity. On the figure below (first row of the maps), the lightning activity is superimposed onto convective precipitation map and correlated in time with the satellite transmission overpass started at 0042 UTC and continuing throughout the morning. Presented slots were chosen to illustrate three stages of the storm development. These maps were constructed with use of data from Polish Lighting Detection System, PERUN.

Statistical scores

Please note that all statistical scores obtained for this study were calculated for the whole day of interest not only for the slots presented on the maps.

The ability of PR-OBS-6A product to recognize the convective precipitation was analyzed using dichotomous statistics parameters. Following the H-SAF methodology, the 0.25 mm/h threshold was used to discriminate rain and no-rain cases. Below, the contingency tables for radar and ATS data as well the Probability of Detection (POD), False Alarm Rate (FAR) and Critical Success Index (CSI) are presented.

	RD			**RG**
	Land	Coast	Sea	(land)
POD	0.51	0.50	0.31	0.90
FAR	0.48	0.37	0.58	0.64
CSI	0.35	0.39	0.22	0.35

The higher values of POD than FAR over land and coast indicate that PR-OBS-6A product ability to recognize the convective precipitation is very good both for ATS and quite good for radar data. This is not valid for results obtained for sea. The POD scores obtained for ATS data are much higher than for radar.

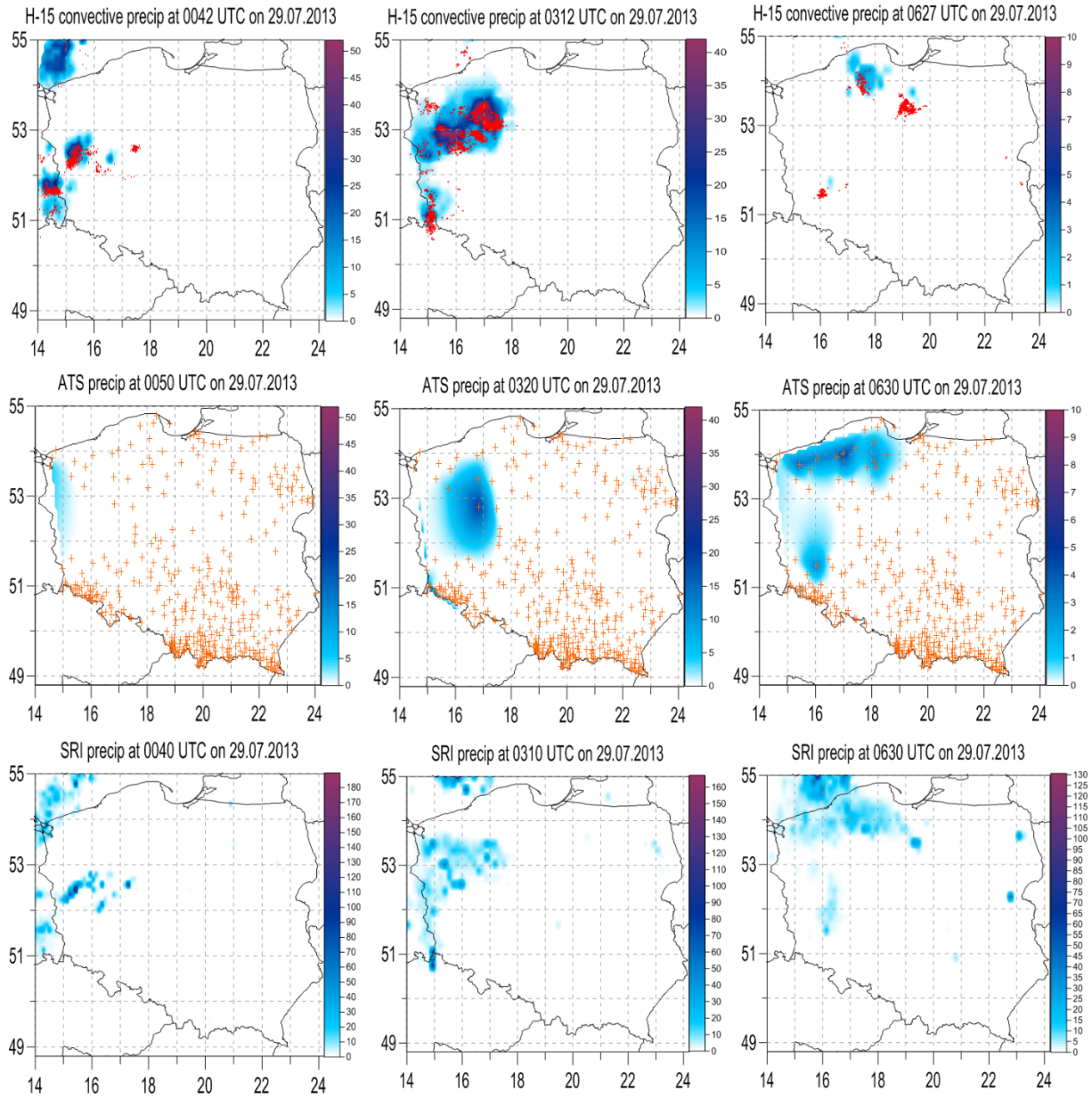

Three stages of the storm evolution described on a set of graphs presenting precipitation distribution over Poland according to H15A, ATS and radar (SRI). The red crosses on the H15A maps represent the lightning activity connected with the storm cells at given time slots while orange crosses on the ATS maps mark the ATS locations in Poland. *Please note the scale difference between radar maps and two other data sources presented.*

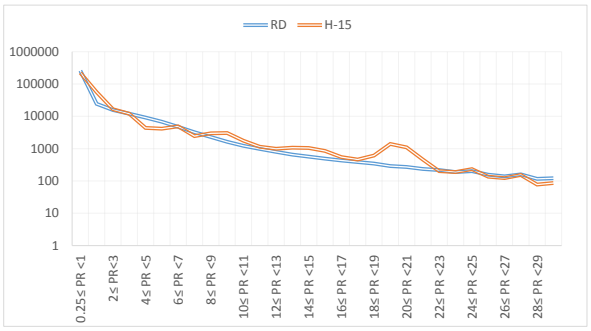

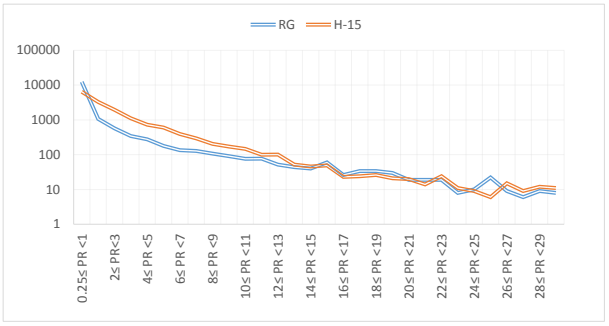

Probability Distribution Function graphs for radar and rain gauge against PR-OBS-6A (land).

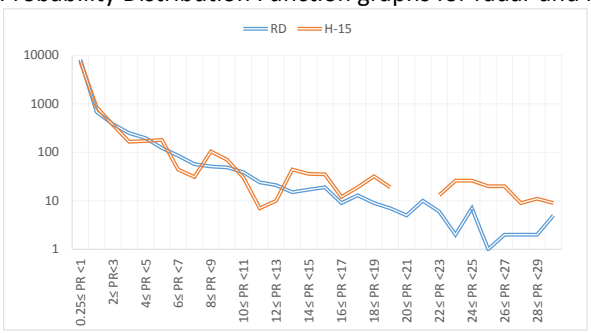

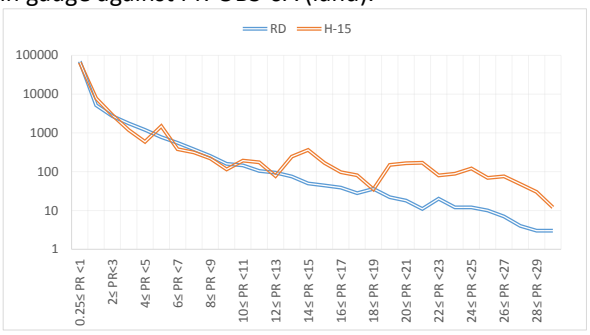

Probability Distribution Function graphs for radar against PR-OBS-6A (coast [left hand side] and sea [right hand side]).

	1 ≤ rr <10	rr ≥ 10
NS	8745	797
NRD	2899	667
ME	0.12	-12.83
SD	4.83	8.66
MAE	3.15	13.14
MB	1.03	0.29
CC	0.01	0.07
RMSE	4.83	15.48
URD %	260.30	73.60

Statistical scores for rain gauges on land.

	1 ≤ rr <10	rr ≥ 10
NS	106881	20057
NRD	79911	9301
ME	-0.45	-14.79
SD	7.49	14.73
MAE	4.03	17.21
MB	0.87	0.25
CC	0.05	-0.003
RMSE	7.50	20.88
URD %	349.30	94.80

Statistical scores for radar on land.

	1 ≤ rr <10	rr ≥ 10
NS	1987	722
NRD	1867	232
ME	5.94	-5.65
SD	16.77	19.997
MAE	9.41	17.79
MB	2.79	0.67
CC	0.06	-0.14
RMSE	17.79	20.77
URD %	875.80	135.50

Statistical scores for radar on coast.

	1 ≤ rr <10	rr ≥ 10
NS	15072	3103
NRD	12993	769
ME	0.42	-11.28
SD	9.16	11.75
MAE	4.71	14.09
MB	1.14	0.28
CC	0.12	-0.01
RMSE	9.17	16.29
URD %	410.60	97.50

Statistical scores for radar on sea.

Some Conclusions

- Concluding, the analysis performed for situation with convective precipitation occurred on the 29th of July 2013 showed quite good ability of PR-OBS-6A product in recognition of precipitation over land and coast. In the case of sea POD score is lower than FAR;
- The area of precipitation was properly recognized by H15A, especially, for the developing and mature convective phases. For the dissipating phase the underestimation was found;
- It needs to be mentioned that both radar and ATS data sets present total precipitation (convective and stratiform) while H15A shows the convective one only;
- The H15A product shows a good correspondence with lightning distribution but also the lack of parallax correction is visible here (see page 2, first row of maps);
- H15A tends to overestimate moderate precipitation while underestimating the high values of precipitation in this case;
- The PDFs over land are in good correspondence with both radar and rain gauge (see page 62).

4.3.2 Case study 2: 15th May, 2014

METEOROLOGICAL EVENT DESCRIPTION

On the 15th of May 2014 the weather over Poland was dominated by low pressure system located in Romanian Carpathians and strongly influencing local weather in south of the country. The rotating system delivered curved cloud structures over the mountain ridges which resulted in orographic intensification of stratiform precipitation in Poland. During the night estimated precipitation in the S regions of Poland was 25 mm while 40 mm at the mountains feet peeking at 50mm in some locations. In the Polish Carpathians snow and melting snow were expected. It resulted in the increase of snow cower in volume of 25 cm in the high mountains. In the rest of the country light liquid precipitation was forecasted. The min temperature in the NW part of the country was estimated at 2°C to 6°C, at the same time in other regions min temperature reached 6°C to 9°C. The predominant N wind was weak and moderate at that day but in the SE part of Poland some wind gusts were recorded. Especially in the high mountains wind gusts speed reached 100km/h at following night.
On the figure below, the 24h cumulation of lightning activity over Poland on 15th of May 2014 is presented. The available data prove that there was no convective precipitation on that day. The main group of lightning strokes is located on Ukraine and Belarus. The map was constructed on the base of data from Polish Lighting Detection System, PERUN.

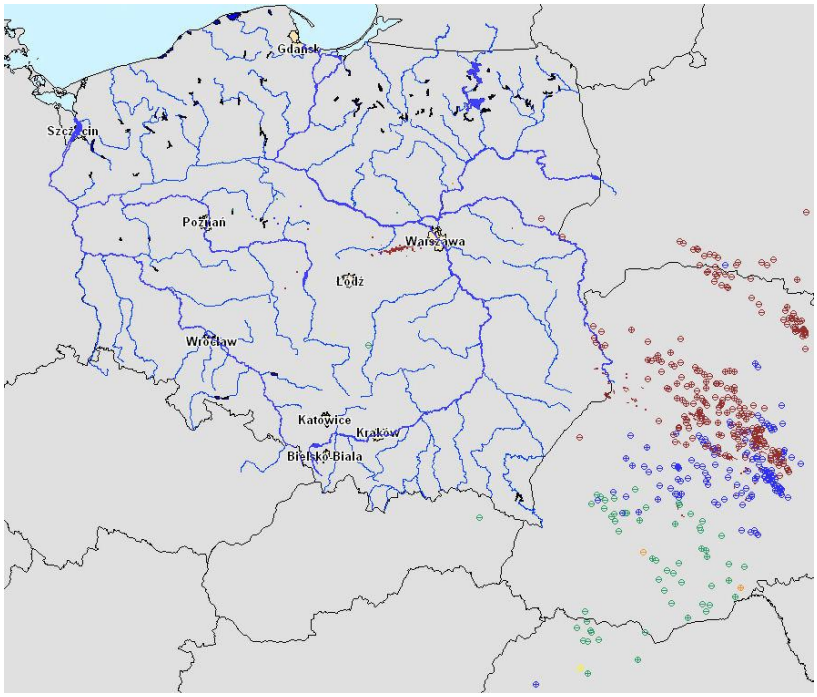

Data and products used

Reference data: data from Polish automatic rain gauges network (IMWM-NRI)
data from Polish meteorological radar network (IMWM-NRI)
H-SAF product: PR-OBS-6A
Ancillary data (used for case analysis):
Polish Lighting Detection System, PERUN (IMWM-NRI)

Comparison

The stratiform precipitation occurred on this day in Poland were captured by morning satellite overpasses started at 0942 UTC and continuing throughout the day.

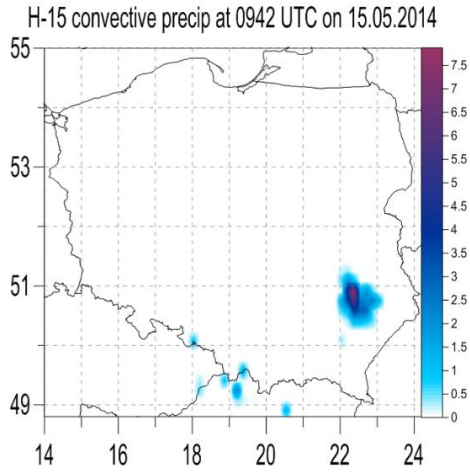

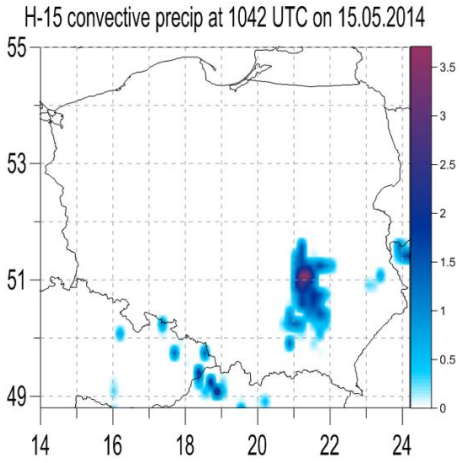

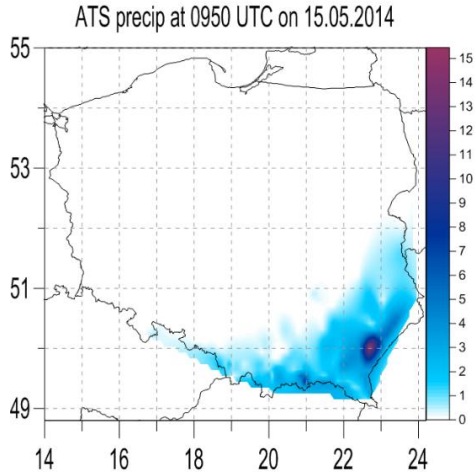

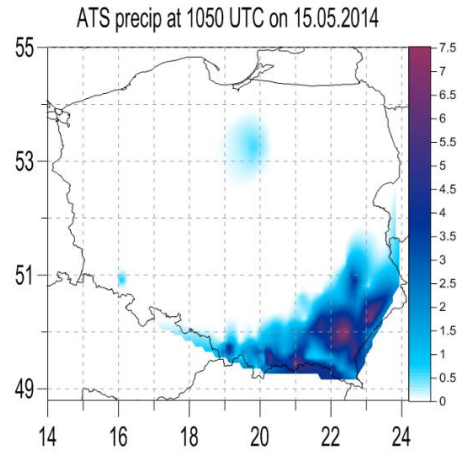

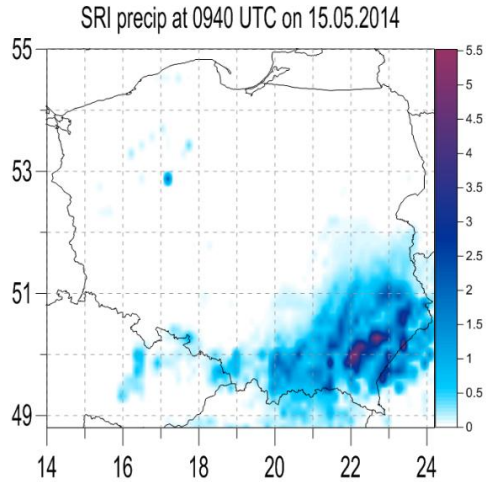

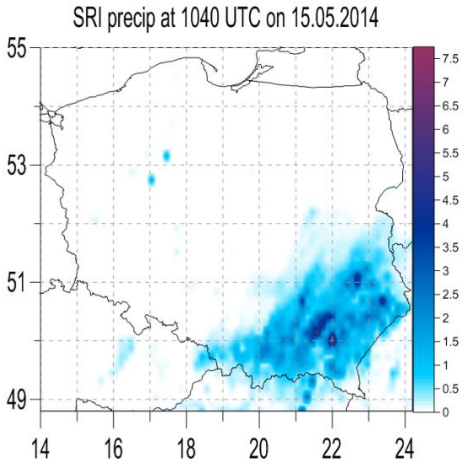

Two stages of the precipitation evolution described on a set of graphs is presented according to H15A, ATS and radar (SRI). *Please note the scale difference between radar maps and two other data sources presented.*

Some Conclusions

The H15A product was tested on the stratiform case to check its behavior. According to the specification of the tested product it should not detect any precipitation at all in this case. Nevertheless, the precipitation area was detected. It means that H15A wrongly classified stratiform precipitation as convective one. The analysis of the statistical scores in this case is pointless.

1. Validation results

6.1 Synopsis of validation results

In this Chapter the validation results of the H15A large statistics analysis are reported for the period (1.6.2013 – 30.06.2014). The validation has been performed on the product release currently in force at the time of writing.

Each Country/Team contributes to this Chapter by providing the monthly contingency tables and the statistical scores. The results are showed for radar and rain gauge, land, sea and coast area for the three precipitation classes defined in Table 5 Classes for evaluating Precipitation Rate products

. The rain rates lower than 0.25 mm/h have been considered as no rain. The precipitation ground networks, instruments and data used for the validation of H15A have been described in Chapter 4.

To assess the degree of compliance of the product with product requirements all the PPVG members provided the long statistic results following the validation methodology reported in Chapter 3.

For product H04 the Product requirements are recorded in following table:

PR-OBS-6A			
Precipitation class	**Requirement (RMSE %)**		
	thresh	**target**	**optimal**
> 10 mm/h	90	80	25
1-10 mm/h	120	105	50

Table 13 Product requirements for H14

This implies that the main score to be evaluated has been the RMSE%. However, in order to give a more complete idea of the product error structure, several statistical scores have been evaluated as reported: Mean Error, Standard Deviation (SD) and Mean Absolute Error (MAE), Mean Bias (MB) Probability Of Detection (POD), False Alarm Rate (FAR) and Critical Success Index (CSI). These scores have been defined in Chapter 3.

The long statistic results obtained in Belgium, Germany, Hungary, Italy, Poland, Slovakia and Turkey will be showed in the next sections. The country validation results are here reported in order to respond not only to the question whether the product meets the requirements or not, but also where it meets or approaches or fails the requirements.

The average performance of H04 for all sites is presented in a compact, synoptic way in this chapter. The contents of the monthly statistical scores have been provided by the individual Countries/Teams and verified by the Validation Cluster Leader, step by step, as described in the Chapter 3. As stressed in Chapter 4, the average scores reported in the following tables have been obtained on measurements collected in heterogeneous geographical, orographic and climatological conditions.

6.2 The continuous statistics

The results obtained by each country, synthetized through error scores computed on monthly-basis, are described in this section by means of temporal-sequence plots, the corresponding annual weighted average being summarized in Table 6.2.1.

It is worth mentioning that a further processing of the country-level error scores has been carried by the Validation Leader . Indeed, anomalous statistical scores (when compared with the general annual trend) were found in correspondence of very limited number of satellite and/or radar pixels to be compared. These values have been filtered out having been considered as outliers based on the following criteria:

a) NS and/or NR <20

b) $X>X_{mean}+2\sigma$ or $X<X_{mean}-2\sigma$

where NS and NR are the number of satellite and radar (or gauges) pixels to be compared. X stands for a generic error score, X_{mean} the average of its temporal distribution and σ the corresponding standard deviation.

Future developments of the validation approach, will evaluate the possibility to implement this basic data control within the common code used for the validation.

6.3 The monthly average

This section summarizes the results obtained by every partner in terms of error scores computed on monthly-basis. For the sake of brevity the results refer to inland areas only.
Looking at Figure 26, showing the temporal sequence of the computed error scores relatively to Belgium, when using the radar-based rainfall estimates as benchmark, we may notice that most of the “absolute” error scores (ME, MAE, SE, RMSE) show a seasonal sensitivity, especially for high precipitation rates, i.e., red curves corresponding to R>10 mm h^{-1}). In this case, the errors are higher during the summer period, which might be explained by the higher occurrence of convective, especially thermo-convective, small-scale storms.

It can be also noticed that, despite the Mean Error (ME) is not negligible, most of RMSE is explained by the Error Standard Deviation (SD), accounting for the spatial and temporal variability.

The “relative” error scores, i.e., Mean Bias and PR-RMSE, show a temporal variability especially for low precipitation rates. However, the PR-RMSE typically ranges around 1.0 (100%) for R>10 mm h^{-1} increasing up to 4.5 (450 %) in June 2014 at moderate rainfall rates (1<R< 10 mm h^{-1}). A comparative analysis with the Mean Error and Mean Bias allows to deduce a clear trend to precipitation underestimation.

Referring to Figure 27, showing the results obtained in Hungary, we may notice a temporal trend similar to that observed for Belgium until February 2014, than the product starts overestimating rainfall at least for R<10 mm h^{-1}. The PR-RMSE varies between about 0.7 (70%) and about 1.2 (120%) for the highest rainfall rate class, reaching up to 6.0 (600%) for the lowest.

Figure 27 -Figure 33 show the results obtained by the other countries, some of them using either radar or rain gauges for the product assessment.

The overall behaviour of H15A seems to be confirmed, a trend to precipitation underestimation, especially at high rain rates.

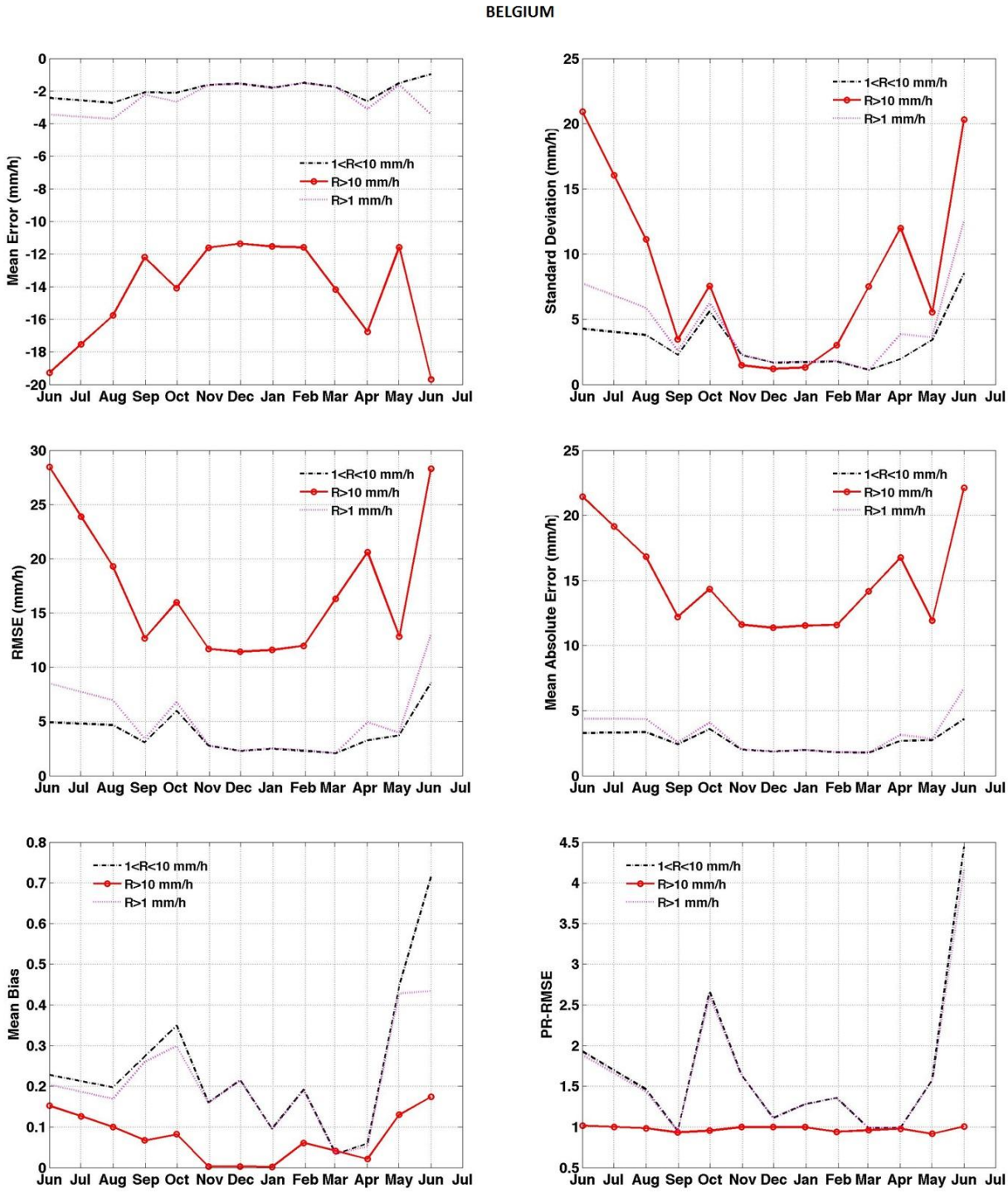

Figure 26 Temporal sequence of the computed error scores relatively to Belgium where the radar-based rainfall estimates have been considered as benchmark. The statistics refers to inland areas, while the reference period is 1st June 2013- 30th June 2014. Note that the PR-RMSE is not expressed in percentage.

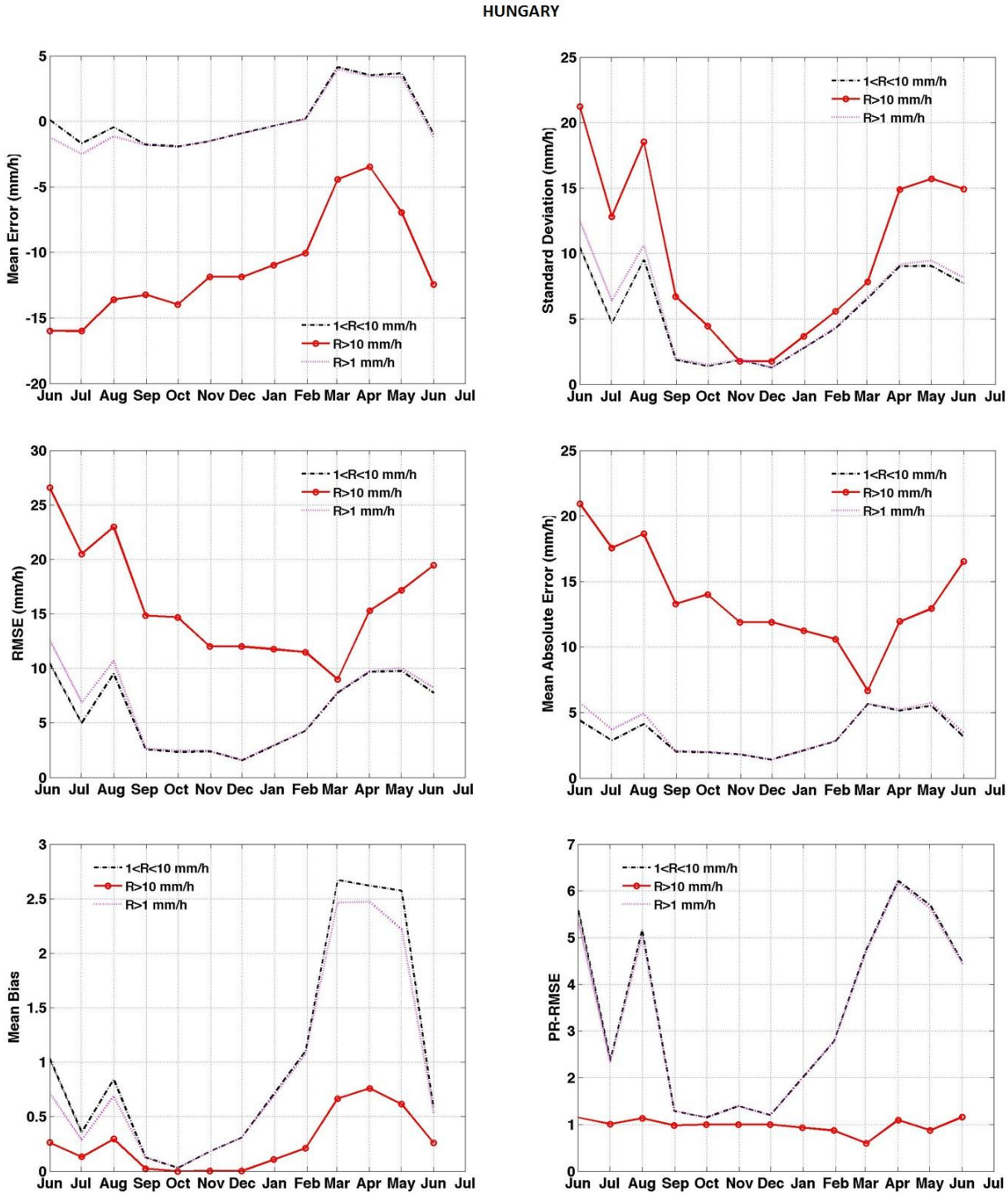

Figure 27 Temporal sequence of the computed error scores relatively to Hungary where the radar-based rainfall estimates have been considered as benchmark. The statistics refers to inland areas, while the reference period is 1st June 2013- 30th June 2014. Note that the PR-RMSE is not expressed in percentage.

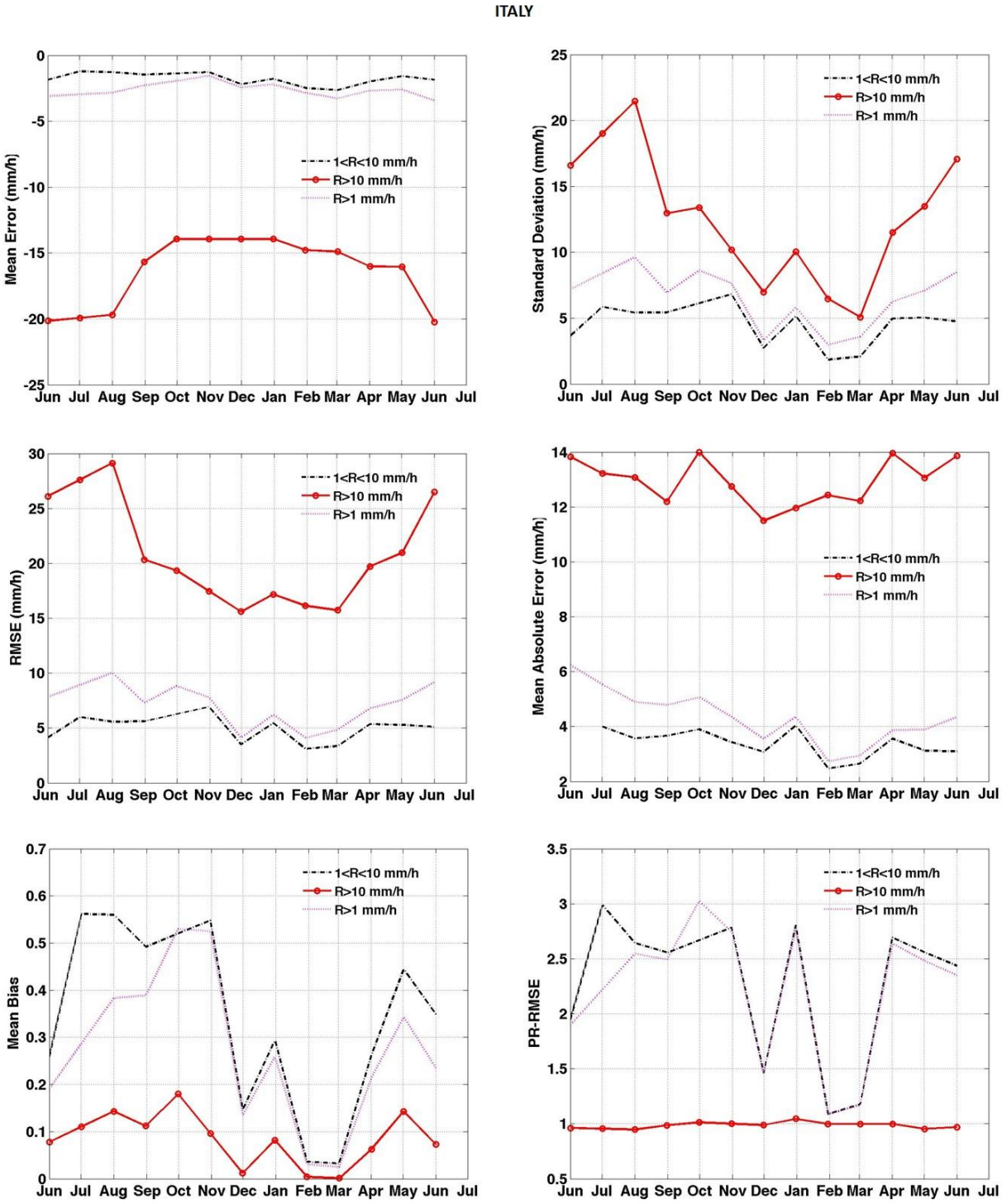

Figure 28 Temporal sequence of the computed error scores relatively to Italy where the radar-based rainfall estimates have been considered as benchmark. The statistics refers to inland areas, while the reference period is 1st June 2013- 30th June 2014. Note that the PR-RMSE is not expressed in percentage.

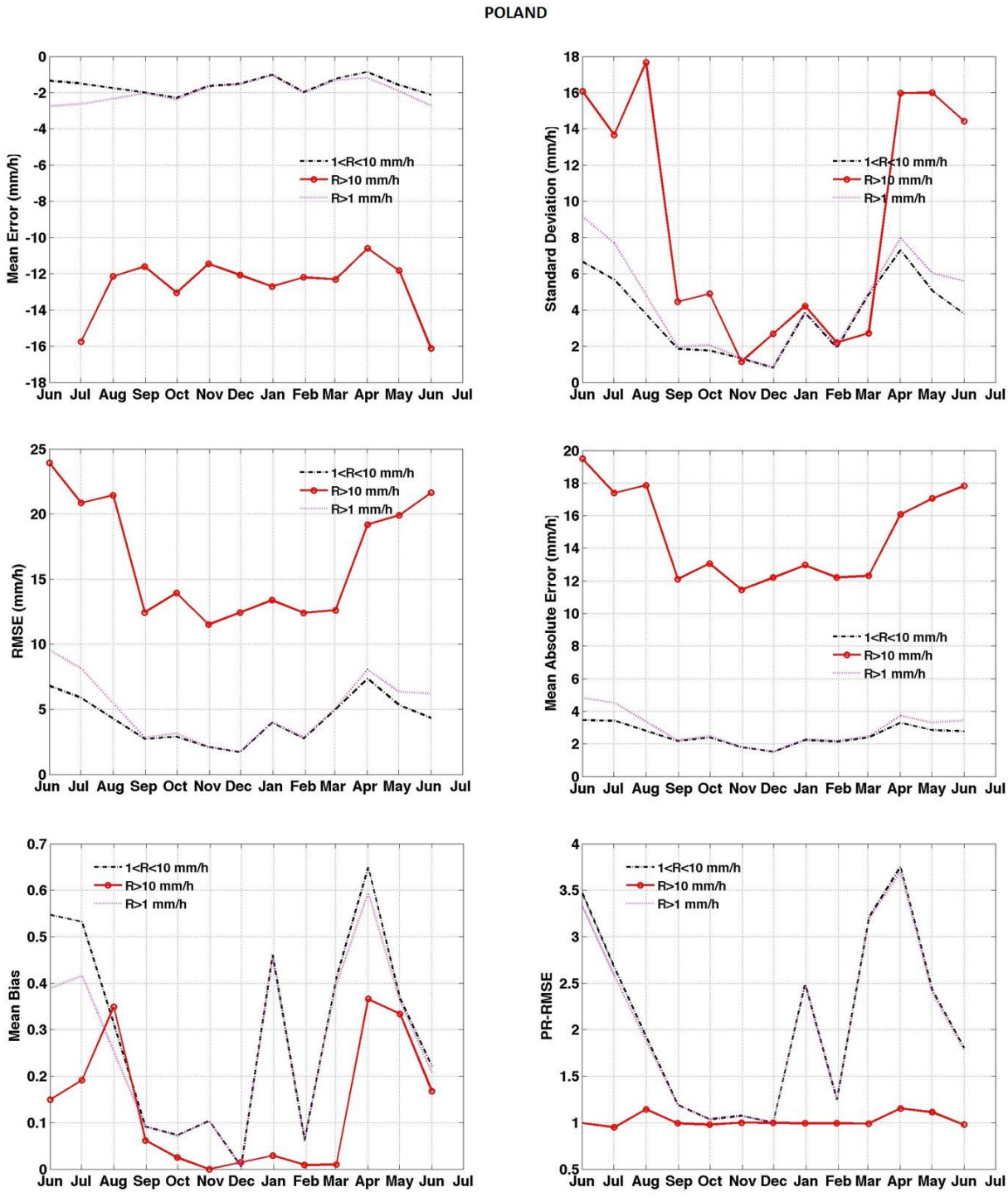

Figure 29 Temporal sequence of the computed error scores relatively to Poland where the radar-based rainfall estimates have been considered as benchmark. The statistics refers to inland areas, while the reference period is 1st June 2013- 30th June 2014. Note that the PR-RMSE is not expressed in percentage.

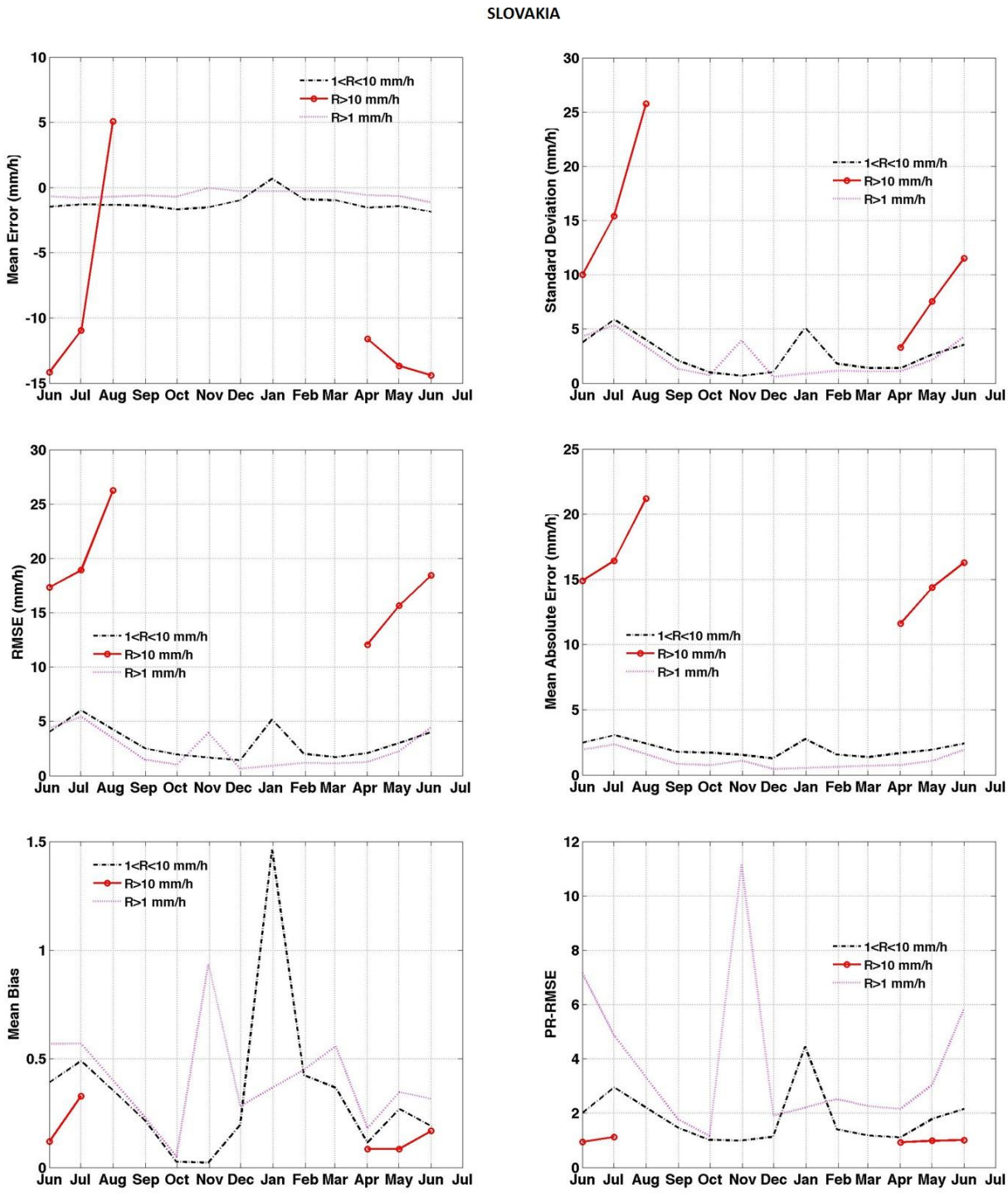

Figure 30 Temporal sequence of the computed error scores relatively to Slovakia where the radar-based rainfall estimates have been considered as benchmark. The statistics refers to inland areas, while the reference period is 1st June 2013- 30th June 2014. Note that the PR-RMSE is not expressed in percentage.

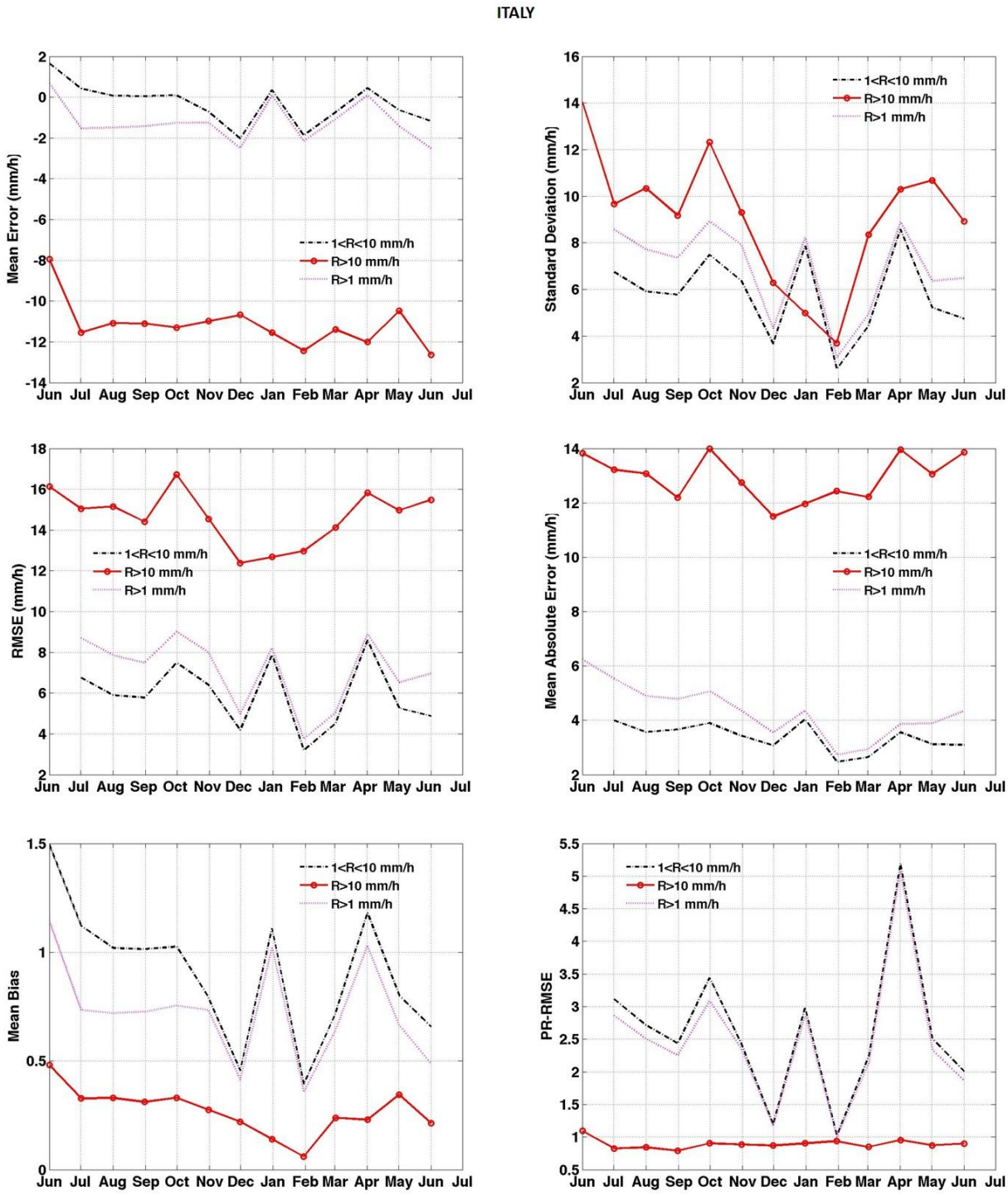

Figure 31 Temporal sequence of the computed error scores relatively to Italy where the gauge-based rainfall estimates have been considered as benchmark. The statistics refers to inland areas, while the reference period is 1st June 2013- 30th June 2014. Note that the PR-RMSE is not expressed in percentage.

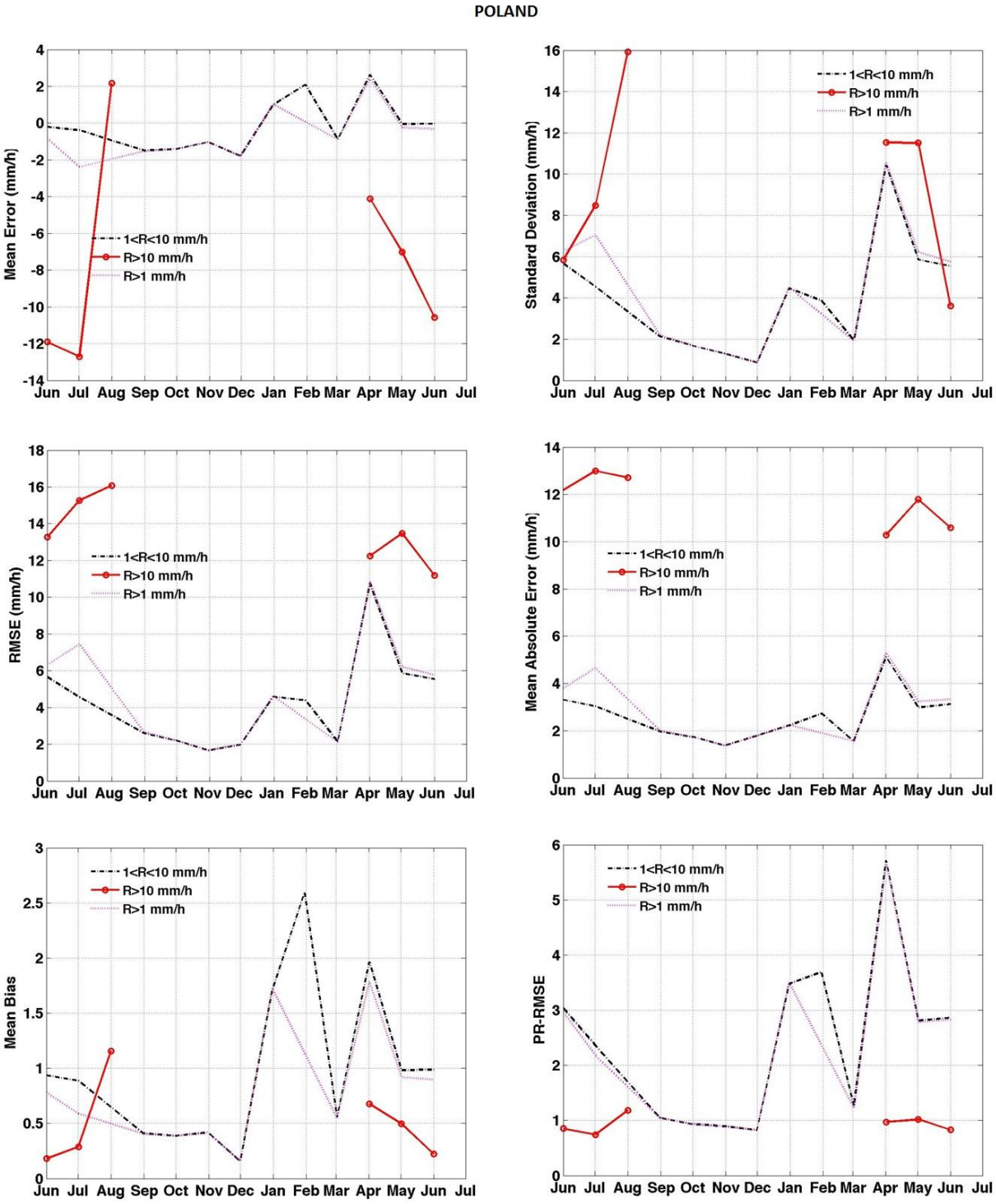

Figure 32 Temporal sequence of the computed error scores relatively to Poland where the gauge-based rainfall estimates have been considered as benchmark. The statistics refers to inland areas, while the reference period is 1st June 2013- 30th June 2014. Note that the PR-RMSE is not expressed in percentage.

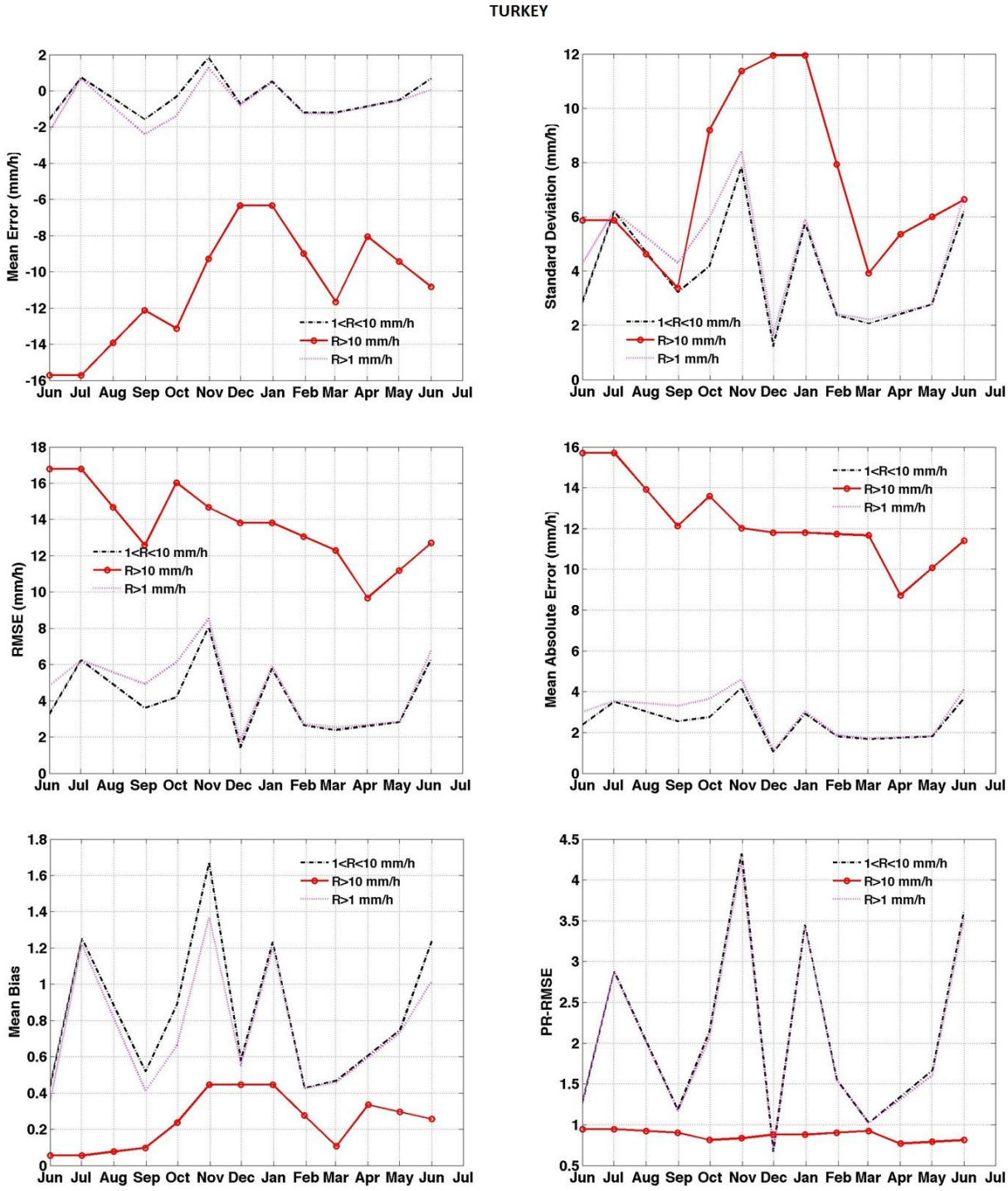

Figure 33 Temporal sequence of the computed error scores relatively to Turkey where the gauge-based rainfall estimates have been considered as benchmark. The statistics refers to inland areas, while the reference period is 1st June 2013- 30th June 2014. Note that the PR-RMSE is not expressed in percentage.

6.4 The annual average

This section summarizes the statistical scores obtained by every partner when aggregated on yearly-basis. For the sake of brevity the results refer to inland areas only. The last column, named "Total", is obtained as a weighted average of the error scores retrieved by each partner, where the weight is represented by the number of Radar or Rain gauge pixels (NR).

Figure 34 and **Errore. L'origine riferimento non è stata trovata.** show the yearly-aggregated error scores as retrieved comparing H15A with radar and rain gauge rainfall estimates, respectively. The results are shown separately for each considered rainfall class. The colour code identifies the country where the scores have been computed.

It can be noticed again the absolute scores are higher for the highest rainfall regime (R>10 mm h^{-1}), as expected. Table 14 summarizes main statistical scores evaluated using the radar estimates as benchmark relatively to the precipitation regime R≥ 1 mm h^{-1}. Whereas, Table 15 refers to the results obtained using the rain gauge rainfall retrieval.

PR-OBS-6A		BE	HU	IT	PL	SK	TOTAL
NR	≥ 1mm/h	65285	144196	376767	236457	90432	
ME	≥ 1mm/h	-2.60	-0.12	-2.52	-2.20	-0.55	-1.87
SD	≥ 1mm/h	5.19	7.74	6.76	5.93	2.51	6.17
MAE	≥ 1mm/h	3.48	4.21	3.85	3.53	1.18	3.53
MB	≥ 1mm/h	0.23	0.96	0.30	0.32	0.43	0.42
RMSE	≥ 1mm/h	5.87	8.08	7.29	6.42	2.60	6.62
PR-RMSE (%)	≥ 1mm/h	179 %	407%	231%	239%	426%	276%

Table 14 The main statistical scores evaluated by PPVG for H15A during 13 months of data 1st June 2013- 30th June 2014 using the radar rainfall estimates as benchmark. The "Total" column is obtained as a weighted average of the contributions provided by each country, the weights being NR.

PR-OBS-6A		IT	PL	TU	TOTAL
NR	≥ 1mm/h	33147	8828	3858	
ME	≥ 1mm/h	-1.35	-0.95	-0.27	-1.14
SD	≥ 1mm/h	7.34	5.37	5.39	6.74
MAE	≥ 1mm/h	4.50	3.34	3.21	4.13
MB	≥ 1mm/h	0.71	0.75	0.89	0.74
RMSE	≥ 1mm/h	7.55	5.57	5.54	6.94
PR-RMSE (%)	≥ 1mm/h	243%	242%	262 %	245%

Table 15 The main statistical scores evaluated by PPVG for H15A during 13 months of data 1st June 2013- 30th June 2014 using the rain gauges rainfall estimates as benchmark. The "Total" column is obtained as a weighted average of the contributions provided by each country, the weights being NR.

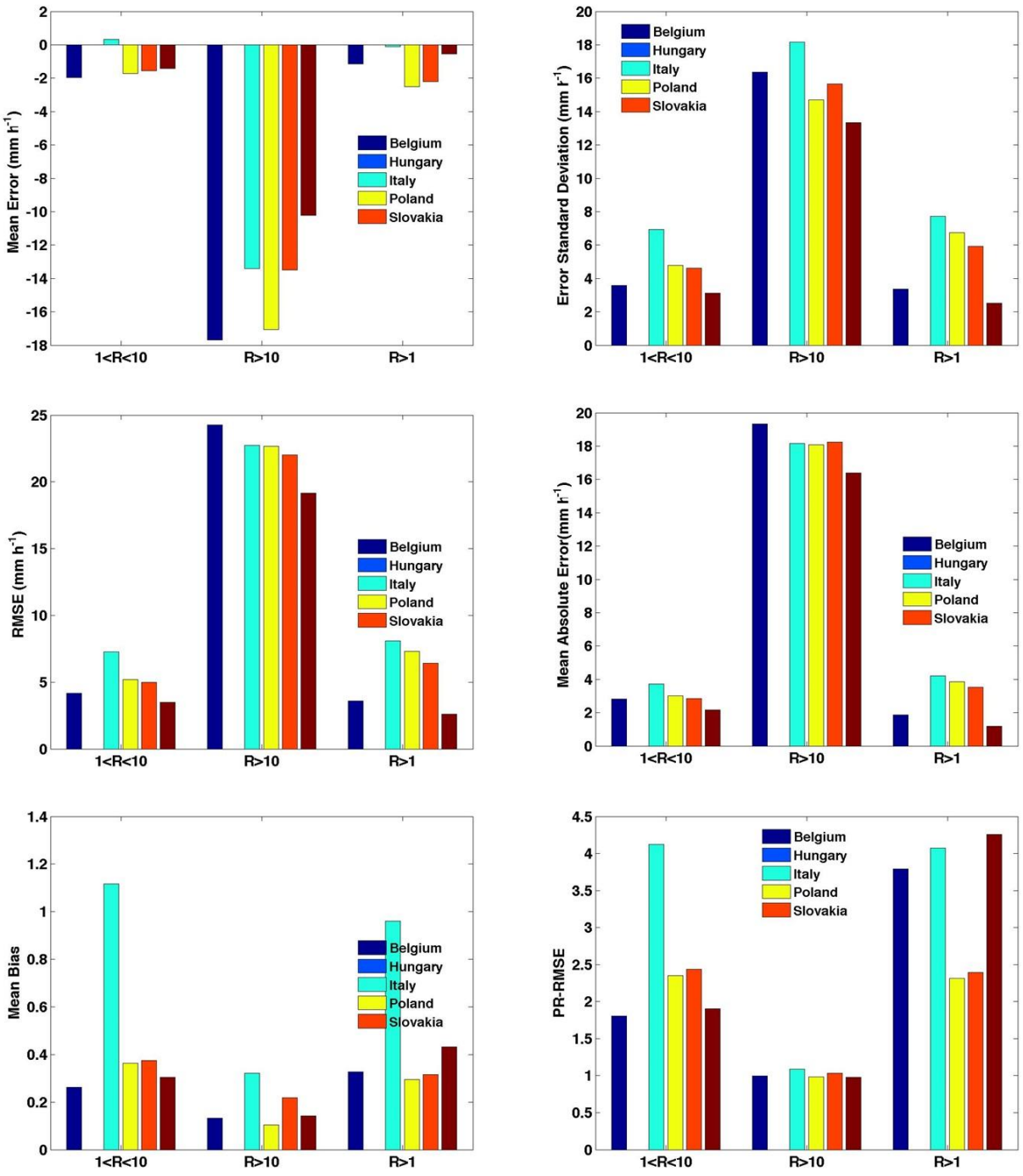

Figure 34 Yearly-aggregated error scores as retrieved using the radar-based rainfall estimates as benchmark. The statistics refers to inland areas, while the reference period is 1st June 2013- 30th June 2014. Note that the PR-RMSE is not expressed in percentage.

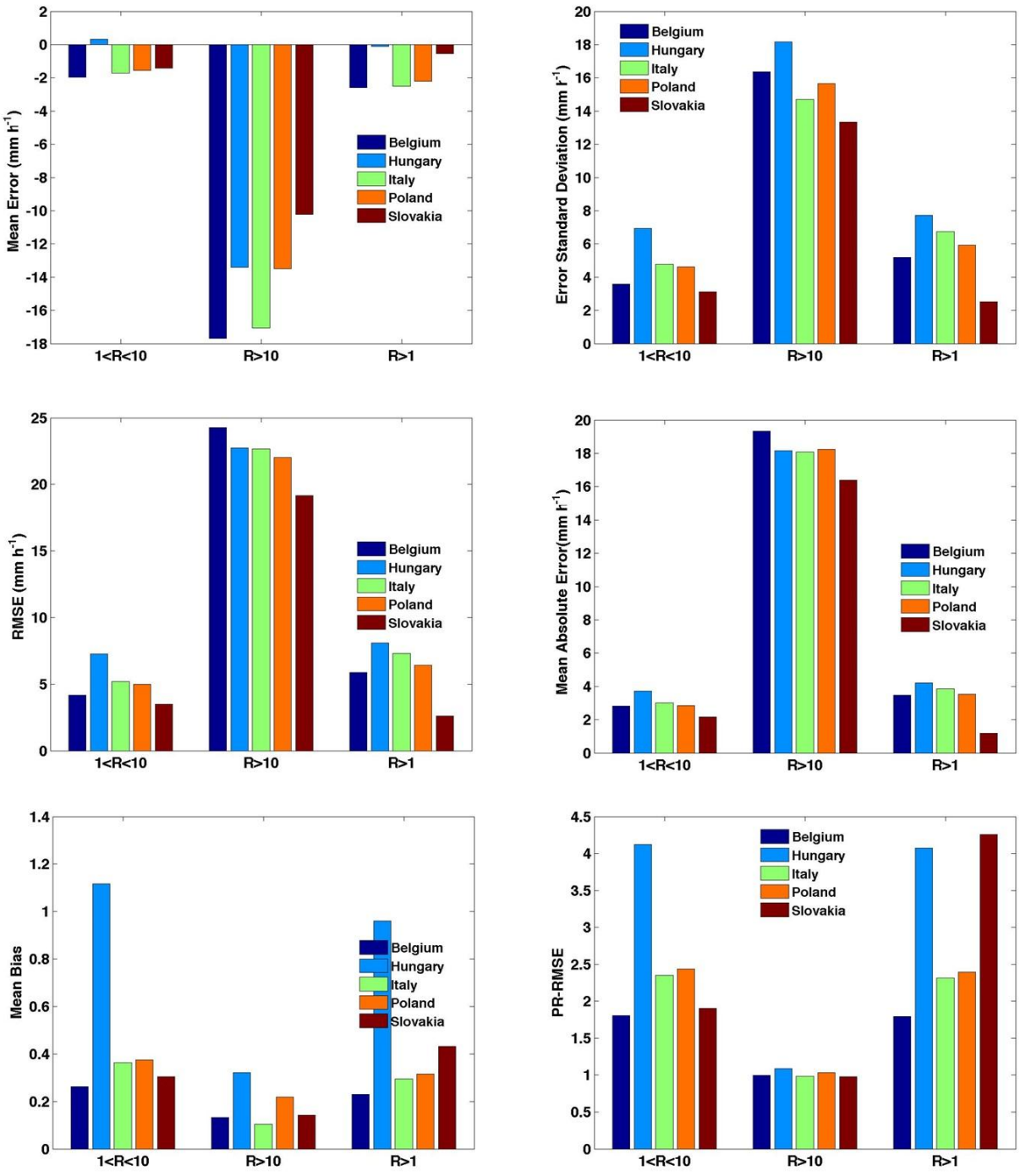

Figure 35 Yearly-aggregated error scores as retrieved using the gauge-based rainfall estimates as benchmark. The statistics refers to inland areas, while the reference period is 1st June 2013- 30th June 2014. Note that the PR-RMSE is not expressed in percentage.

6.5 The multi-categorical statistics

Two sets of validation have been performed:

- one set for Countries/Teams that has compared satellite data with meteorological radar in inner land areas: Belgium/BE, Hungary/HU, Italy, Poland/PL and Slovakia/SK;
- one set for Countries/Teams that has compared satellite data with rain gauges in inner land areas: Italy/IT, Poland/PL and Turkey/TR.

Each Country/Team contributes to this Chapter by providing the monthly contingency table and the statistical scores. The Validation Cluster Leader has collected all the validation files, has verified the consistency of the results and evaluated the monthly and yearly contingency tables and the statistical scores.

Radar validation

	Jun-2013	Jul-2013	Aug-2013	Sep-2013	Oct-2013	Nov-2013	Dec-2013	Jan-2014	Feb-2014	Mar-2014	Apr-2014	May-2014	Jun-2014	TOT
POD	0.28	0.40	0.34	0.25	0.16	0.25	0.16	0.13	0.05	0.076	0.13	0.33	0.22	0.21
FAR	0.77	0.65	0.59	0.58	0.81	0.80	0.91	0.84	0.90	0.94	0.93	0.87	0.87	0.89
CSI	0.14	0.23	0.23	0.19	0.10	0.12	0.06	0.08	0.03	0.03	0.05	0.1	0.09	0.07

Table 16 The averages POD, FAR and CSI deduced comparing H15A with radar data for the precipitation class R≥ 1mm/h.

The multi-category scores computed on the entire considered validation period are 0.21, 0.89 and 0.07, respectively for POD, FAR and CSI.

Rain gauge validation

	Jun-2013	Jul-2013	Aug-2013	Sep-2013	Oct-2013	Nov-2013	Dec-2013	Jan-2014	Feb-2014	Mar-2014	Apr-2014	May-2014	Jun-2014	TOT
POD	0.25	0.65	0.65	0.58	0.67	0.52	0.53	0.53	0.38	0.51	0.46	0.64	0.59	0.55
FAR	0.95	0.81	0.69	0.71	0.61	0.63	0.57	0.68	0.77	0.90	0.92	0.81	0.71	0.84
CSI	0.04	0.17	0.26	0.24	0.33	0.28	0.30	0.25	0.17	0.09	0.07	0.17	0.25	0.14

Table 17 The average POD, FAR and CSI deduced comparing H15A with rain gauge data for the precipitation class R≥ 1mm/h.

The multi-category scores computed on the entire considered validation period are 0.36, 0.90 and 0.08, respectively for POD, FAR and CSI.

6.7 Product requirement compliance

Table 18 summarizes the statistical scores obtained by the yearly validation of H15A with radar and rain gauge data . For the highest precipitation class H15A performs relatively well considering that RMSE% slightly exceeds (inland) the threshold when compared with the radar observations, while it is in between threshold and target using the rain gauge for comparison. Regarding the intermediate precipitation class, i.e. 1<R<10 mm h^{-1}, the RMSE% exceeds the threshold by more than 50%.

Between target and optimal	Between threshold and target	Threshold exceeded by < 50 %	Threshold exceeded by ≥ 50 %

PR-OBS-6A				Annual average of RMSE%		
Precipitation class	Requirement (RMSE %)			radar land	gauge land	radar coast
	thresh	target	optimal			
> 10 mm/h	90	80	25	102%	87%	104 %
1-10 mm/h	120	105	50	262%	258%	319 %

Table 18 Product requirement and compliance analysis for product H15A**.**

As shown in Chapter 4 it is not possible to consider radar and rain gauge fields like the 'ground truth'. It is well know that radar and rain gauge rainfall estimation is influenced by several error sources that should be carefully handled and characterized before using these data as reference for ground validation of any satellite-based precipitation products. An inventory of the precipitation ground networks, instruments and data available inside the PPVG has been provided in Chapter 4 in order to highlight the main error sources and to present a possible methodology for selecting the ground data that are more reliable. It is important to evaluate the limits of the "available truth", to estimate the errors of the data used to validate the satellite products and to understand if a direct comparison of the product requirements with the result of validation is completely correct.

The product requirements indicate what ***error*** is allowed by the user to the satellite product to be significantly useful (*threshold*), or to produce a step improvement in the application (*target*) or to produce the maximum improvement before entering saturation (*optimal*); it is the RMSE of satellite versus truth. Besides the result of validation activities indicate the ***difference*** between the satellite measurement and the ground measurement utilized as a reference; it is the RMSD of satellite versus reference data.

Obviously, RMSD > RMSE, since RMSD is inclusive of:
1) the error of satellite measurements RMSEsat;
2) the error of ground measurements RMSEground;
3) the error of the comparison methodology RMSEcomparison.

There are also errors related to satellite data used by H15A, not related to the algorithm, that have an impact on the H15A performances:
- pixel geolocation is retrieved by using the information made available by satellite owners, and it is not perfect; it is necessary to evaluate how much mislocations impact on the accuracy of the comparison. The effect is clearly larger for convective precipitation.
- parallax errors introduce mislocation of satellite precipitation, with associated comparison errors, larger for convective precipitation because of deeper penetration in the upper troposphere.

7. Summary conclusions on the status of product validation

The H15A product has been validated by the PPVG on one year of data 1st June 2013- 30th June 2014. Each Country/Team have provided case study and long statistics analysis using radar and rain gauge following the validation methodology reported in Chapter 3.

The results of the Precipitation Validation Programme are reported in this Product Validation Report (PVR). A precipitation product validation section of the H-SAF web page is under development. This validation web section will be continuously updated with the last validation results and studies coming from the Precipitation Product Validation Group (SPVG).

It is well know that radar and rain gauge rainfall estimation is influenced by several error sources that should be carefully handled and characterized before using these data as reference for ground validation of any satellite-based precipitation products. A complete inventory of the precipitation ground networks, instruments and data available inside the PPVG has been provided in Chapter 4 in order to highlight the main error sources and to present possible methodology for selecting the ground data more reliable.

Four case study have been analysed in Chapter 5. Convective precipitations during summer and winter periods have been analysed in different countries. Rain gauges with 10 minutes refresh time, radar data and nowcasting tools have been used to highlight different characteristics of the satellite product. The case studies proposed have pointed out that different statistical score values are obtained during summer and winter period.

In Chapter 6 the validation results of the H15A long statistics analysis obtained for the period (1.6.2013 – 30.06.2014), has been presented. To assess the degree of compliance of the product with product requirements Each Country/Team has provided the monthly contingency tables and the statistical scores. The results have been showed using radar and rain gauge as benchmark, over land and coast areas for the two precipitation classes defined in fig. 11 of Chapter 3.

For the highest precipitation class H15A performs relatively well considering that RMSE% slightly exceeds (inland) the threshold when compared with the radar observations, while it is in between threshold and target using the rain gauge for comparison. Regarding the intermediate precipitation class, i.e. 1<R<10 mm h^{-1}, the RMSE% exceeds the threshold by more than 50%.
This might be acceptable considering that the products has been conceived to deal with convective precipitation.

Annex 1: Introduction to H-SAF

The EUMETSAT Satellite Application Facilities

H-SAF is part of the distributed application ground segment of the "*European Organization for the Exploitation of Meteorological Satellites (EUMETSAT)*". The application ground segment consists of a "*Central Application Facilities*" located at EUMETSAT Headquarters, and a network of eight "*Satellite Application Facilities (SAFs)*", located and managed by EUMETSAT Member States and dedicated to development and operational activities to provide satellite-derived data to support specific user communities (see Figure 36):

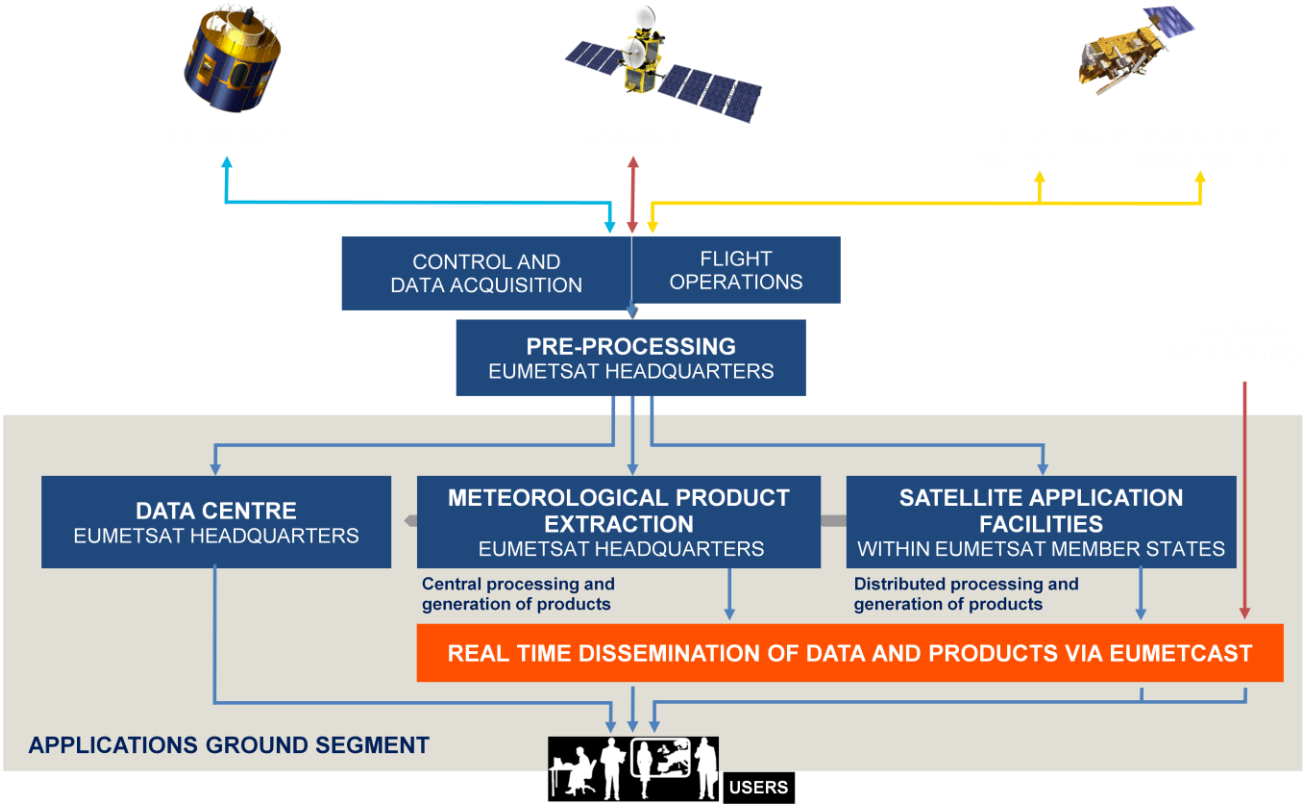

Figure 36: Conceptual scheme of the EUMETSAT Application Ground Segment

Figure 37, here following, depicts the composition of the EUMETSAT SAF network, with the indication of each SAF's specific theme and Leading Entity.

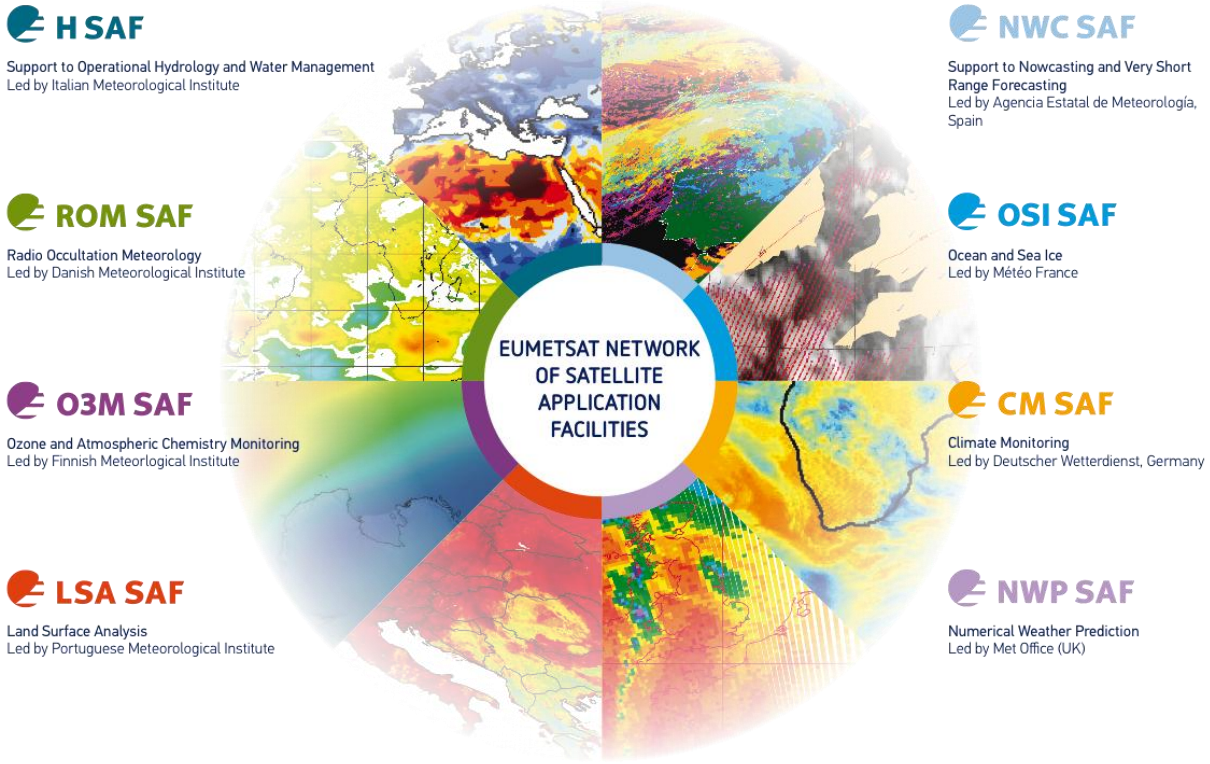

Figure 37: Current composition of the EUMETSAT SAF Network

Purpose of the H-SAF

The main objectives of H-SAF are:

a. ***to provide new satellite-derived products*** from existing and future satellites with sufficient time and space resolution to satisfy the needs of operational hydrology, by generating, centralizing, archiving and disseminating the identified products:

- precipitation (liquid, solid, rate, accumulated);
- soil moisture (at large-scale, at local-scale, at surface, in the roots region);
- snow parameters (detection, cover, melting conditions, water equivalent);

b. ***to perform independent validation of the usefulness of the products*** for fighting against floods, landslides, avalanches, and evaluating water resources; the activity includes:

- downscaling/upscaling modelling from observed/predicted fields to basin level;
- fusion of satellite-derived measurements with data from radar and raingauge networks;
- assimilation of satellite-derived products in hydrological models;
- assessment of the impact of the new satellite-derived products on hydrological applications.

Products / Deliveries of the H-SAF

For the full list of the Operational products delivered by H-SAF, and for details on their characteristics, please see H-SAF website hsaf.meteoam.it.

All products are available via EUMETSAT data delivery service (EUMETCast, http://www.eumetsat.int/website/home/Data/DataDelivery/EUMETCast/index.html), or via ftp download; they are also published in the H-SAF website hsaf.meteoam.it.

All intellectual property rights of the H-SAF products belong to EUMETSAT. The use of these products is granted to every interested user, free of charge. If you wish to use these products, EUMETSAT's copyright credit must be shown by displaying the words "copyright (year) EUMETSAT" on each of the products used.

System Overview

H-SAF is lead by the Italian Air Force Meteorological Service (ITAF USAM) and carried on by a consortium of 21 members from 11 countries (see website: hsaf.meteoam.it for details)

Two major areas can be distinguished within the H-SAF system context:

- Product generation area
- Central Services area (for data archiving, dissemination, catalogue and any other centralized services)
- Validation services area which includes Quality Monitoring/Assessment and Hydrological Impact Validation.

Products generation area is composed of 5 processing centres physically deployed in 5 different countries; these are:

- for precipitation products: ITAF CNMCA (Italy)
- for soil moisture products: ZAMG (Austria), ECMWF (UK)
- for snow products: TSMS (Turkey), FMI (Finland)

Central area provides systems for archiving and dissemination; located at ITAF CNMCA (Italy), it is interfaced with the production area through a front-end, in charge of product collecting.

A central archive is aimed to the maintenance of the H-SAF products; it is also located at ITAF CNMCA.

Validation services provided by H-SAF consists of:

- Hydrovalidation of the products using models (hydrological impact assessment);
- Product validation (Quality Assessment and Monitoring).

Both services are based on country-specific activities such as impact studies (for hydrological study) or product validation and value assessment.

Hydrovalidation service is coordinated by IMWM (Poland), whilst Quality Assessment and Monitoring service is coordinated by DPC (Italy): The Services' activities are performed by experts from the national meteorological and hydrological Institutes of Austria, Belgium, Bulgaria, Finland, France, Germany, Hungary, Italy, Poland, Slovakia, Turkey, and from ECMWF.

Annex 2: First Report "Rain gauge data used in PPVG "

Coordinator: Federico Porcù (University of Ferrara), Silvia Puca (DPC), Italy
Participants: Emmanuel Roulin and Angelo Rinollo (Belgium), Gergana Kozinarova (Bulgaria), Claudia Rachimow and Peter Krahe (Germany), Rafal Iwanski and Bozena Lapeta (Poland), Ibrahim Sonmez and Ahmet Oztopal (Turkey), Emanuela Campione (Italy).

0. Introduction

This document reports on the outcomes of the inventory completed about the raingauges used as "ground reference" within the validation groups. Moreover, some general conclusion is drawn, based on the raingauges validation activities carried on in the last years by the Validation Group of H-SAF. The inventory was structured in three sections, dealing with the instruments used, the operational network and the approach to match gauge data with the satellite estimates. The results are summarized in the next pages.

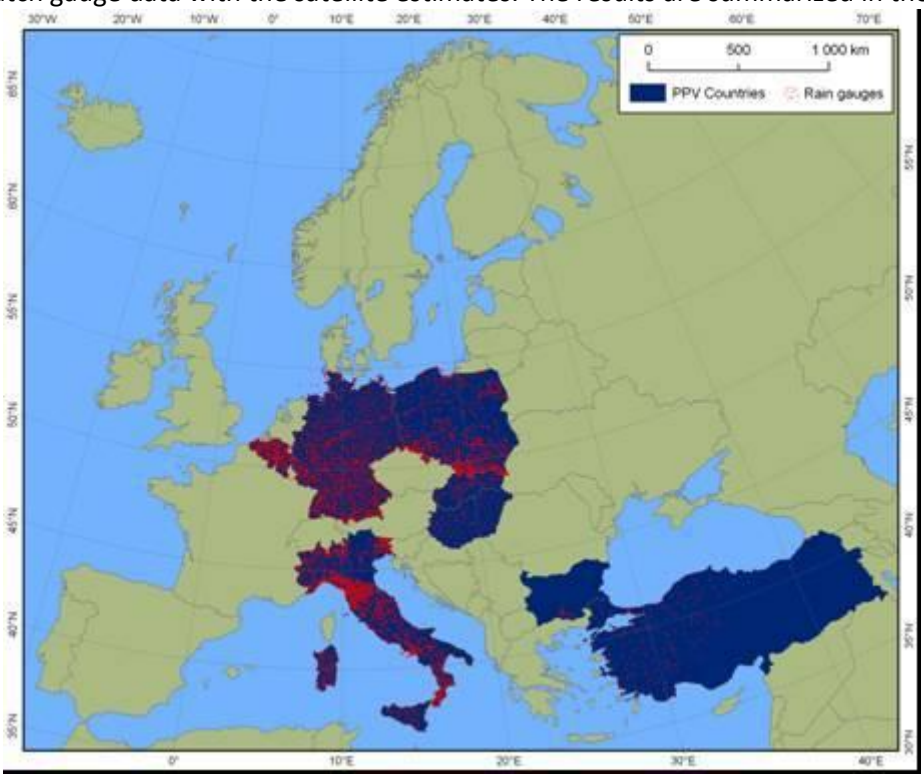

Figure 38 Rain gauge networks in PPVG

1. The Instruments

Most of the gauges used in the National networks by the Precipitation Product Validation Group (PPVG) Partners are of the tipping bucket type, which is the most common device used worldwide to have continuous, point-like rainrate measurement. Nevertheless, several source of uncertainty in the measurements are well known but difficult to mitigate. First, very light rainrates (1 mm h^{-1} and less) can be incorrectly estimated due to the long time it takes the rain to fill the bucket (Tokay et al., 2003). On the other side, high rainrates (above 50 mm h^{-1}) are usually underestimated due to the loss of water during the tips of the buckets (Duchon and Biddle, 2010). Drifting wind can also greatly reduce the size of the effective catching area, if rain does not fall vertically, resulting in a rainrate underestimation quantitatively assessed in about 15% for an average event (Duchon and Essenberg, 2001).
Further errors occur in case of solid precipitation (snow or hail), when frozen particles are collected by the funnel but not measured by the buckets, resulting in a temporal shift of the measurements since the

melting (and the measure) can take place several hours (or days, depending on the environmental conditions) after the precipitation event (Leitinger et al, 2010, Sugiura et al, 2003). This error can be mitigated by an heating system that melts the particles as soon as are collected by the funnel. All these errors can be mitigated and reduced, but in general not eliminated, by a careful maintenance of the instrument.
A number of *a posteriori* correction strategies have been developed in order to correct precipitation data measured by raingauges, but mainly apply at longer accumulation intervals, daily to monthly (Wagner, 2009)

Country	Minimum detectable rainrate	Maximum detectable rainrate (mm h^{-1})	Heating system (Y/N)	cumulation interval (min)
Belgium	0.1 mm	N/A**	N	60
Bulgaria	0.1 mm	2000	Y	120, 1440
Germany	0.05 mm h^{-1}	3000	Y	60
Italy	0.2 mm	N/A**	Y/N*	60
Poland	0.1 mm	N/A**	Y	10
Turkey	0.2 mm	720	Y	1

Table 19 Summary of the raingauge characteristics

* only 300 out of 1800 gauges are heated
** information not available at the moment: a value about 300 mmh^{-1} can be assumed for tipping bucket raingauges.

Most of these shortcomings could be avoided by using instruments based on different principle or mechanisms. The German network, and a part of the Bulgarian network, as an example, are equipped by precipitation weighting gauges, that allow continuous precipitation (both solid and liquid) measurements with higher accuracy. Other option could be the use of disdrometers, that give more information about the precipitation structure and a more accurate rainrate measure.
In table 1 relevant characteristics of the raingauges used in the different countries are reported.

2. The networks

The validation work carried on with raingauges uses about 3000 instruments across the 6 Countries, as usual, irregularly distributed over the ground. A key characteristics of such networks is the distance between each raingauge and the closest one, averaged over all the instruments considered in the network and it is a measure of the raingauge density. Instruments number and density are summarized in table 2.
The gauges density ranges between 7 (for Bulgaria, where only 3 river basins are considered) to 27 km (for Turkey). These numbers should be compared with the decorrelation distance for precipitation patterns at mid-latitude. Usually the decorrelation distance is defined as the minimum distance between two measures to get the correlation coefficient (Pearson Coefficient) reduced to e^{-1}. A recent study on the H-SAF hourly data for Italy, shows this decorrelation distance varies from about 10 km in warm months (where small scale convection dominates) to 50 km in cold months, when stratified and long lasting precipitation mostly occur. In next figure the value of the linear correlation coefficient is computed between each raingauge pair in the Italian hourly 2009 dataset, as function of the distance between the two gauges.

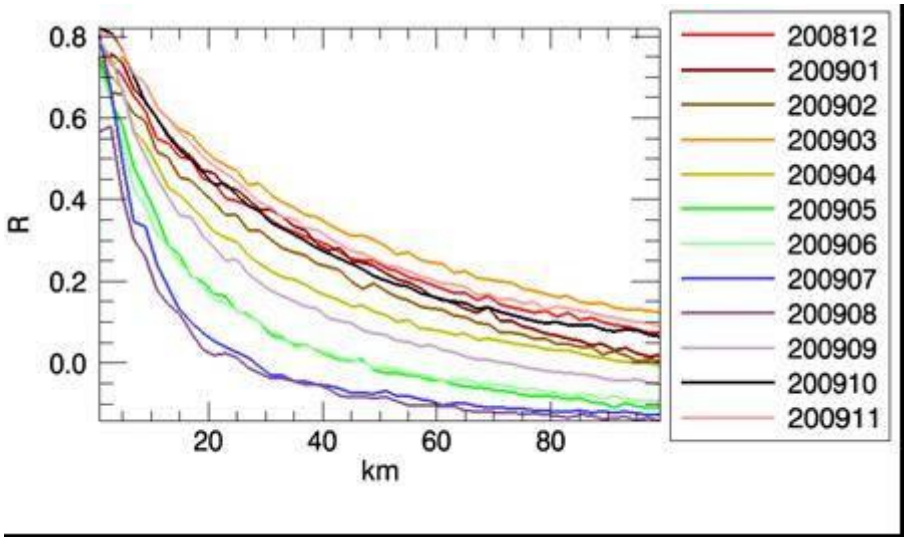

Figure 39 Correlation coefficient between raingauge pairs as function of the distances between the gauges. Colours refer to the months of the year 2009

Assuming these values significant for the other Countries involved in this study, we can conclude the distribution of gauges is capable to resolve the spatial structure of rain patterns only for stratified systems but it is inadequate for small scale convective events.

Country	Total number of gauges *	Average minimum distance (km)
Belgium	89**	11.2
Bulgaria	37***	7
Germany	1300	17
Italy	1800	9.5
Poland	330-475	13.3
Turkey	193****	27

Table 20 Number and density of raingauges within H-SAF validation Group

* the number of raingauges could vary from day to day due to operational efficiency within a maximum range of 10-15%.
** only in the Wallonia Region
*** only in 3 river basins
**** only covering the western part of Anatolia

3. Data processing

The partners of the Validation Group have been using a variety of different strategies to treat gauge data and to compare them with satellite estimates. Some are using interpolation algorithms to get spatially continuous rainfall maps, while others process directly the measurements of individual gauges. All the data in the network (except for cold months in Poland) are quality controlled: there is no information about the techniques used, but usually quality control rejects data larger than a given threshold and in case of too high rainrate difference (exceeding given thresholds) among neighbouring gauges and between subsequent measures of the same instrument. Table 21 summarizes the data pre-processing performed in different Countries, while Table 22 and Table 23 reports the different matching approaches for H01-H02 and H03-H05, respectively.
As for the temporal matching, the used approaches are rather homogeneous within the Groups: instantaneous measurements are matched with next ground cumulated values over the different available

intervals, ranging from 1 minute (Turkey) to 1 hour (Italy, Germany). Cumulated estimates, obviously, are compared to ground measured rain amounts over the same cumulation intervals.
As for spatial matching, different approaches are considered, also taking into account the different spatial structure of the satellite IFOVs. Two basic ideas are pursued: pixel-by-pixel matching or ground measure averaging inside satellite IFOV. The second approach seems to be more convenient, especially when the "large" IFOV of H01 and H02 are concerned. Probably it is mandatory for H02 also take into account that the size of the IFOV changes across the track and could become very large. The first approach, e.g. nearest neighbour, can be more effective for H03 and H05 products.

Country	Type of interpolation	Quality control (Y/N)
Belgium	Barnes over 5x5 km grid	Y
Bulgaria	Co kriging	Y
Germany	Inverse square distance	Y
Italy	Barnes over 5x5 km grid	Y
Poland	No	Y (except cold months)
Turkey	No	Y

Table 21 Data pre-processing strategies

	H01		H02	
Country	Spatial matching	Temporal matching	Spatial matching	Temporal matching
Belgium*	N/A	N/A	N/A	N/A
Bulgaria*	N/A	N/A	N/A	N/A
Germany	matching gauges are searched on a radius of 2.5 km from the IFOV centre	each overpass is compared to the next hourly rain amount	matching gauges are searched on a radius of 2.5 km from the IFOV centre	each overpass is compared to the next hourly rain amount
Italy	mean gauges value over 15x15 km area centred on satellite IFOV	each overpass is compared to the next hourly rain amount	Gaussian-weighted mean gauges value centred on satellite IFOV	each overpass is compared to the next hourly rain amount
Poland	mean gauges value over the IFOV area (rectangular)	each overpass is compared to the next 10-minutes rain amount	mean gauges value over the IFOV area (rectangular)	each overpass is compared to the next 10-minutes rain amount
Turkey	weighted mean (semi variogram) gauges value centred on satellite IFOV	each overpass is compared to the corresponding 1-minute rain rate	weighted mean (semi variogram) gauges value over centred on satellite IFOV	each overpass is compared to the corresponding 1-minute rain rate

Table 22 Matching strategies for comparison with H01 and H02

*Belgium and Bulgaria use raingauges only for cumulated precipitation validation.

	H03		H05	
Country	Spatial matching	Temporal matching	Spatial matching	Temporal matching
Belgium*	N/A	N/A	Nearest neighbour	rain amounts in the same number of hours are compared (24 hours)
Bulgaria*	N/A	N/A	Nearest neighbour	rain amounts in the

				same number of hours are compared (3 and 24 hours)
Germany	matching gauges are searched on a radius of 2.5 km from the IFOV centre	each overpass is compared to the next hourly rain amount	matching gauges are searched on a radius of 2.5 km from the IFOV centre	rain amounts in the same number of hours are compared (3, 6, 12 and 24 hours).
Italy	Nearest neighbour	the average rainrate over a given hour Is compared to next hourly rain amount	Nearest neighbour	rain amounts in the same number of hours are compared (3,6,12 and 24 hours).
Poland	mean gauges value over the pixel area	each overpass is compared to the next 10-minutes rain amount	mean gauges value over the pixel area	rain amounts in the same number of hours are compared(3,6,12 and 24 hours).
Turkey	weighted mean (semi variogram) gauges value centred on satellite IFOV	each overpass is compared to the corresponding 1-minute rain rate	weighted mean (semi variogram) gauges value over centred on satellite IFOV	rain amounts in the same number of hours are compared (3,6,12 and 24 hours).

Table 23 Matching strategies for comparison with H03 and H05

*Belgium and Bulgaria use raingauges only for cumulated precipitation validation.

Conclusions

After this inventory some conclusion can be drawn.
First, it seems the raingauge networks used in this validation activities are surely appropriated for the validation of cumulated products (1 hour and higher), while for instantaneous estimates the use of hourly cumulated ground measurements surely introduces intrinsic errors in the matching scores, that can be estimated as very large. The validation of instantaneous estimates should be carried on only when gauges cumulation interval is 10 to 15 minutes (as in Poland). Values cumulated over shorter intervals (5 or even one minute, as it is done in Turkey) are affected by large relative errors in cases of low/moderate rainrates.
Different approaches for the estimates matching are considered, and probably could be a good idea to harmonize them among partners. As an example, for H02 a document was delivered by the developers, where the best estimate-ground reference matching strategy was indicated, and also Angelo Rinollo delivered few years ago the code for the Gaussian weight of the antenna pattern in the AMSU/MHS IFOV.
Anyway, different approaches over different Countries are leading to very similar values in the considered skill scores, indicating probably two things: 1) none of the considered approaches can be considered as inadequate and (more important) 2) the differences between ground fields and satellite estimates are so large that different views in the data processing do not results in different numbers.

5. References

Duchon, C.E. and G.R. Essenberg, G. R., 2001, Comparative rainfall observations from pit and aboveground gauges with and without wind shields, *Water Resour. Res.*, **37**, 3253–3263.

Duchon, C.E. and C.J. Biddle, 2010, Undercatch of tipping-bucket gauges in high rain rate events. *Adv. Geosci*., **25**, 11–15.

Leitinger, G., N. Obojes and U. Tappeiner, 2010, Accuracy of winter precipitation measurements in alpine areas: snow pillow versus heated tipping bucket rain gauge versus accumulative rain gauge, EGU General Assembly 2010, held 2-7 May, 2010 in Vienna, Austria, p.5076.

Sevruk, M. Ondrás, B. Chvíla, 2009, The WMO precipitation measurement intercomparisons, *Atmos. Res.,* **92**, 376-380.

Sugiura, K., D. Yang, T. Ohata, 2003, Systematic error aspects of gauge-measured solid precipitation in the Arctic, Barrow, Alaska. *Geophysical Research Letters,* **30**, 1-5.

Schutgens, N.A.J. and R.A. Roebeling, 2009, Validating the validation: the influence of liquid water distribution in clouds on the intercomparison of satellite and surface observations, *J. Atmos. Ocean. Tech.*, **26**, 1457-1474

Tokay, A., D.B. Wolff, K.R. Wolff and P. Bashor, 2003, Rain Gauge and Disdrometer Measurements during the Keys Area Microphysics Project (KAMP). *J. Atmos. Oceanic Technol.*, **20**, 1460-1477.

Wagner, A., 2009, Literature Study on the Correction of Precipitation Measurements, FutMon C1-Met-29(BY), 32 p. available at *www.futmon.org*.

Annex 3: First Report "Radar data used in PPVG "

Coordinators: Estezr Labo (HMS) Hungary and Gianfranco Vulpiani (DPC), Italy
Contributors: Angelo Rinollo (Belgium), Jan Kanak and Luboslav Okon (Slovakia), Firat Bestepe (Turkey), Rafal Iwanski (Poland), Claudia Rachimow (Germany)

Description of tasks:
In the HSAF project, satellite-based precipitation estimations are compared regularly with the radar-derived precipitation fields. However, radar rainfall products are influenced by several error sources that should be carefully analyzed and possibly characterized before using it as a reference for validation purposes.
However, we have to emphasize that the radar data used for validation purposes is not developed by the validation groups themselves. They are developed within specialized radar working teams in many of the countries. Therefore, it should not be the aim of the work of the Radar WG to improve the radar data used; however, it is specifically expected from the current activities to characterize radar data and error sources of the ground data coming from the radar networks of the Precipitation Validation Group (PPVG).
Main error sources of radar rainfall estimations are listed in the Radar Working Group description document:

- system calibration,
- contamination by non-meteorological echoes, i.e. ground clutter, sea clutter, "clear air" echoes (birds, insects), W-LAN interferences,
- partial or total beam shielding,
- rain path attenuation,
- wet radome attenuation,
- range dependent errors (beam broadening, interception of melting snow),
- contamination by dry or melting hail ("hot spots"),
- variability of the Raindrop Size Distribution (RSD) and its impact on the adopted inversion techniques

Moreover, several studies have been on radar quality assessments like *S´ alek M, Cheze J-L, Handwerker J, Delobbe L, Uijlenhoet R. 2004.: Radar techniques for identifying precipitation type and estimating quantity of precipitation. COST Action 717, Working Group 1 – A review. Luxembourg, Germany*; or *Holleman, I., D., Michelson, G. Galli, U. Germann and M. Peura, Quality information for radars and radar data, Technical rapport: 2005, EUMETNET OPERA, OPERA_2005_19, 77p.*

Our main purpose for the first step was to collect characteristics (polarization, beam width, maximum range, range, resolution, scan frequency, geographical coordinates, scan strategy [elevations]…) of the radar networks which composes the PPVG adopted processing chain; and the generated products (including the quality map, if any). This report is intended to present the results of the overview of different radar capacities and instruments in each of the participating countries.

Radar sites and radars:
In the PPVG group, we have all together 54 radars used, or in the plan to be used. Their distribution in the countries is:

- Belgium (1 radar)
- Germany (16 radars – not BfG products)
- Hungary (3 radars)
- Italy (18 radars)
- Slovakia (2 radars)
- Poland (8 radars)
- Turkey (6 radars)

These radars cover wide range of geographical area: from the longitude 5.50562 in Wideumont, Belgium to the most Eastern area with longitude 32°58'15" in Ankara, Turkey; and from the Northern latitude of 54°23’03,17’’ in Gdańsk, Poland to the latitude of 36°53'24" in Mugla, Turkey and lat 37,462 in Catania, Italy.
Radars are built at different elevations above the sea level. In mountainous countries, they are placed at elevations more than 1000m above sea level; whereas in flat countries like Hungary or Belgium, their height position is not exceeding 400m. This information collected will be useful in the future steps of the Working Group to assess the partial or total beam shielding by mountains in the propagation way of the radar signals.

All radars are C-band radars, working at frequency in C-band, at 5.6 GHz. This is important to know that our radar system is comparable.
All radars are equipped by Doppler capacity which means that ground clutters can be removed from the radar data measurements effectively; however, not all of them have dual polarization which would be important to correct rain path attenuation.

Scan strategies:
We have explored the scan strategy for each of the radars used. In this matter, all countries have shared their information on the number of elevations, minimum and maximum elevations, scan frequency, maximum nominal range distance, and range resolution.

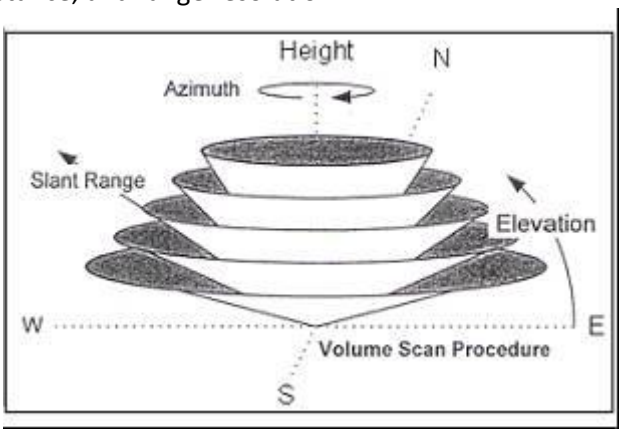

We can conclude that the scan frequency ranges from 5 minutes in Belgium, Germany and Slovakia to 10 minutes in Turkey and Poland, and 15 minutes in Hungary; and varying frequency for Italian radars.
The number of elevation stays between 4 and 15, in average around 10.
The range distance used is 240 km in general. But in some places in Italy, and for the Turkish radars, the maximum range distance used is 120 km, or even less, e.g. 80 km.
Range resolution is 250 m in Belgium, 250, 340, 225, and sometimes 500 m for the Italian radars, 500 m for one of the Hungarian radars, and 250m for the other two, Polish radars can work with 125 m and 250 m resolution, and in Turkey it is 250 m for all the radars.
All in all, the scan strategies within the PPVG countries are well-balanced and similar to each other; though they vary from one radar to the other, even within countries.

All radars are regularly maintained and calibrated, which is a good indicator of the continuous supervision of quality of radar data, and the important element to sustain radar data quality.

Overview of radar products used for validation in the HSAF project:

The Table at the end of the report is provided to summarize the available products generated from radar measurements, and the processing chain used to generate them. Finally, the list of the radar products used for the validation work is included in the last row.
Radar rainfall products are obtained after processing the measured radar reflectivities at different elevations of the radar scan strategy. After each elevation, the PPI (Plan Position Indicator) products and the CAPPI (Constant Altitude PPI) products are calculated. PPI is the measurement of the radar antenna rotating 360 degrees around the radar site at a fixed elevation angle. CAPPI products are derived from this, by taking into account the radar displays which give a horizontal cross-section of data at constant altitude. The CAPPI is composed of data from several different angles that have measured reflectivity at the requested height of CAPPI product.
The PPVG group uses mostly CAPPI products for calculation of rainfall intensities; except for Hungary, which uses the CMAX data (maximum radar reflectivity in each pixel column among all of the radar elevations) for deriving rainfall intensities. However, the rest of the countries have also chosen different elevation angles for the CAPPI product which provides the basis for rain rate estimations. Additionally, we have to say that the countries apply different techniques of composition of radar data that were not specified in this questionnaire. The composition technique is important in areas which are covered by more than one radar measurements. Also, the projection applied is varying from one country to the other.
To sum up, the radar products used are not harmonized, different techniques are applied. However, each of them is capable to grasp rainfall and to estimate rainfall intensity.

As for the accumulated products, we see that Belgium uses 24-hourly accumulations, with rain gauge correction, Italy uses 3, 6, 12, 24h accumulations without gauge-correction; in Hungary 3, 6, 12, 24h data is used, but only the 12h and 24 hourly accumulations are corrected by rain gauges, in Poland and Slovakia no rain gauge correction is applied. Poland has only 6, and 24 hourly data. Turkey has 3,6,12,24h data, and applies rain gauge correction for 1 hourly data. It is important to note that techniques used for accumulation are numerous, even within the same country the can differ from one accumulation period to another. E.g. in Hungary, the 3,6h accumulations are derived from summing up the interpolation of the 15minute-frequent measurements into 1 minute-intervals; whereas the 12, and 24 h accumulations are summed up from 15 minute measurements, but corrected with rain gauge data.
All above implies that more probably the quality and error of rainfall and rain rate accumulations is differing from one country to another; and cannot be homogeneously characterized.

Conclusion of the questionnaire

Maintenance

All the contributors declared the system are kept in a relatively good status.

Correction factors for error elimination:

These correction factors are diverse in the countries, not homogeneous distribution of correction methods:

- all contributors compensate for non-meteorological echoes (Clutter)
- RLAN interferences implemented in Hungary, Slovakia- in development.
- Poland and Slovakia correct attenuation. In other countries, it is not accounted for.
- Some of the countries are testing new procedures for dealing with VPR (Italy) and Partial Beam Blockage, PBB effects. VPR (Vertical Profile of Refelctivity) used in Turkey.

This means that the corresponding rainfall estimates are diverse, and the estimation of their errors cannot be homogenized.
However, each county can provide useful information of the error structure of its rainfall products based on its own resources: e.g. if they have already defined Quality Indicators, or estimations of errors based on studies of comparison of radar and rain gauge data in the country itself.

In the future, possible separation of reliable and quasi-reliable radar fields would be possible. Separation would be based on radar site/geographical areas/event type/radar products. Selected cases will be suitable enough to be used as a reference for the H-SAF products validation.

Satellite product testing will be carried out in areas with higher reliability. Statistical results will be evaluated and compared to previous data. As such, the accuracy of statistical results of PPVG with radar data as ground reference will be able to be established.

References

References have been collected from each country describing radar data, radar data quality, and radar data quality estimation techniques. This list will be the baseline for further work of the Radar WG.

The following list of references has been set up:

Belgium

Goudenhoofdt, E. and Delobbe, L.: Evaluation of radar-gauge merging methods for quantitative precipitation estimates, Hydrol. Earth Syst. Sci., 13, 195-203, doi:10.5194/hess-13-195-2009, 2009. http://radar.meteo.be/en/3302595-Publications.html

Berne, A., M. ten Heggeler, R. Uijlenhoet, L. Delobbe, Ph. Dierickx, and M. De Wit, 2005. A preliminary investigation of radar rainfall estimation in the Ardennes region. Natural Hazards and Earth System Sciences, 5, 267-274. http://radar.meteo.be/en/3302595-Publications.html

Italy

Fornasiero A., P.P. Alberoni, G. Vulpiani and F.S. Marzano, "Reconstruction of reflectivity vertical profiles and data quality control for C-band radar rainfall estimation", Adv. in Geosci., vol. 2, p. 209-215, 2005. http://www.adv-geosci.net/2/index.html

R. Bechini, L. Baldini, R. Cremonini, E. Gorgucci . Differential Reflectivity Calibration for Operational Radars, Journal of Atmospheric and Oceanic Technology, Volume 25, pp. 1542-1555, 2008. http://journals.ametsoc.org/doi/pdf/10.1175/2008JTECHA1037.1

Silvestro, F., N. Rebora, and L. Ferraris, 2009: An algorithm for real-time rainfall rate estimation using polarimetric radar: Rime. J. Hydrom., 10, 227–240.

Vulpiani, G., P. Pagliara, M. Negri, L. Rossi, A. Gioia, P. Giordano, P. P. Alberoni, Roberto Cremonini, L. Ferraris, and F. S. Marzano, 2008: The Italian radar network within the national early-warning system for multi-risks management. Proceed. of 5th European Radar Conference (ERAD), Helsinki (Finland); http://erad2008.fmi.fi/proceedings/extended/erad2008-0184-extended.pdf

Vulpiani, G., M. Montopoli, L. Delli Passeri, A. Gioia, P. Giordano and F. S. Marzano, 2010: On the use of dual-polarized C-band radar for operational rainfall retrieval in mountainous areas. submitted to J. Appl. Meteor and Clim. http://www.erad2010.org/pdf/oral/tuesday/radpol2/5_ERAD2010_0050.pdf

Hungary

Péter Németh: Complex method for quantitative precipitation estimation using polarimetric relationships for C-band radars. Proceed. of 5th European Radar Conference (ERAD), Helsinki (Finland); http://erad2008.fmi.fi/proceedings/extended/erad2008-0270-extended.pdf

Slovakia

D. Kotláriková, J. Kaňák and I. Strmiska: Radar horizon modelling as a requirement of SHMI radar network enhancement, Physics and Chemistry of the Earth, Volume 25, Issues 10-12, 2000, Pages 1153-1156 First European Conference on Radar Meteorology, doi:10.1016/S1464-1909(00)00170-2

Poland

Szturc, J., Ośródka, K., and Jurczyk, A., 2008. Parameterization of QI scheme for radar-based precipitation data. Proceedings of ERAD 2008.
http://erad2008.fmi.fi/proceedings/extended/erad2008-0091-extended.pdf
Szturc, J., Ośródka, K., and Jurczyk, A., 2009. Quality index scheme for 3D radar data volumes, 34th Conf. on Radar Meteorology. Proceedings. AMS, 5-9.10.2009, Williamsburg VA, USA;
Katarzyna Osrodka, Jan Szturc, Anna Jurczyk, Daniel Michelson, Gunther Haase, and Markus Peura: Data quality in the BALTRAD processing chain., Proceed. of 6th European Radar Conference (ERAD 2010), Sibiu (Romania);
http://www.erad2010.org/pdf/oral/wednesday/dataex/06_ERAD2010_0240.pdf
Szturc, J., Ośródka, K. and Jurczyk, A. , Quality index scheme for quantitative uncertainty characterization of radar-based precipitation. Meteorological Applications, 2010 (doi: 10.1002/met.230)

	BELGIUM	ITALY	HUNGARY
List of Available Products.	Rain rate 240 Km; rain rate 120 Km; velocity (120 Km); MAX (240 Km); VVP2 Windprofiles; Hail Probability; Hail Probability 24h Overview; 1, 3, 24 Hr Rainrate accumulation;		CMAX, PPI, CAPPI(2.5 km), VIL, ETops, Base, HailProbability
Is any quality map available?	NO	YES	NO
Processing chain	Clutter removal (time-domain Doppler filtering and static clutter map); Z-R: a=200, b=1.6	Clutter suppression by Fuzzy Logic scheme using Clutter map, Velocity, Texture. Z-R: a=200, b=1. VPR correction under testing.	RLAN(wifi) filter; Clutter removal; atttenuation correction + beam blocking correction => next Year (2012) VPR => No Z-R: a=200, b=1.6
Description of instanteneous radar product used in HSAF Validation Activities	PCAPPI-1500m Cartesian grid, 600m resolution	Nationale composite: CAPPI 2 km, CAPPI 3 km, CAPPI 5 km, VMI, SRI Projection: Mercator Resolution: 1 km Threshold: No	National composite, (CMAX) Projection: stereographic (S60) Resolution: 2 km Threshold: 7dBZ No rain gauge correction
Description of accumulated radar product used in HSAF Validation Activities	24-h accumulation with range-dependent gauge adjustment, Cartesian grid, 600m resolution	Acc. periods: 1, 3, 6, 12, 24h Projection: Mercator Resolution: 1 km Threshold: No No rain gauge correction	Acc.periods: 3,6,12,24h National composite, (CMAX) Projection: stereographic (S60) Resolution: 2 km Threshold: 7dBZ Rain gauge correction applied for 12, 24 hourly data

	POLAND	**SLOVAKIA**	**TURKEY**
List of Available Products.	PPI, PCAPPI, RHI, MAX, EHT, SRI, PAC, VIL, VVP, HWIND, VSHEAR, HSHEAR, LTB, SWI, MESO, WRN. List of non-operational products: LMR, CMAX, UWT, VAD, SHEAR, SWI, MESO, ZHAIL, RTR, CTR, WRN.	CAPPI 2 km, Etops, PPI 0.2, Base, Cmax, Hmax, VIL, Precip. Intensity, 1h-, 3h-, 6h-, 24h-acc. precip., 1h-acc. SRI 1km, 2km agl	MAX, PPI, CAPPI, VIL, ETOPS, EBASE, RAIN Acumulation (1,3,6,12,24h)
Processing chain	Doppler method clutter removal; atenuation correction - yes; VPR => No Z-R: a=200, b=1.6	Clutter filtering: frequency-domain IIR filter; Atmospheric attenuation correction; Z-R: a=200, b=1.6 RLAN filtering in development	Clutter Removal, VPR Correction, Z-R: A=200 b=1.6
Is any quality map available?	NO, in development	NO	NO
Description of instanteneous radar product used in HSAF Validation Activities	National composite, (SRI); Projection: azimutal equidistant (standard: elipsoid); Resolution: 1 km; Threshold: 5 dBZ; No rain gauge correction.	National composite CAPPI 2 km Projection: Mercator Resolution: 1 km Threshold: -31.5 dBZ No rain gauge correction	CAPPI, Projection: Azimuthal Equidistant Resolution: 250 m Threshold: ? Rain Gauge Correction (with limited number of gauges)
Description of accumulated radar product used in HSAF Validation Activities	Acc. Periods: 1, 6, 24h; National composite (PAC), Projection: azimuthal equidistant (standard: elipsoid); Resolution: 1 km; Treshold: 0,1 mm; No rain gauge correction	Acc. periods: 3, 6, 12, 24h National composite CAPPI 2 km Projection: Mercator Resolution: 1 km Threshold: -31.5 dBZ No rain gauge correction	Acc.periods: 1,3,6,12,24h Projection: Azimuthal Equidistant Resolution: 250 m Threshold: ? Rain gauge correction applied for 1h Rain Acc.

Annex 4: Study on evaluation of radar measurements quality indicator with regards to terrain visibility

Ján Kaňák, Ľuboslav Okon, SHMÚ

For validation of H-SAF precipitation products it is necessary to know errors distribution of used ground reference. In this case precipitation intensity or accumulated precipitation measured by SHMÚ radar network is considered as a ground reference. To find distribution of errors in radar range next steps must be done:

- simulations of terrain visibility by radar network using 90m digital terrain model
- statistical comparison of radar data against independent rain gauge data measurements
- derivation of dependence (regression equation) describing the errors distribution in radar range with regard to terrain visibility, based on rain gauge and radar data statistical evaluation
- computation of error distribution maps using regression equation and terrain visibility

24-hour cumulated precipitation measurements from 68 automatic precipitation stations from the period 1 May 2010 – 30 September 2010 were coupled with radar based data. Distribution of gauges according their elevation above the sea level is shown in next figure.

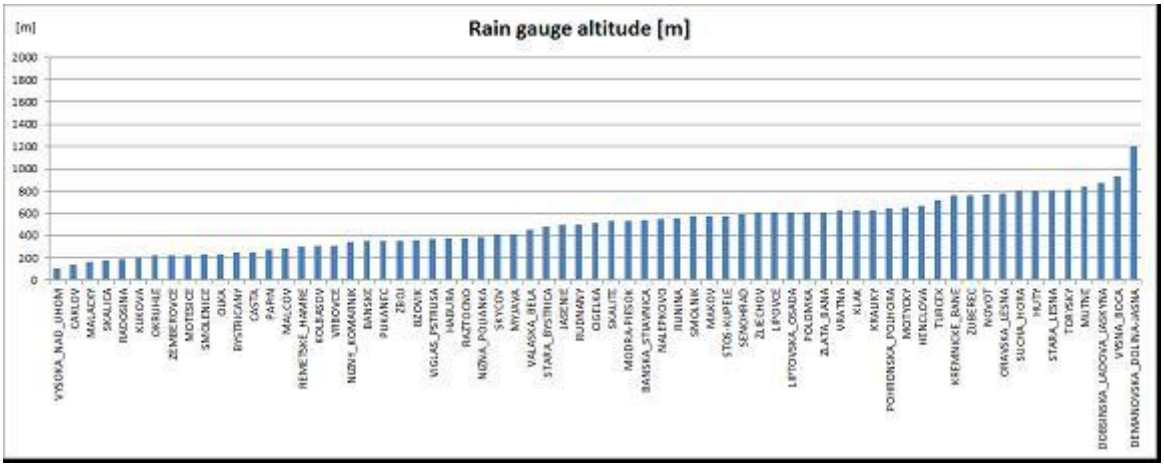

Figure 40 Distribution of rain gauges according their altitude above the sea level

To simulate terrain visibility by meteorological radars Shuttle Radar Topography Mission (SRTM) data were used as an input into radar horizon modeling software developed in SHMÚ. Details about SRTM can be found at http://en.wikipedia.org/wiki/Shuttle_Radar_Topography_Mission or directly at http://www2.jpl.nasa.gov/srtm/ SRTM model provides specific data set of terrain elevations in 90 m horizontal resolution in the whole HSAF area where HSAF validation by radars is performed. Modelling software parameters were adjusted for single radar according real scanning strategy:

Radar Site	Malý Javorník	Kojšovská hoľa
Tower height	25m	25m
Range	1200pixels/240km	1200pixels/200km
Resulted resolution	200m/pixel	166,67m/pixel
Min elevation	-0,1 deg	-0,8 deg
Refraction	1,3 (standard atmosphere)	1,3 (standard atmosphere)
Elevation step	0,01 deg	0,01 deg
Azimuth step	1/40 deg	1/40 deg
Layer minimum	500 m	500 m

Layer maximum	1000 m	1000 m
Max displayed height	5000 m	5000 m

Radar horizon model provides the following outputs (maps of radar range):

- terrain elevation
- minimum visible height above the sea level
- minimum visible height above the surface
- Layer visibility (defined by minimum and maximum levels)

Results of the horizon model for Malý Javorník and Kojšovská hoľa radar sites are shown on Figure 41. To evaluate the radar visibility over the whole radar network composite picture of minimum visible height above the surface was created and is shown on figure below.

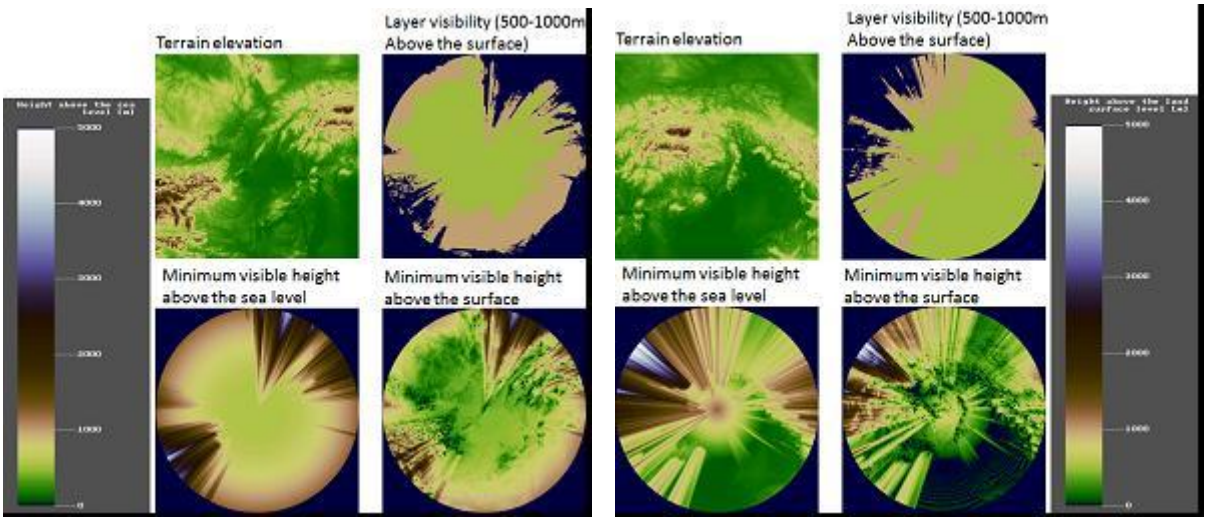

Figure 41 Radar horizon model output for Malý Javorník (left) and Kojšovská hoľa (right) radar sites

Colour scale on left corresponds to the products showing heights above the sea level, scale on right corresponds to the products showing heights above the surface.

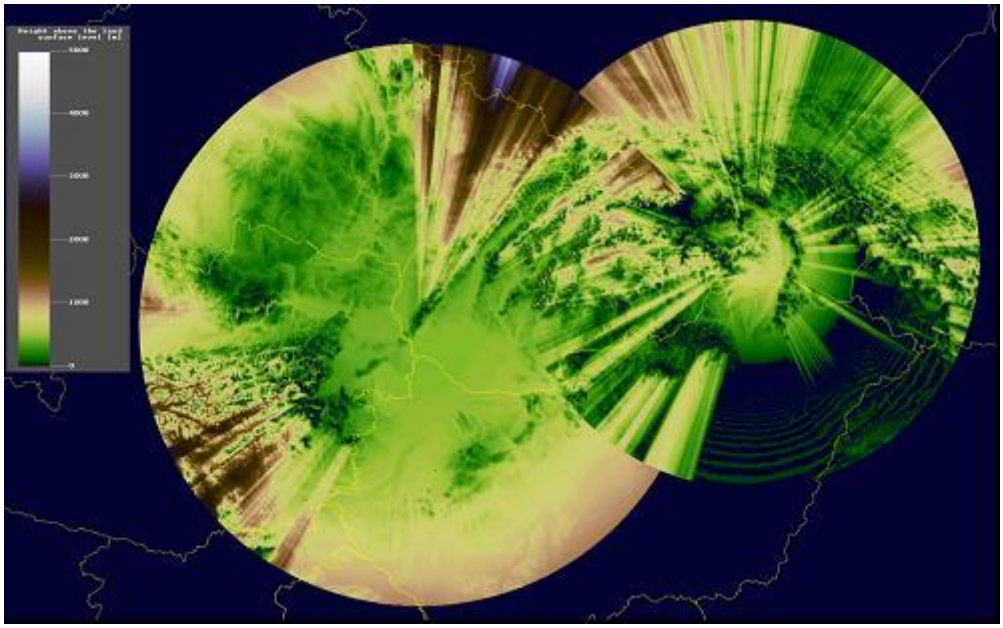

Figure 42 Composite picture of minimum visible height above the surface over the whole radar network. Compositing algorithm selects the minimum value from both radar sites

In next step minimum visible heights above the rain gauge stations were derived from the composite picture. Distribution of rain gauges according to the minimum visible height of radar beam is shown on next figure. It should be noted that while radar beam elevation is reaching 3000m in northern central part of composite picture, no rain gauge station was available in this region. Only rain gauge stations with minimum visible heights in the interval (0m; 1100m) were available in this study.

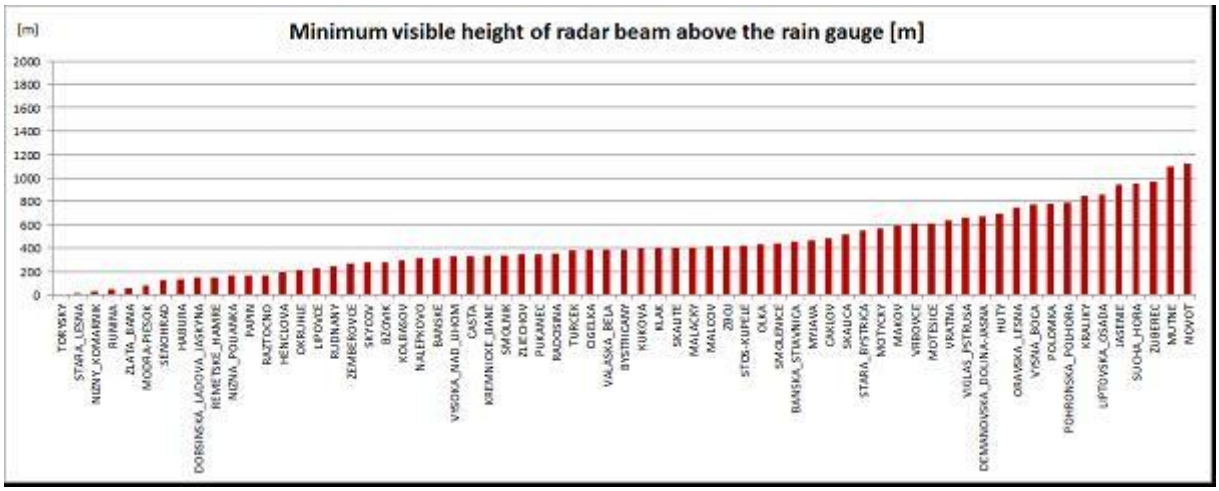

Figure 43 Distribution of rain gauges according to the minimum visible height of radar beam

To understand dependence of radar precipitation estimations and rain gauge values on gauge altitude above the sea and on radar beam altitude the scatterplots of log(R/G) versus station altitude shown on Next figure and log(R/G) versus radar beam altitude shown on Fig.6 were generated. Quite wide scattering can be observed but quadratic polynomial trend lines indicate that in general radar underestimates precipitation and this underestimation is proportional to station elevation and radar beam elevation.

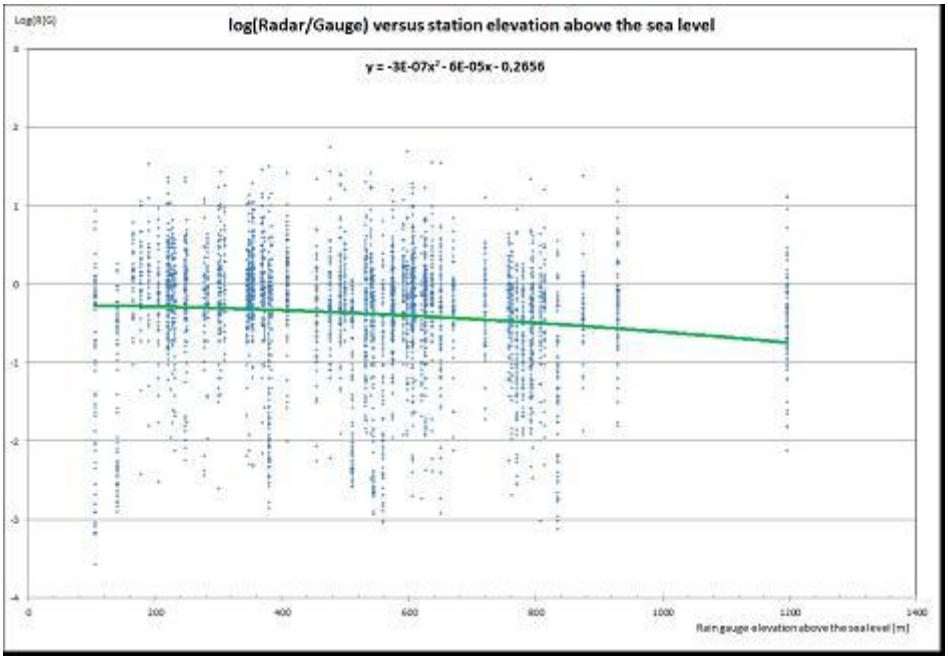

Figure 44 Scatterplot of log(R/G) versus station altitude shows general underestimation of precipitation by radar

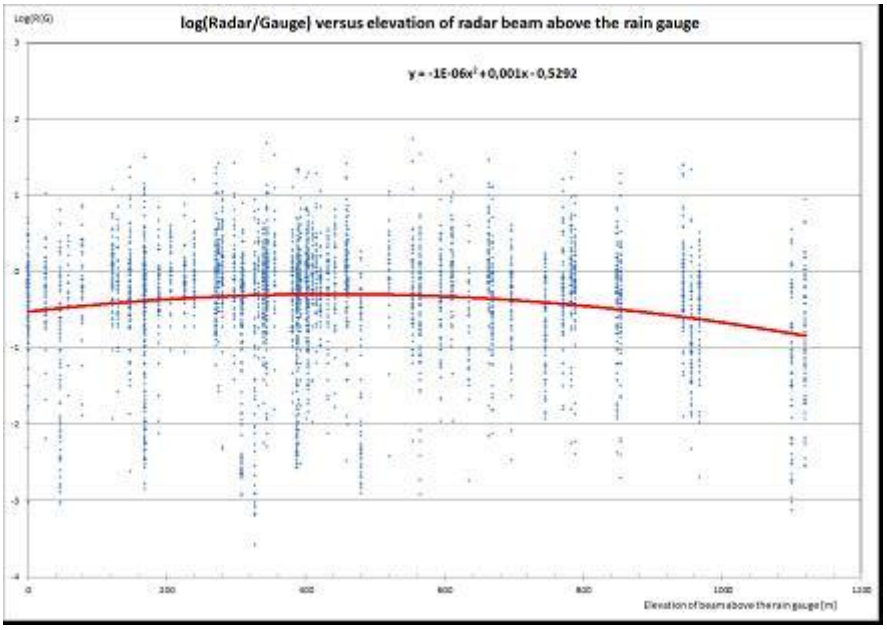

Figure 45 Scatterplot of log(R/G) versus radar beam altitude shows increased underestimation of radar for high and close to zero radar beam elevations

Polynomial trend line on the two figures above are different. While in case of rain gauge altitudes the lowest underestimation by radar can be observed for the lowest rain gauge altitudes, in case of radar beam altitudes the lowest underestimation by radar is observed for radar beam elevation about 500m. Stronger underestimation for rain gauges with close to zero radar beam elevation can be explained by partial signal blocking by terrain obstacles. These are the cases when rain gauge station is close to the top of terrain obstacle.

Finally set of statistical parameters for each single rain gauge station was computed: mean error, standard deviation, mean absolute error, multiplicative bias, correlation coefficient, RMSE and relative RMSE. Relative RMSE and Mean Error were selected to be specified for radar precipitation measurement over the whole radar range. For this purpose quadratic or linear polynomial trend lines were created as is shown on next figure.

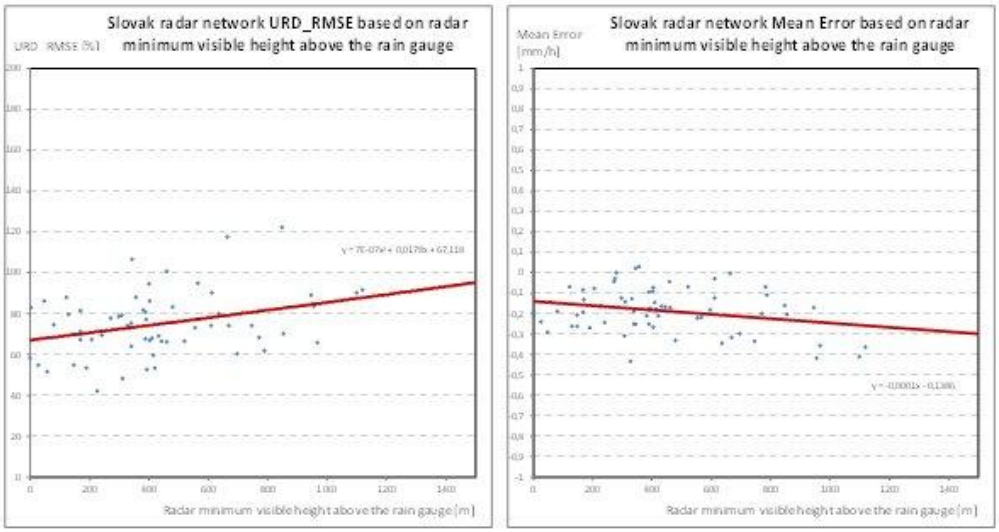

Figure 46 Relative RMSE (left) and Mean Error (right) computed independently for each rain gauge station in radar range and corresponding trend lines extrapolated for beam elevation up to 1500m

Relative RMSE and Mean Error can be specified for each pixel of radar network composite map using regression equations which describe dependence on minimum radar beam elevation above the surface. This can be considered as quality indicator maps of radar measurements with regard to terrain visibility by current radar network of SHMÚ as is shown in next two figures.

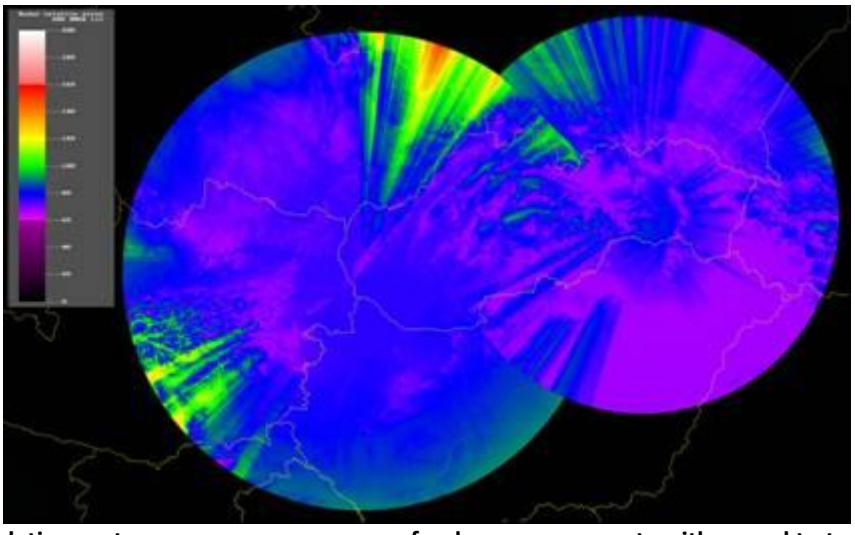

Figure 47 Final relative root mean square error map of radar measurements with regard to terrain visibility by current radar network of SHMÚ

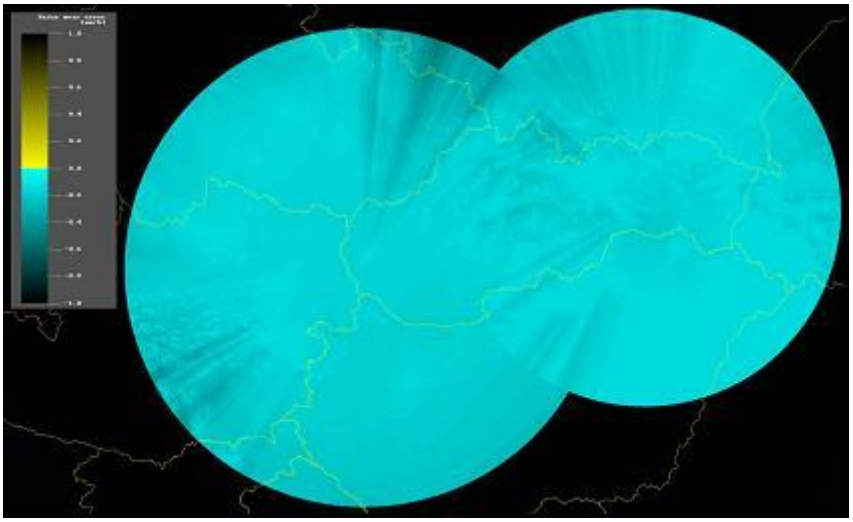

Figure 48 Final mean error map of radar measurements with regard to terrain visibility by current radar network of SHMÚ. General underestimation of precipitation by radars is observed

Conclusions

Considering the fact that reference precision of rain gauges used in this study is not sufficient and they do not reflect real ground reference of precipitation fields, obtained results can be considered as a ceiling guess of radar measurements quality indicator with regards to terrain visibility. This result includes also the error of rain gauge network itself.

Also averaged mean error, root mean square error and relative root mean square error values were computed for 68 rain gauge stations located in radar horizons:

Averaged mean error: -0,184 mm/h for instantaneous or -4,42 mm for 24 hours cumulated precipitation
Averaged RMSE: 0,395 mm/h for instantaneous or 9,48 mm for 24 hours cumulated precipitation
Averaged URD_RMSE: 69,3 % for 24 hours cumulated precipitation

It should be noted that all computations in this study were based on 24 hour cumulated precipitation and only re-calculated into instantaneous precipitation. Values of errors in case of instantaneous precipitation can be significantly higher because of short time spacing. Therefore it is planned in the future to calculate errors of radar measurements separately for instantaneous and for cumulated precipitation.

Annex 5: Radar and rain gauge integrated data

Coordinator: Jan Kanak (SHMU)
Participants: Claudia Rachimow and Peter Krahe (Germany), Ľuboslav Okon, Jozef Vivoda and Michal Neštiak (Slovakia), Rafal Iwanski and Bozena Lapeta (Poland), Silvia Puca (Italy)

Introduction

This report presents outcomes of the initial activities performed within the "INCA products" working group. In the first part information on the INCA or INCA-like systems available in the participating countries are summarized. The second part of the report presents several case studies comparing precipitation fields estimated by radars, raingauges and the INCA system. Results of the statistical comparison of the PR-OBS-2 product with the different reference fields for selected precipitation events are also included.

Summary of the INCA system survey

As a first step of survey experts/contact persons were identified inside the INCA group community as listed in the next table.

Country	Contact person/expert	E-mail address
Slovakia	Jozef Vivoda Michal Neštiak	jozef.vivoda@shmu.sk michal.nestiak@shmu.sk
Poland	Rafal Iwanski	rafal.iwanski@imgw.pl
Germany	Claudia Rachimow Peter Krahe	rachimow@bafg.de krahe@bafg.de

Table 24 List of contact persons

Within the participating countries there are two types of systems providing precipitation analyses usable for H-SAF validation: **INCA** (developed by ZAMG, Austria) and **RADOLAN** (DWD, Germany).
The INCA system is currently under development as INCA-CE (Central Europe) and is used in pre-operational mode in Slovakia and Poland. The RADOLAN system is used in Germany operationally and is already utilized for the H-SAF products validation.

Figure 49 Coverage of Europe by the INCA and RADOLAN systems

Here below a brief description of the INCA and RADOLAN systems follows. More information on both systems can be found in the documentation which is available on the H-SAF ftp server: /hsaf/WP6000/precipitation/WG_groups/WG3-inca/documentation

Brief description of the INCA system

The INCA (Integrated Nowcasting through Comprehensive Analysis) analysis and nowcasting system is being developed primarily as a means of providing improved numerical forecast products in the nowcasting and very short range forecasting. It should integrate, as far as possible, all available data sources and use them to construct physically consistent analyses of atmospheric fields. Among the input data sources belong:

- NWP model outputs in general (P, T, H, clouds …)
- Surface station observations (T, precipitation)
- Radar measurements (reflectivity, currently 2-d, 3-d in development)
- Satellite data (CLM, Cloud type, in development for use in precipitation analysis)
- Elevation data (high resolution DTM, indication of flat and mountainous terrain, slopes, ridges, peaks)

The INCA system provides:

- **High-resolution analyses** – interest of validation WG-3
- Nowcasts
- Improved forecasts

of the following variables:

- Temperature (3-d field)
- Humidity (3-d)
- Wind (3-d)
- **Precipitation (2-d)** – interest of validation WG-3
- Cloudiness (2-d)
- Global radiation (2-d)

The INCA precipitation analysis is a combination of station data interpolation including elevation effects, and radar data. It is designed to combine the strengths of both observation types, the accuracy of the point measurements and the spatial structure of the radar field. The radar can detect precipitating cells that do not hit a station. Station interpolation can provide a precipitation analysis in areas not accessible to the radar beam.

The precipitation analysis consists of the following steps:

- Interpolation of station data into regular INCA grid (1x1 km) based on distance weighting (only nearest 8 stations are taken into account to reduce bull-eyes effect)
- Climatological scaling of radar data by means of monthly precipitation totals of raingauge to radar ratio (partial elimination of the range dependance and orographical shielding)
- Re-scaling of radar data using the latest rain gauge observations
- Final combination of re-scaled radar and interpolated rain gauge data
- Elevation dependence and orographic seeding precipitation

In the final precipitation field the raingauge observations are reproduced at the raingauge station locations within the limits of resolution. Between the stations, the weight of the radar information becomes larger the better the radar captures the precipitation climatologically.

Important factor affecting the final precipitation analysis is accuracy and reliability of the raingauge stations. In order to eliminate the influence of raingauge stations providing evidently erroneous data, the SHMÚ is developing the blacklisting technique which temporarily excludes such stations from the analysis. Currently, the stations can be put into the blacklist only manually but development of the automated blacklisting is expected in near future.

Brief description of the RADOLAN system

RADOLAN is a routine method for the online adjustment of radar precipitation data by means of automatic surface precipitation stations (ombrometers) which has started on a project base at DWD in 1997. Since June 2005, areal, spatial and temporal high-resolution, quantitative precipitation data are derived from online adjusted radar measurements in real-time production for Germany.

The data base for the radar online adjustment is the operational weather radar network of DWD with 16 C-band sites on the one hand, and the joined precipitation network of DWD and the federal states with automatically downloadable ombrometer data on the other hand. In the course of this, the precipitation scan with five-minute radar precipitation data and a maximum range of 125 km radius around the respective site is used for the quantitative precipitation analyses. Currently, from more than 1000 ombrometer station (approx. 450 synoptic stations AMDA I/II-and AMDA III/S-of DWD; approx. 400 automatic precipitation stations AMDA III/N of DWD; approx. 150 stations of the densification measurement network of the federal states) the hourly measured precipitation amount is used for the adjustment procedure.

In advance of the actual adjustment different preprocessing steps of the quantitative radar precipitation data are performed. These steps, partly already integrated in the offline adjustment procedure, contain the orographic shading correction, the refined Z-R relation, the quantitative composite generation for Germany, the statistical suppression of clutter, the gradient smoothing and the pre-adjustment. Further improvements of these procedures are being developed.

Precipitation distribution of the rain gauge point measurements | Precipitation distribution of the areal original radar measurements | RADOLAN precipitation product

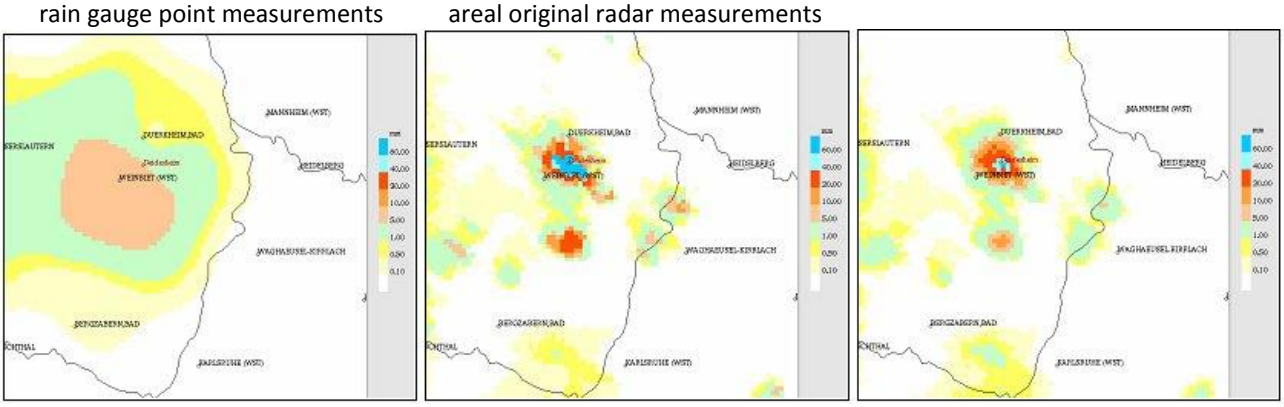

Figure 50 Procedure of the RADOLAN online adjustment (hourly precipitation amount on 7 August 2004 13:50 UTC)

In order to collect more detailed information about both types of systems a questionnaire was elaborated and completed by Slovakia, Poland and Germany. The questionnaire provided details such as geographical coverage, input data inventory or availability of different instantaneous and cumulated precipitation products.

The final version of the questionnaire is shown in the next table and is also available on the H-SAF ftp server: /hsaf/WP6000/precipitation/WG_groups/WG3-inca/questionnaire.

Group of information	Item	GERMANY	POLAND	SLOVAKIA domain1	SLOVAKIA domain2
Availability of documentation for INCA or similar (German) system [Yes/No]	If possible please attach link or documentation	Dokumentation received during Helsinki validation meeting	Documentation available from ZAMG	Documentation available from ZAMG	Documentation should be issued in future
Definition of geographical area covered by INCA or similar (in Germany) system	Grid size in pixels	900x900	741x651	501x301	1193x951
	Min longitude	3.5943 E	13.82 E	15.99231 E	8,9953784943 E
	Max longitude	15.71245 E	25.334 E	23.09630 E	25,9996967316 E
	Min latitude	46.95719 N	48.728 N	47.13585 N	45,0027313232 N
	Max latitude	54.73662 N	55.029 N	50.14841 N	53,000579834 N
	Space resolution	1 km	1 km	1 km	1 km
Input data	Number of radars in network	Composite of 16 national radars	Composite of 8 national radars	Composite of 2 national radars	Composite of 5 international radars
	Number of precipitation stations	1300	475 (Poland only)	397 (SHMU, CHMI, ZAMG, IMWM)	TBD
	Blacklist for precipitation stations [Yes/No]	?	Yes	Yes	Yes
Density of raingauge stations	Map of density of precipitation stations [Yes/No]	?	TBD	TBD	TBD
Output data	Instantaneous precipitation based only on raingauge network, time resolution, timelines	5 min	No	Yes, 15 min	Yes, 15 minute
	Instantaneous precipitation based only on radar network, time resolution, timelines	5 min	No	Yes, 5 minute	Yes, 5 minute
	Instantaneous precipitation based on combined raingauge and radar network, time resolution, timelines	5 min	Yes, 10 minutes	Yes, 5 minutes	Yes, 5 minutes
	Cumulative precipitation based only on raingauge network, time intervals, timelines	5 min, 1,3,6,12,18,24 hours	No	Yes, min 5 min, available 1,3,6,12,24 hours	Yes, min 5 min, available 1,3,6,12,24 hours
	Cumulative precipitation based only on radar network, time intervals, timelines	5 min, 1,3,6,12,18,24 hours	No	Yes, min 5 min, available 1,3,6,12,24 hours	Yes, min 5 min, available 1,3,6,12,24 hours
	Cumulative precipitation based on combined raingauge and radar network, time intervals, timelines	5 min, 1,3,6,12,18,24 hours	Yes, min 10 minutes, available in future	Yes, min 5 min, available 1,3,6,12,24 hours	Yes, min 5 min, available 1,3,6,12,24 hours
Dates for selected case studies	Case 1	will be set	No	29.3.2009	
	Case 2		No	1.-3.6.2010	
	Case 3		No	20.6.2010	
	Case 4		No	15.-16.8.2010	
	Case 5		No		
Availability of own software for upscaling INCA data into native satellite grid	H01	yes	No	No	No
	H02	yes	No	No	No
	H03	yes	No	No	No
	H04	no	No	No	No
	H05	yes	No	No	No
	H06	yes	No	No	No

Table 25 Questionnaire

Case studies

Several case studies comparing the INCA analyses with their source precipitation fields from radars and raingauges and with selected H-SAF products have been elaborated at SHMÚ. The precipitation fields from individual observations have been compared visually but have also been used as a "ground reference" for statistical analysis of the PR-OBS-2 product during selected precipitation events.

Case study PR-OBS-1 vs. INCA,15 August 2010 15:00 UTC

This is the first case study elaborated at SHMÚ which compares the PR-OBS-1 product with precipitation fields produced by the INCA system. In order to make precipitation fields from the microwave instruments and ground observations at 1 km resolution comparable, the INCA precipitation fields have been upscaled into the PR-OBS-1 native grid using the Gaussian averaging method.

Ellipses in next figure represent the satellite instrument IFOVs with colour corresponding to the upscaled radar, rain-gauge and INCA analysis rain-rate value in case of next figure (from a) to c)) respectively, or the satellite rain-rate value in case of next figure, part d)).
As can be seen in next figure, part b) the rain-gauge network captured intense precipitation near the High Tatras mountain in the northern part of Slovakia where only low precipitation rates were observed by radars (next figure, part a)) The resulting INCA analysis is shown in (next figure, part c)).
The corresponding PR-OBS-1 field (next figure, part d) shows overestimation even when compared with the rain-gauge adjusted field of the INCA analysis.

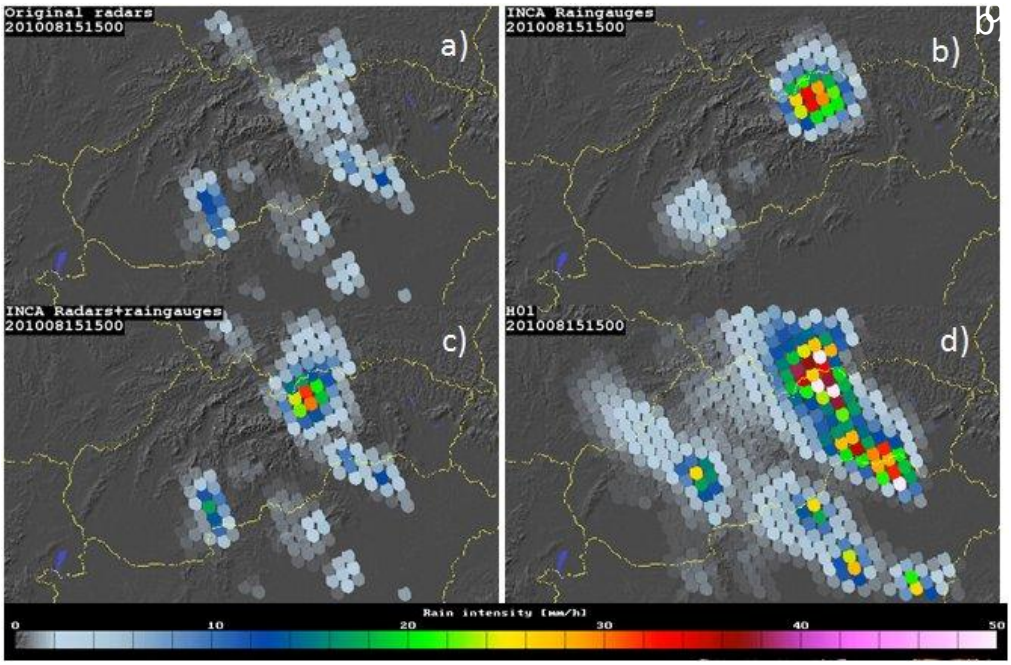

Figure 51 Precipitation intensity field from 15 August 2010 15:00 UTC obtained by a) radars, b) interpolated raingauge data, c) INCA analysis and d) PR-OBS-1 product

Visual comparison of the precipitation fields

In this section two case studies from 15 August 2010 focused on performance of the INCA analyses are presented.

15 August 2010, 06:00 UTC

This case illustrates potential of the INCA system to correct errors in radar precipitation measurements due to radar beam attenuation in heavy precipitation. As can be seen in next figure, part a) the radar measured precipitation near centre of the circled area was relatively weak. However, as next figure, part c) suggests, the precipitation was probably underestimated by radars because an intense convective cell occurred directly in path of the radar beam (dashed line in next figure, part c). The raingauge network (next figure, part b) captured the intense precipitation underestimated by radars and improved the INCA analysis (next figure, part c).

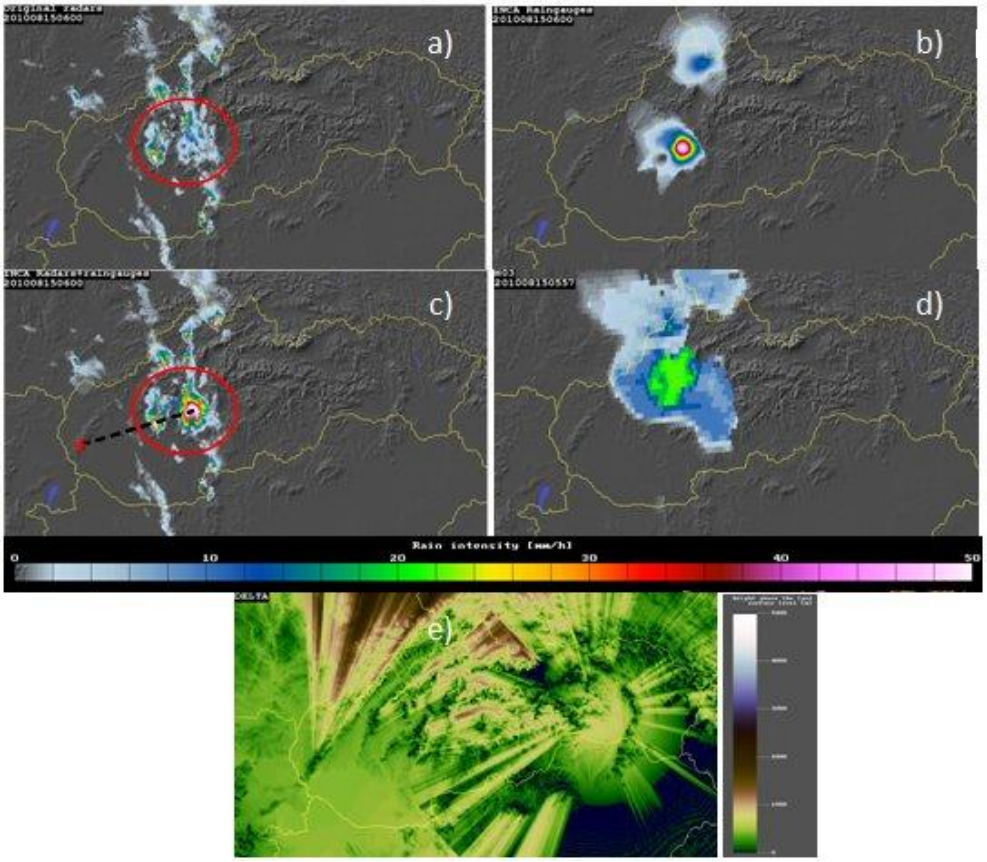

Figure 52 Precipitation intensity field from 15 August 2010 6:00 UTC obtained by a) radars, b) interpolated raingauge data, c) INCA analysis and d) PR-OBS-3 product (5:57 UTC) supplemented with map of minimum visible height above surface level of the SHMU radar network e)

15 August 2010, 08:00 UTC

The case from 08:00 UTC (next figure) gives an example of partial correction of radar beam orographical blocking by the INCA analysis. The radar precipitation field in the north-western part of Slovakia (next figure a)) is affected by orographical blocking as indicated by relatively high minimum elevations of radar beam above this location in next figure e)). Also in this case information from raingauge network (next figure b)) supplemented the radar field in the resulting INCA analysis (next figure c)).

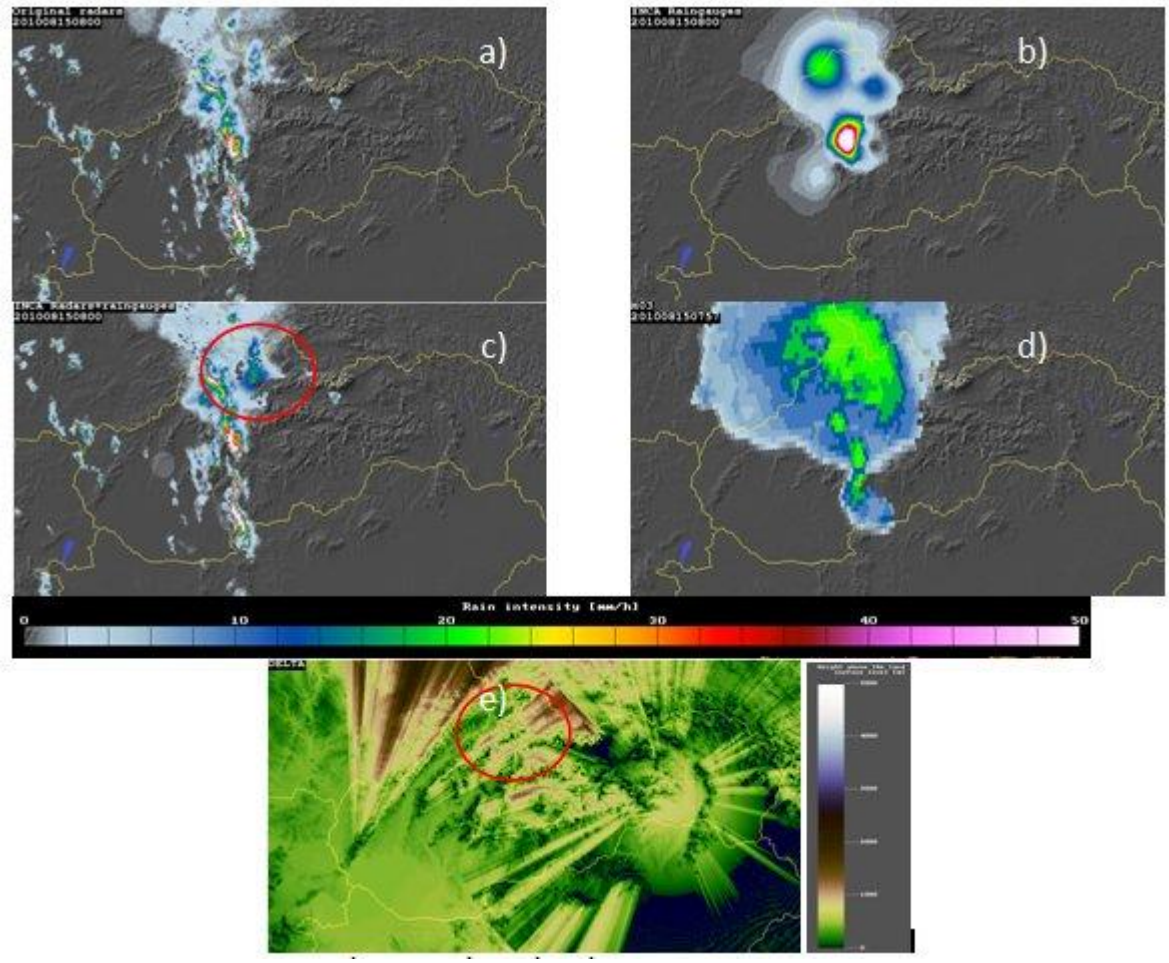

Figure 53 As in previous figure except for 8:00 UTC

Statistical analysis of the PR-OBS-2 product on selected precipitation events

As a first step towards utilizing the INCA precipitation analyses for the H-SAF validation, it has been decided to perform at SHMÚ a statistical analysis of the H-SAF products using the precipitation fields from INCA, radars and raingauges as a "ground reference" data for selected precipitation events. Since this task required modification of the SHMÚ software currently used for upscaling radar data, until now results for the PR-OBS-2 product are only available.

In order to eliminate interpolation artifacts in the areas outside the raingauge network occuring in the INCA analyses, only the PR-OBS-2 data falling inside the Slovakia territory were taken into account in the statistical analysis.

Overall five precipitation events with different prevailing type of precipitation have been selected for the statistical analysis as listed in next table.

Event	Period (UTC)	Precipitation type
1	15 August 2010 00:00 - 21:00	convective
2	16 August 2010 06:00 - 23:45	convective
3	15 September 2010 15:00 - 18 September 2010 09:00	mixed
4	21 November 2010 20:00 -	stratiform

	22 November 2010 23:45	
5	28 November 2010 15:00 - 29 November 2010 10:00	stratiform

Table 26 List of precipitation events selected for statistical analysis

For each precipitation event and each "ground reference" data a set of continuous and dichotomous statistical scores was computed. The scores and thresholds of the precipitation classes were adopted from the H-SAF common validation methodology.

As an example, the results of selected statistical scores obtained with different reference data for the event 1 and 4 are shown in next two figures respectively.

Due to the small number of compared PR-OBS-2 observations during the selected precipitation events (overall convective: 1864 observations, stratiform: 2251, mixed: 3409) the obtained results may not be representative enough. Therefore it is questionable if any conclusion about dependence of the investigated "ground reference" data on the long-term validation results can be made. It is proposed that statistical analysis using longer validation period will have to be performed.

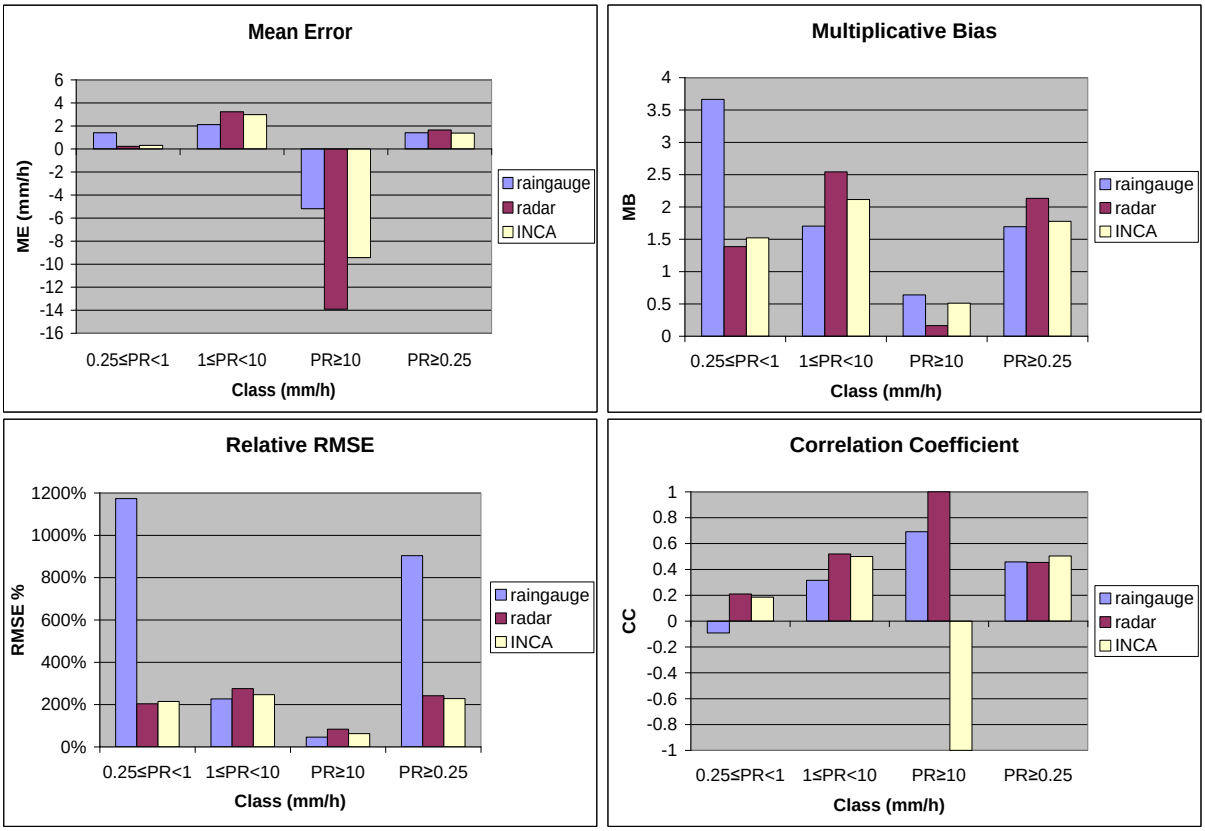

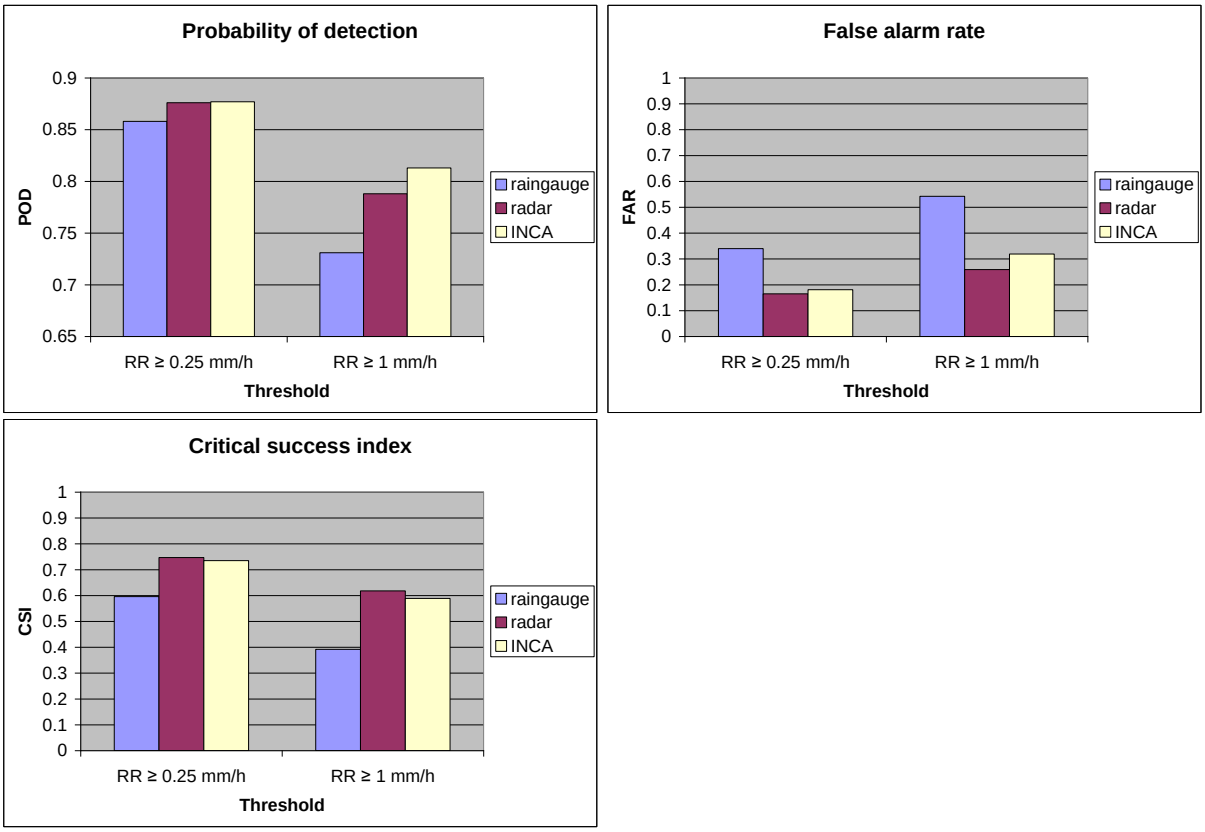

Figure 54 Comparison of selected statistical scores for the PR-OBS-2 product obtained by different "ground reference" data; valid for event 1 (convective)

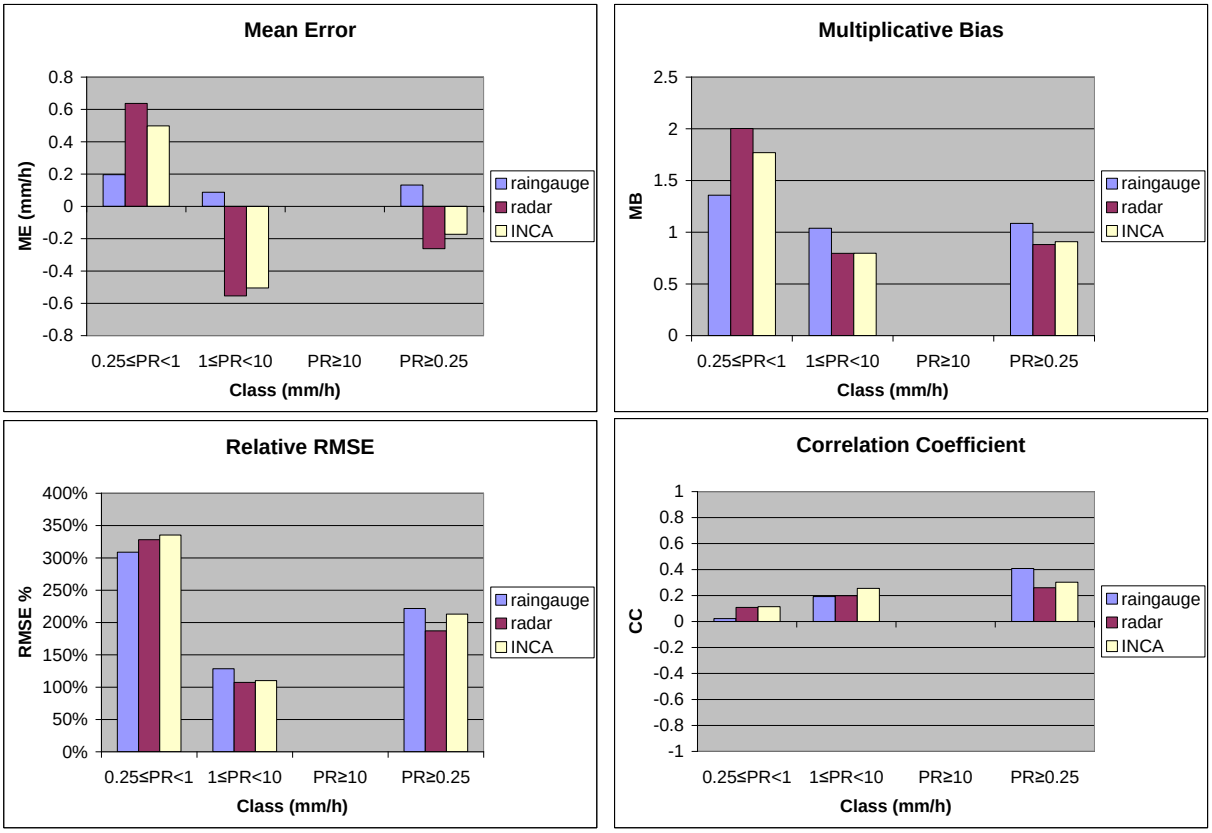

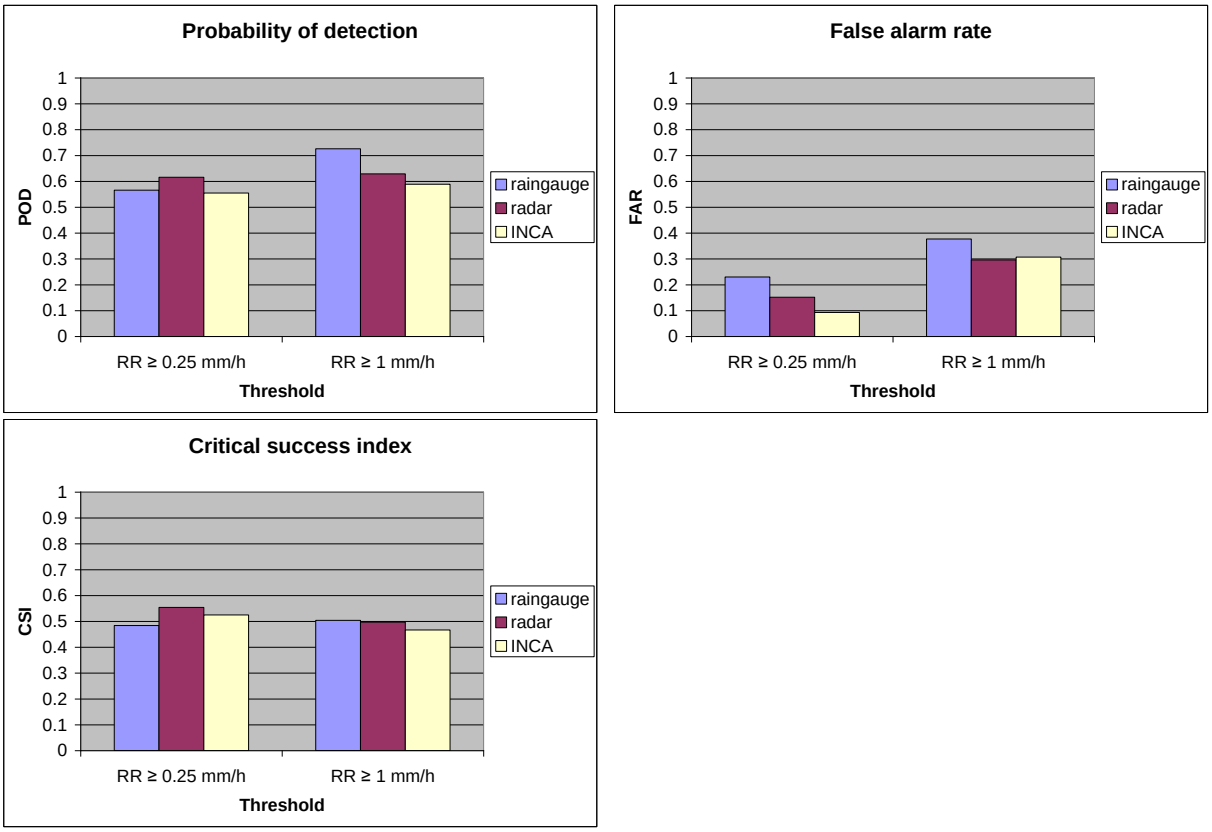

Figure 55 As in previous figure except for event 4 (stratiform)

Conclusions

The INCA system as a potential tool for the precipitation products validation is available in Slovakia and Poland, in both countries being run in pre-operational mode. It is still relatively new system undergoing continuous development. More sophisticated algorithms of the precipitation analysis (e.g. assimilation of the 3-D radar data) can be expected from its development in frame of the ongoing INCA-CE project.

In Germany similar precipitation analysis system called RADOLAN is being run operationally. This tool is already used for validation of the H-SAF precipitation products in this country.

The accuracy and reliability of the raingauge stations significantly affect final precipitation analysis of the INCA or INCA-like systems and therefore need to be checked. In order to solve this problem an automated blacklisting technique is going to be developed at SHMÚ (currently blacklisting is used in manual mode).

The case studies presented in the report comparing the INCA analyses with corresponding input precipitation fields from radars and raingauges pointed out the benefits of the INCA system. It has been shown that the system has potential to compensate errors due to effects like radar beam orographical blocking but also to correct instantaneous factors affecting radar measurement quality like radar beam attenuation in heavy precipitation what can not be achieved by standard methods of climatological radar data adjustment.

First attempts to utilize the INCA analyses as a “ground reference” data for the H-SAF products validation have been done by statistical analysis of the PR-OBS-2 product during selected precipitation events.

The software for upscaling the INCA precipitation field into the H-SAF products grid will have to be developed. Since the grids of INCA and RADOLAN have similar horizontal resolution to the common radar grid, the radar upscaling techniques can be applied also on the INCA or RADOLAN data. In frame of the

unification of the validation methodologies the same common upscaling software could be shared between both radar (WG2) and INCA (WG3) working groups in the future.

References:

T.Haiden, A. Kann, G. Pistotnik, K. Stadlbacher, C. Wittmann: Interated Nowcasting through Comprehensive Analysis (INCA) System description. ZAMG, Vienna, Austria, 4 January 2010

André Simon, Alexander Kann, Michal Neštiak, Ingo Meirold-Mautner, Ákos Horváth, Kálmán Csirmaz, Olga Ulbert, Christine Gruber: Nowcasting and very short range forecasting of wind gusts generated by deep convection. European Geosciences Union General Assembly 2011, Vienna, Austria, 03 - 08 April, 2011

Ingo Meirold-Mautner, Benedikt Bica, Yong Wang: INCA-CE: A Central European initiative in nowcasting applications. Central Institute for Meteorology and Geodynamics, Hohe Warte 38, 1190 Vienna, Austria

Ingo Meirold-Mautner, Yong Wang, Alexander Kann, Benedikt Bica, Christine Gruber, Georg Pistotnik, Sabine Radanovics: Integrated nowcasting system f or the Central European area: INCA-CE. Central Institute for Meteorology and Geodynamics (ZAMG), Hohe Warte 38, 1190 Vienna, Austria

Annex 6: Geographical maps – distribution of error

Coordinator: Bozena Lapeta (IMGW, Poland)
Members: Ibrahim Somnez (ITU, Turkey)

Introduction

The Working Group 5 aims at creating geographical maps of H-SAF products' error and analyzing its usefulness for H-SAF validation. The idea of this work stemmed from hydrological validation community that is interested in distribution of the error over the catchments. In this report the results obtained during the first step of WG5 activities aiming at selection of the best method for mean error specialization are presented.

Selection of spatialisation algorithm – first results

The most important issue in creating geographical distribution of any parameter is the algorithm for spatial interpolation. As there is no universal spatial interpolation method that can be applied for any parameters, the first step in the creation of maps of H-SAF precipitation products error was the selection of the interpolation algorithm. Commonly used Ordinary Kriging, Inverse Distance Weighted and Natural Neighbour methods were tested firstly. The analysis was performed for monthly average mean error of H-05 3 h cumulated precipitation for selected months. In the analysis data from Polish rain gauges were used. In the next figure the example mean error maps for July 2010 obtained using three mentioned above algorithms are presented.

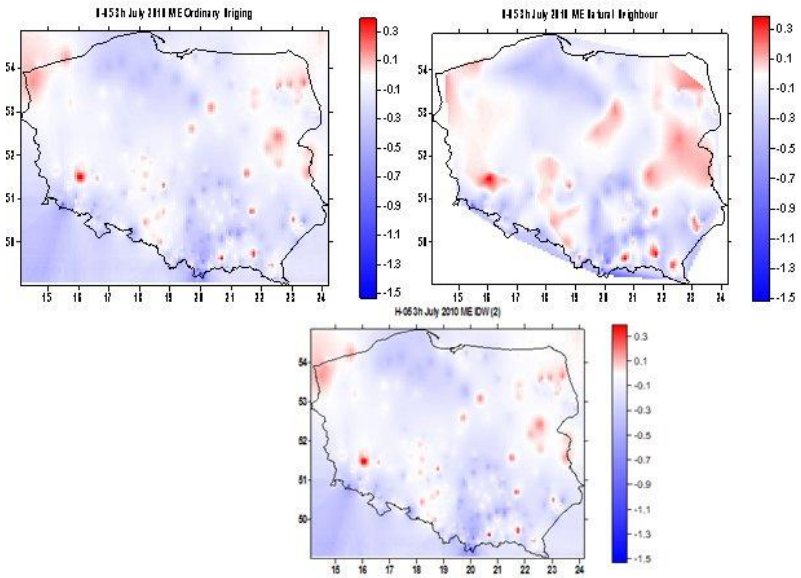

Figure 56 Distribution of the monthly average H-05 3 h cumulated precipitation Mean Error calculated for July 2010 using three methods: (clockwise from upper left) Ordinary Kriging, Natural Neighbour, and IDW (2)

One can see that the obtained maps do not differ significantly, however, for the map created with the use of Natural Neighbour method, the maximum and minimum values are less pronounced that on the other two maps. Moreover, application of Natural Neighbour method does not allow for extrapolating the distribution beyond the area defined by stations.

In order to evaluate the quality of the error distribution, the cross validation was performed and the results are presented on the next figure.

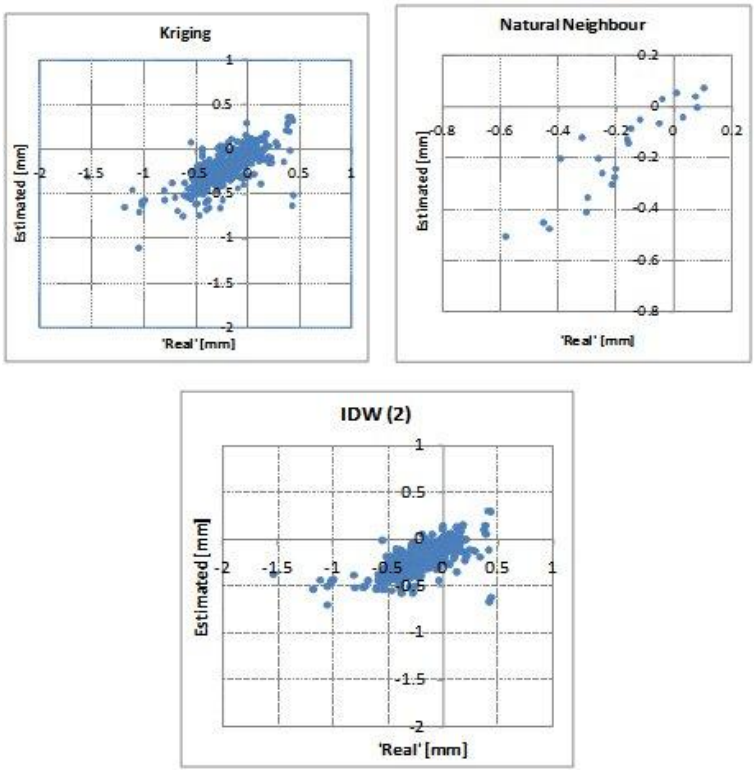

Figure 57 Cross validation results obtained for three different methods for spatial interpolation

For all methods, the results are similarly scattered around the perfect estimation, however, for IDW(2) some underestimation was found for negative ME values. The values of Mean Residual and Mean Absolute Residual defined as mean and mean absolute difference between Estimated and Real values of ME are presented in the next table.

	Mean Residual	Mean Absolute Residual
Kriging	-0.004	0.09
Natural Neighbour	0.007	0.06
IDW(2)	-0.009	0.10

Table 27 Mean Residual and Mean Absolute Residual values obtained for three algorithms for spatial interpolation using cross-validation approach

The lowest value of Mean Absolute Residual was found for Natural Neighbour method, what indicates that application of this algorithm may allow for minimizing the systematical error introduced by spatialisation method. Therefore this method seems to be the best for creating the geographical distribution of H-SAF products error for countries characterized by terrain geographical configuration similar to the Polish one.

Conclusions

The analysis performed for ME of H-05 3 h cumulated product obtained using data from Polish network of rain gauges showed that Natural Neighbour interpolation method seems to be the best one for creating maps of H-SAF products error. However, application of Natural Neighbour method does not allow for extrapolating the distribution beyond the area defined by stations, what is a disadvantage of this methods.

As the maps are to be created for the whole H-SAF domain, presented above results should be verified over other countries. Therefore, in the next step of WG5 activities the study will be performed for other countries and for the errors calculated using radar data.

Annex 7: Acronyms

AMSU	Advanced Microwave Sounding Unit (on NOAA and MetOp)
AMSU-A	Advanced Microwave Sounding Unit - A (on NOAA and MetOp)
AMSU-B	Advanced Microwave Sounding Unit - B (on NOAA up to 17)
ATDD	Algorithms Theoretical Definition Document
AU	Anadolu University (in Turkey)
BfG	Bundesanstalt für Gewässerkunde (in Germany)
CAF	Central Application Facility (of EUMETSAT)
CDOP	Continuous Development-Operations Phase
CESBIO	Centre d'Etudes Spatiales de la BIOsphere (of CNRS, in France)
CM-SAF	SAF on Climate Monitoring
CNMCA	Centro Nazionale di Meteorologia e Climatologia Aeronautica (in Italy)
CNR	Consiglio Nazionale delle Ricerche (of Italy)
CNRS	Centre Nationale de la Recherche Scientifique (of France)
DMSP	Defense Meteorological Satellite Program
DPC	Dipartimento Protezione Civile (of Italy)
EARS	EUMETSAT Advanced Retransmission Service
ECMWF	European Centre for Medium-range Weather Forecasts
EDC	EUMETSAT Data Centre, previously known as U-MARF
EUM	Short for EUMETSAT
EUMETCast	EUMETSAT's Broadcast System for Environmental Data
EUMETSAT	European Organisation for the Exploitation of Meteorological Satellites
FMI	Finnish Meteorological Institute
FTP	File Transfer Protocol
GEO	Geostationary Earth Orbit
GRAS-SAF	SAF on GRAS Meteorology
HDF	Hierarchical Data Format
HRV	High Resolution Visible (one SEVIRI channel)
H-SAF	SAF on Support to Operational Hydrology and Water Management
IDL©	Interactive Data Language
IFOV	Instantaneous Field Of View
IMWM	Institute of Meteorology and Water Management (in Poland)
IPF	Institut für Photogrammetrie und Fernerkundung (of TU-Wien, in Austria)
IPWG	International Precipitation Working Group
IR	Infra Red
IRM	Institut Royal Météorologique (of Belgium) (alternative of RMI)
ISAC	Istituto di Scienze dell'Atmosfera e del Clima (of CNR, Italy)
ITU	İstanbul Technical University (in Turkey)
LATMOS	Laboratoire Atmosphères, Milieux, Observations Spatiales (of CNRS, in France)
LEO	Low Earth Orbit
LSA-SAF	SAF on Land Surface Analysis
Météo France	National Meteorological Service of France
METU	Middle East Technical University (in Turkey)
MHS	Microwave Humidity Sounder (on NOAA 18 and 19, and on MetOp)
MSG	Meteosat Second Generation (Meteosat 8, 9, 10, 11)
MVIRI	Meteosat Visible and Infra Red Imager (on Meteosat up to 7)
MW	Micro Wave
NESDIS	National Environmental Satellite, Data and Information Services
NMA	National Meteorological Administration (of Romania)
NOAA	National Oceanic and Atmospheric Administration (Agency and satellite)
NWC-SAF	SAF in support to Nowcasting & Very Short Range Forecasting
NWP	Numerical Weather Prediction
NWP-SAF	SAF on Numerical Weather Prediction
O3M-SAF	SAF on Ozone and Atmospheric Chemistry Monitoring
OMSZ	Hungarian Meteorological Service

ORR	Operations Readiness Review
OSI-SAF	SAF on Ocean and Sea Ice
PDF	Probability Density Function
PEHRPP	Pilot Evaluation of High Resolution Precipitation Products
Pixel	Picture element
PMW	Passive Micro-Wave
PP	Project Plan
PPVG	Precipitation Products Validation Group (sometimes also PVG, Precipitation Validation Group)
PR	Precipitation Radar (on TRMM)
PUM	Product User Manual
PVR	Product Validation Report
RMI	Royal Meteorological Institute (of Belgium) (alternative of IRM)
RR	Rain Rate
RU	Rapid Update
SAF	Satellite Application Facility
SEVIRI	Spinning Enhanced Visible and Infra-Red Imager (on Meteosat from 8 onwards)
SHMÚ	Slovak Hydro-Meteorological Institute
SSM/I	Special Sensor Microwave / Imager (on DMSP up to F-15)
SSMIS	Special Sensor Microwave Imager/Sounder (on DMSP starting with S-16)
SYKE	Suomen ympäristökeskus (Finnish Environment Institute)
T_{BB}	Equivalent Blackbody Temperature (used for IR)
TKK	Teknillinen korkeakoulu (Helsinki University of Technology)
TMI	TRMM Microwave Imager (on TRMM)
TRMM	Tropical Rainfall Measuring Mission UKMO
TSMS	Turkish State Meteorological Service
TU-Wien	Technische Universität Wien (in Austria)
U-MARF	Unified Meteorological Archive and Retrieval Facility
UniFe	University of Ferrara (in Italy)
PR-RMSE	User Requirements Document
UTC	Universal Coordinated Time
VIS	Visible
ZAMG	Zentralanstalt für Meteorologie und Geodynamik (of Austria)